

**DEVELOPMENT OF SYNTHETIC METHODOLOGY TO ACCESS
GLYCEROL-3-PHOSPHATE ACYLTRANSFERASE INHIBITORS**

by

Victor Kenneth Outlaw

A dissertation submitted to The Johns Hopkins University in conformity with the requirements
for the degree of Doctor of Philosophy

Baltimore, Maryland
May 15, 2015

© 2015 Victor Kenneth Outlaw
All rights reserved

Abstract

Despite a rising demand for anti-obesity therapeutics, few effective pharmacological options are clinically available that target the synthesis and accumulation of body fat. Moderate inhibition of mammalian glycerol-3-phosphate acyltransferase (GPAT) with 2-(alkanesulfonamido)benzoic acids has recently been described *in vitro*, accompanied by promising weight loss *in vivo*. Docking studies with 2-(octanesulfonamido)benzoic acid modeled into the active site of squash GPAT revealed an unoccupied volume lined with hydrophobic residues proximal to C-4 and C-5 of the benzoic acid ring. In an effort to produce more potent GPAT inhibitors, a series of 4- and 5-substituted analogs were designed, synthesized, and evaluated for inhibitory activity. In general, compounds containing hydrophobic substituents at the 4- and 5-positions, such as biphenyl and alkylphenyl hydrocarbons, exhibited an improved inhibitory activity against GPAT *in vitro*. The most active compound, a *p*-biphenylketo-substituted analog, demonstrated an IC_{50} of 8.5 μ M and represents the best GPAT inhibitor discovered to date. Conversely, further substitution with polar hydroxyl or fluoro groups led to a 3-fold decrease in activity. These results are consistent with the presence of a hydrophobic pocket and may support the binding model as a potential tool for developing more potent inhibitors.

The design and synthesis of indole analogs based on the sulfonamidobenzoic scaffold was also undertaken. Since existing methods for their preparation were insufficient, a flexible and efficient route to substituted 7-amino-5-cyanoindoles from pyrrole-3-carboxaldehydes was developed. The route commences with a one-pot, three-component Wittig reaction of the aldehydes with fumaronitrile and a trialkylphosphine. The predominantly *E*-alkene product

positions the allylic nitrile for facile intramolecular Hoeben-Hoesch reaction in the presence of $\text{BF}_3 \cdot \text{OEt}_2$. Syntheses of 2,5- and 3,5-disubstituted 7-aminoindoles are illustrated. Additionally, dianion alkylation of the allylic nitrile is demonstrated to furnish, after cyclization, 5,6-disubstituted 7-aminoindoles.

Isosteres of indole, N-fused heteroaromatic bicycles were also desired as inhibitor candidates. An efficient route to these heterocycles, including indolizines, imidazo[1,2-*a*]pyridines, and imidazo[1,5-*a*]pyridines from azole aldehydes was developed using a related but mechanistically distinct method. A similar three-component Wittig olefination of the aldehydes was optimized to afford predominantly *E*-alkenes that, upon in situ treatment with catalytic KOH, undergo rapid cycloaromatization. Substituent control of the 1-, 2-, and 3-positions of the resulting heteroaromatic bicycles is demonstrated. Alternatively, the isolable *E*-alkene Wittig product from pyrrole-2-carboxaldehyde, under dianionic conditions, undergoes selective alkylation with various electrophiles, followed by in situ annulation to indolizines additionally substituted at the 6-position. These routes allow for the rapid generation of heterocyclic libraries for evaluation of GPAT inhibition.

Thesis Advisor:

Dr. Craig A. Townsend, Department of Chemistry, The Johns Hopkins University

Readers:

Dr. John D. Tovar, Department of Chemistry, The Johns Hopkins University

Dr. Rebekka S. Klausen, Department of Chemistry, The Johns Hopkins University

Acknowledgements

There are several people without whom the work described in this thesis would not have been possible. First, I would like to thank Dr. Townsend for his financial and academic support during my time in his lab. At a time when many PIs were consolidating research projects due to the current harsh funding climate, he allowed me to follow the chemistry and pursue my own ideas long after they had strayed quite far from the lab's traditional research areas. I believe this has made me a far better scientist, and I am grateful for his support and guidance. I would also like to thank the rest of the Johns Hopkins Chemistry faculty and staff, particularly my thesis committee readers, for their assistance and tutelage through the years. Next, I would like to thank my family for their love and support. They've encouraged me throughout my academic career and were always available with advice or an attentive ear depending on which of the two the situation called for. I'd also like to thank my friends in the Townsend lab, as well as other labs. Whether it was productive discussion over coffee, air-guitaring to 80s hits, away-team-heckling at Camden Yards, or pounding Bohs en route to one of several Harm City championships, they could always be counted on when I needed to blow off steam. Finally, I'd like to thank my wife Megan who has been with me from the start. She has talked me off several metaphorical ledges, and, without her emotional support, I am sure I would not have made it through graduate school.

Publications Drawing Upon This Thesis

1. Outlaw, V. K.; Wydysh, E. A.; Vadlamudi, A.; Medghalchi, S. M.; Townsend, C. A. Design, synthesis, and evaluation of 4- and 5-substituted *o*-(octanesulfonamido)benzoic acids as inhibitors of glycerol-3-phosphate acyltransferase. *Med. Chem. Comm.* **2014**, *5*, 826–830.
2. Outlaw, V. K.; Townsend, C. A. A Practical Route to Substituted 7-Aminoindoles from Pyrrole-3-carboxaldehydes. *Org. Lett.* **2014**, *16*, 6334–6337.
3. Outlaw, V. K.; D'Andrea, F. B.; Townsend, C. A. One-Pot Synthesis of Highly Substituted N-Fused Heteroaromatic Bicycles from Azole Aldehydes. *Org. Lett.* **2015**, *17*, 1822–1825.

Table of Contents

Chapter 1: Introduction to Current Antiobesity Therapeutics.....	1
1.1 Introduction.....	1
1.2 Antiobesity Therapies Targeting Food Intake.....	2
1.3 Antiobesity Therapies Targeting Biochemical Processes after Food Intake.....	4
1.4 Glycerol-3-Phosphate Acyltransferase as an Antiobesity Drug Target.....	7
1.5 Summary.....	11
1.6 Thesis Goals.....	11
1.7 References.....	11
Chapter 2: Design, Synthesis, and Evaluation of <i>o</i>-(Octanesulfonamido)benzoic Acids as Inhibitors of Glycerol-3-phosphate Acyltransferase.....	15
2.1 Introduction.....	15
2.2 Inhibitor Design and Molecular Modeling.....	16
2.3 Synthesis of 4- and 5-Substituted Analogs.....	18
2.4 Inhibitory Data.....	20
2.5 Conclusions.....	24
2.6 Experimental.....	25
2.7 References.....	60

Chapter 3: A Practical Route to Substituted 7-Aminoindoles from Pyrrole-3-

carboxaldehydes.....	62
3.1 Introduction.....	62
3.2 One-Pot, Three-Component Wittig Reaction: Optimization.....	66
3.3 One-Pot, Three-Component Wittig Reaction: Scope.....	68
3.4 Alkylation of C-6.....	69
3.5 Lewis Acid-Mediated Annulation: Optimization.....	70
3.6 Lewis Acid-Mediated Annulation: Scope.....	71
3.7 One-Pot, Tandem Wittig/Annulation Sequence.....	72
3.8 Application to Synthesis of Benzofurans and Benzothiophenes.....	73
3.9 Functional Group Transformations.....	74
3.10 Conclusions.....	75
3.11 Experimental.....	76
3.12 References.....	94

Chapter 4: One-Pot Synthesis of Highly Substituted N-Fused Heteroaromatic Bicycles from

Azole Aldehydes.....	97
4.1 Introduction.....	97
4.2 Design of Synthetic Route.....	98
4.3 Optimization of Method.....	100
4.4 Scope of Method.....	101
4.5 Dianionic Approach to C-6 Substituted Indolizines.....	103
4.6 Conclusions.....	104

4.7	Experimental.....	105
4.8	References.....	118
 Chapter 5: Summary and Conclusions.....		121
5.1	Obesity Epidemic.....	121
5.2	GPAT as a Therapeutic Target for Obesity.....	121
5.3	Second-Generation GPAT Inhibitors: Probing for an Active Site Hydrophobic Pocket.....	122
5.4	Development of Methodology to Access Substituted Indoles.....	124
5.5	Development of Methodology to Access Substituted <i>N</i> -Fused Heteroaromatic Bicycles.....	126
5.6	Conclusions.....	128
5.7	References.....	129

List of Figures, Schemes, and Tables

Chapter 1: Introduction to Current Antiobesity Therapeutics

Figure 1.1. Leading causes of death in the United States in 2010.....	1
Figure 1.2. Antiobesity drugs targeting the central nervous system.....	2
Figure 1.3. Lipolysis of TAG by pancreatic lipases and mechanism of inhibition by orlistat.....	5
Figure 1.4. Biosynthesis of fatty acids by FAS.....	7
Figure 1.5. Structure of FAS inhibitor cerulenin.....	7
Figure 1.6. Competition of GPAT and CPT1 for fatty acyl-CoAs: biosynthesis of TAG versus fatty acid oxidation.....	8
Figure 1.7. First generation GPAT inhibitors designed as mimics of enzymatic transition state.....	10

Chapter 2: Design, Synthesis and Evaluation of *o*-(Octanesulfonamido)benzoic Acids as Inhibitors of Glycerol-3-phosphate Acyltransferase

Figure 2.1. Structure of <i>o</i> -(alkanesulfonamido)benzoic acid GPAT inhibitors.....	16
Figure 2.2. Inhibitors 1c and 14b docked into the active site of squash GPAT.....	17
Figure 2.3. Inhibitor design for 4- and 5-substituted derivatives of 1c.....	18
Figure 2.4. Synthesis of GPAT inhibitor analogs.....	19
Table 2.1. GPAT Inhibition by 4- and 5-Substituted Derivatives.....	21
Figure 2.5. 4- and 5-substituted analogs with linkers: structures and IC ₅₀ data.....	22

Chapter 3: A Practical Route to Substituted 7-Aminoindoles from Pyrrole-3-carboxaldehydes

Figure 3.1. Design of heteroaromatic bicyclic inhibitors and general structure of indole scaffold.....	63
Figure 3.2. Prominent indole syntheses from benzenoid precursors.....	64
Figure 3.3. Tunable regioselectivity for electrophilic reactions of pyrroles.....	65
Figure 3.4. Proposed route to substituted 7-aminoindoles.....	66
Figure 3.5. Representative medicinal chemistry targets.....	66
Table 3.1. Optimization of Wittig Reaction with Aldehyde 1a.....	68
Table 3.2. Scope of Wittig Reaction.....	69
Table 3.3. Alkylation of Allylic Nitrile 3a.....	70
Table 3.4. Optimization of Cyclization to Indole 3a.....	71
Table 3.5. Scope of Indole Annulation.....	72
Figure 3.6. One-pot synthesis of indole 3a.....	73
Figure 3.7. Application to the synthesis of benzofuran and benzothiophene derivatives.....	73
Figure 3.8. Functional group conversion of 3a to precursors of medicinal chemistry targets.....	74

Chapter 4: One-Pot Synthesis of Highly Substituted *N*-Fused Heteroaromatic Bicycles from Azole Aldehydes

Figure 4.1. Design of GPAT inhibitors containing <i>N</i> -fused heteroaromatic bicycles.....	98
Figure 4.2. Proposed route to <i>N</i> -fused heterocycles.....	99
Table 4.1. Optimization of Reaction Conditions.....	101
Figure 4.3. Scope of one-pot annulation of azole aldehydes.....	102

Table 4.2. Tandem Alkylation/Cyclization Sequence.....	104
--	-----

Chapter 5: Summary and Conclusions

Figure 5.1. Structures and *in vitro* inhibitory data for *o*-(alkanesulfonamido)benzoic acids

1a-c.....	122
-----------	-----

Figure 5.2. (Octanesulfonamido)benzoic acid docked in GPAT and proposed inhibitor

analogs.....	123
--------------	-----

Figure 5.3. Hydrophobic- and chloro-substituted inhibitors with most potent activity.....124

Figure 5.4. Design of indole-based GPAT inhibitors and proposed synthetic intermediate....125

Figure 5.5. Synthesis of 2-, 3-, and 6-substituted 7-amino-5-cyanoindoles.....126

Figure 5.6. Design of *N*-fused heteroaromatic bicycles inhibitors of GPAT.....127

Figure 5.7. One-pot synthesis of *N*-fused heteroaromatic bicycles.....127

Figure 5.8. Tandem alkylation/cycloaromatization route to 6-substituted indolizines.....128

Chapter 1

Introduction to Current Antiobesity Therapeutics

1.1 Introduction

The incidence of obesity, defined as having a Body Mass Index (BMI) of 30.0 or higher, has been steadily increasing with approximately 400 million adults being affected worldwide. A recent study estimated that 68.0% of U.S. adults are overweight (BMI greater than 25.0) with 33.8% classified as obese at an annual cost approaching \$300 billion.¹ Obesity has been implicated in multiple diseases including heart disease^{2,3}, type 2 diabetes⁴, stroke⁵, nonalcoholic fatty liver disease⁴, infertility⁶, and certain types of cancer⁷. In fact, of the five leading causes of death in the U.S. in 2010, as shown in Fig. 1.1, four carried some association with obesity. Every year, obesity results in hundreds of thousands of lives lost and billions of dollars wasted, making pharmacological intervention for the disease an attractive option.

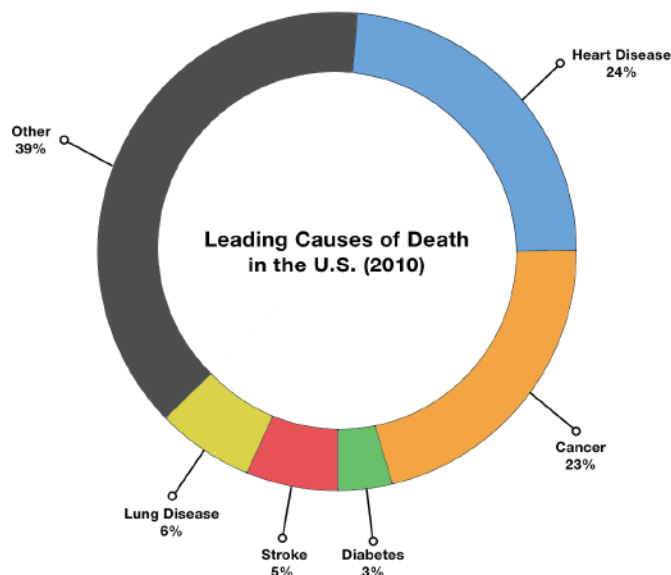


Figure 1.1 Leading causes of death in the United States in 2010

1.2 Antiobesity Therapies Targeting Food Intake (CNS)

Despite the rising demand for antiobesity therapeutics, few drugs have been cleared for clinical treatment (Fig. 1.2). The majority of these drugs target receptors in the central nervous system (CNS) and were originally studied for neurological disorders such as depression and drug dependence. For many of these centrally-acting drugs, antiobesity therapy was considered only after researchers observed anorectic side effects in clinical patients. As with many drugs targeting the CNS, several of these therapies have also been linked to severe side effects, leading to limited or discontinued clinical use.

Drugs Targeting Appetite (Central Nervous System)

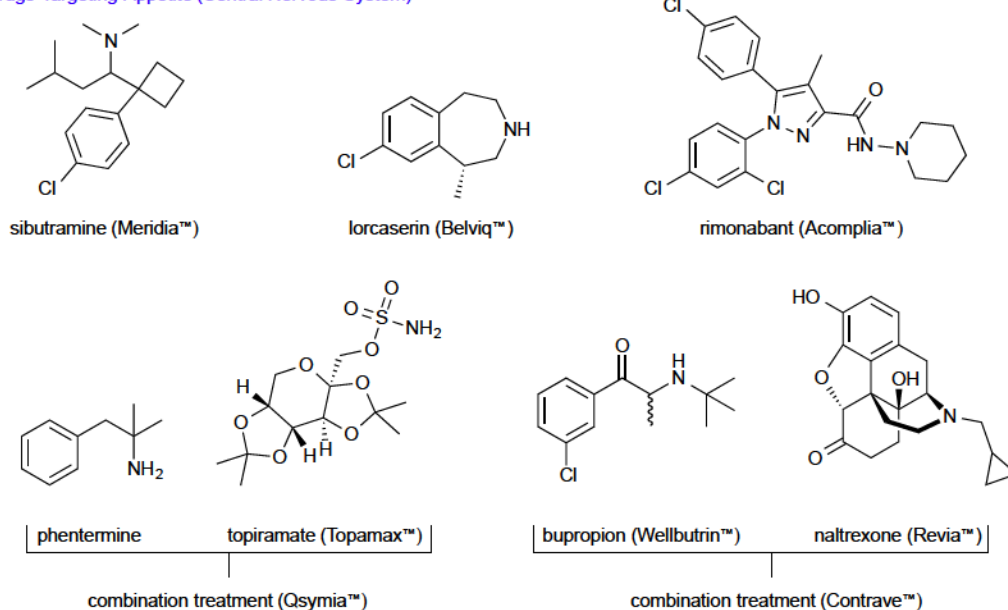


Figure 1.2 Antiobesity drugs targeting the central nervous system

Sibutramine acts as a serotonin-norepinephrine reuptake inhibitor (SNRI) and was originally tested as an antidepressant, but its ability to suppress appetite caused a reduction in food intake and led to weight loss in patients.⁸ It was approved for treatment of obesity in the U.S. in 1997. Following several reports of cardiovascular events such as strokes and heart attacks, however, it was withdrawn by Abbott Laboratories in 2010 under pressure from the FDA.^{9,10}

Lorcaserin, developed by Arena Pharmaceuticals, acts as a 5HT_{2C} receptor agonist.¹¹ While the cascading effects of the serotonergic activity are poorly understood, lorcaserin treatment resulted in an increase in anorectic activity and subsequent decrease in weight. Initial studies indicating increased tumor formation in rats led the FDA in 2010 to reject its approval for the treatment of obesity.¹² After additional studies, however, the FDA in 2012 approved lorcaserin for clinical use in restricted subsets of obese patients.¹³ Psychiatric dependency in patients led the drug to be categorized as a Schedule IV substance by the Drug Enforcement Agency in 2013.¹⁴

Rimonabant acts as an inverse agonist to the cannabinoid receptor CB₁ and was studied as a therapy for substance abuse for cocaine, marijuana, tobacco, and alcohol dependency.¹⁵ While tetrahydrocannabinol, the psychoactive component of marijuana, acts as a potential agonist of CB₁ leading to, among other effects, increased appetite, the inverse agonism of Rimonabant results in appetite suppression and weight loss.¹⁶ For this reason, Sanofi-Aventis won approval for Rimonabant as an antiobesity drug in the European Union in 2006. In the U.S., the FDA denied approval, citing increased psychiatric problems such as depression and suicidal thoughts.¹⁷ Because of these side effects, it was withdrawn from the European markets in 2009.

The combination therapy Qsymia™ includes the amphetamine derivative phentermine along with the anticonvulsant topiramate. Phentermine has shown previous weight loss effects when combined with fenfluramine, a combination popularly referred to as fen-phen.¹⁸ Fen-phen was withdrawn after being directly linked to fatal heart valve defects and pulmonary hypertension.¹⁹ Phentermine itself, however, has not yet been shown to have significant toxicity and, combined with topiramate, acts as an appetite suppressant. Qsymia™ was approved by the FDA in 2012 but has so far been denied approval by the European Union owing to increased cardiovascular risk.²⁰

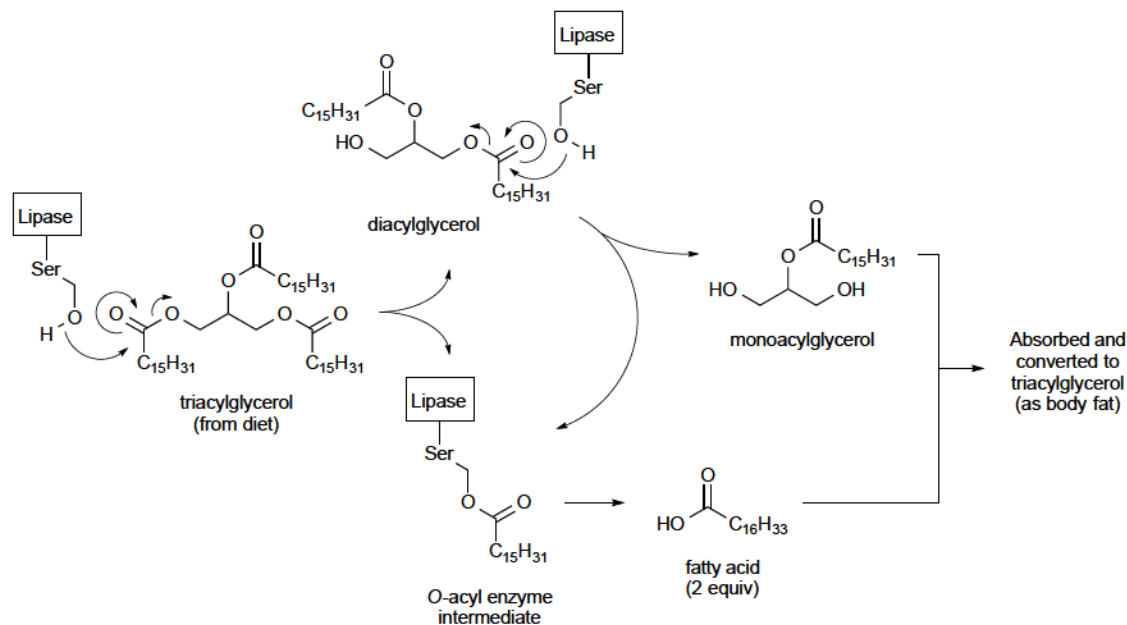
Finally, the combination therapy Contrave™ combines the opioid receptor antagonist naltrexone with the antidepressant bupropion to achieve a significant reduction in body weight.²¹ Both drugs have individually demonstrated anorectic activity and are believed to synergistically work to suppress appetite. The FDA approved the combination therapy for obesity in late 2014 along with boxed warnings of increased mood disorder and suicidal thoughts.²²

1.3 Antiobesity Therapies Targeting Biochemical Processes after Food Intake (Peripheral)

Compared to the plethora of antiobesity therapies targeting the CNS for appetite suppression, relatively few drugs have been developed that target the myriad biochemical processes that take place after food intake. Because these processes occur in the peripheral tissues, pharmacological intervention carries a lower risk of psychiatric side effects such as those observed in centrally-acting drugs. Orlistat, for example, is a saturated derivative of the natural product lipstatin and acts as a potent pancreatic lipase inhibitor.²³ Typically, triacylglycerol (TAG) from the diet, which itself is poorly absorbed, is hydrolyzed by pancreatic lipases into two equivalents of fatty acid and one equivalent of monoacylglycerol (MAG) which can be absorbed by enterocytes along the intestinal wall and eventually converted into body fat (Fig. 1.3A). The β -lactone of orlistat functions as an acylglycerol mimic and acylates the nucleophilic hydroxyl moiety on the catalytic serine of pancreatic lipases (Fig. 1.3B). This covalent inhibition prevents the breakdown of dietary TAG, decreasing the amount of fat absorbed and excreting the remaining fat in the stools. Patients treated with orlistat demonstrated 3.5% greater increase in weight loss compared with the placebo control after 1 year.²⁴ The weight loss in treated patients correlated with a mild decrease in incidence of type-2 diabetes and a reduction in blood

pressure levels.^{25, 26} While orlistat is moderately effective as a weight loss therapeutic, the unabsorbed dietary fat causes undesirable side effects such as steatorrhea and fecal incontinence. Also, the fat-soluble vitamins A, D, E, and K bind to and are excreted with the unabsorbed dietary fat necessitating additional vitamin supplementation.²⁷

A) Mechanism for Pancreatic Lipolysis of Dietary Triacylglycerol



B) Mechanism of Lipase Inhibition by Orlistat

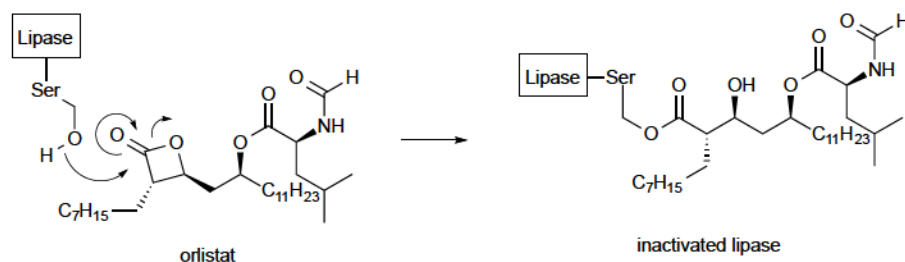


Figure 1.3 A) Lipolysis of TAG by pancreatic lipases; B) Mechanism of lipase inhibition by orlistat

Another therapeutic approach to obesity involves exploiting the enzymatic mechanisms of fatty acid biosynthesis. Fatty acid synthase (FAS) in humans is a large, multi-domainal protein responsible for catalyzing the biosynthesis of long chain fatty acids, such as palmitate, from acetyl-CoA and malonyl-CoA substrates. Eight distinct domains, shown in Fig. 1.4, exist within

its structure including the acyl carrier protein (ACP), acetyl-CoA:ACP transacylase (AT), malonyl-CoA:ACP transacylase (MAT), β -ketoacyl:ACP synthase (KS), β -ketoacyl:ACP reductase (KR), β -hydroxyacyl:ACP dehydratase (DH), enoyl:ACP reductase (ER), and acyl:ACP thioesterase domains. Fatty acid biosynthesis commences by transthioesterification of acetyl-CoA onto the ACP phosphopantetheine arm catalyzed by the AT domain, followed by trans-thioesterification to load the acetyl group onto the active site cysteine of the KS domain. Malonyl-CoA is then loaded onto the ACP phosphopantetheine arm catalyzed by the MAT domain, and a decarboxylative Claisen condensation occurs to form a β -ketoacyl:ACP intermediate. NADPH-dependent reduction of the β -ketone is then catalyzed by the KR domain to afford a β -hydroxyacyl:ACP intermediate, which undergoes dehydration catalyzed by the DH domain. The resulting ACP-bound α , β -unsaturated thioester undergoes another NADPH-dependent reduction, catalyzed by the ER domain, to give the fully saturated C₄ intermediate. This intermediate is loaded back onto the KS and the four-step chain extension/reduction/dehydration/reduction sequence is repeated until a C₁₆ saturated fatty acyl:ACP intermediate is formed. Finally, the TE domain catalyzes the hydrolysis of this intermediate to release the free fatty acid palmitate.

Because FAS is the enzyme responsible for the *de novo* biosynthesis of fatty acids, its domains have attracted interest as targets for antiobesity drugs. Cerulenin (Fig. 1.5), for example, is a natural product isolated from *Cephalosporium caerulens* that binds to the KS domain of FAS, preventing chain extension and inhibiting fatty acid synthesis.^{28,29} Researchers reported up to 30% weight loss in mice treated with 60 mg/kg/day of cerulenin after 1 week.³⁰ The lost weight was recovered upon cessation of treatment with no reported toxicity.

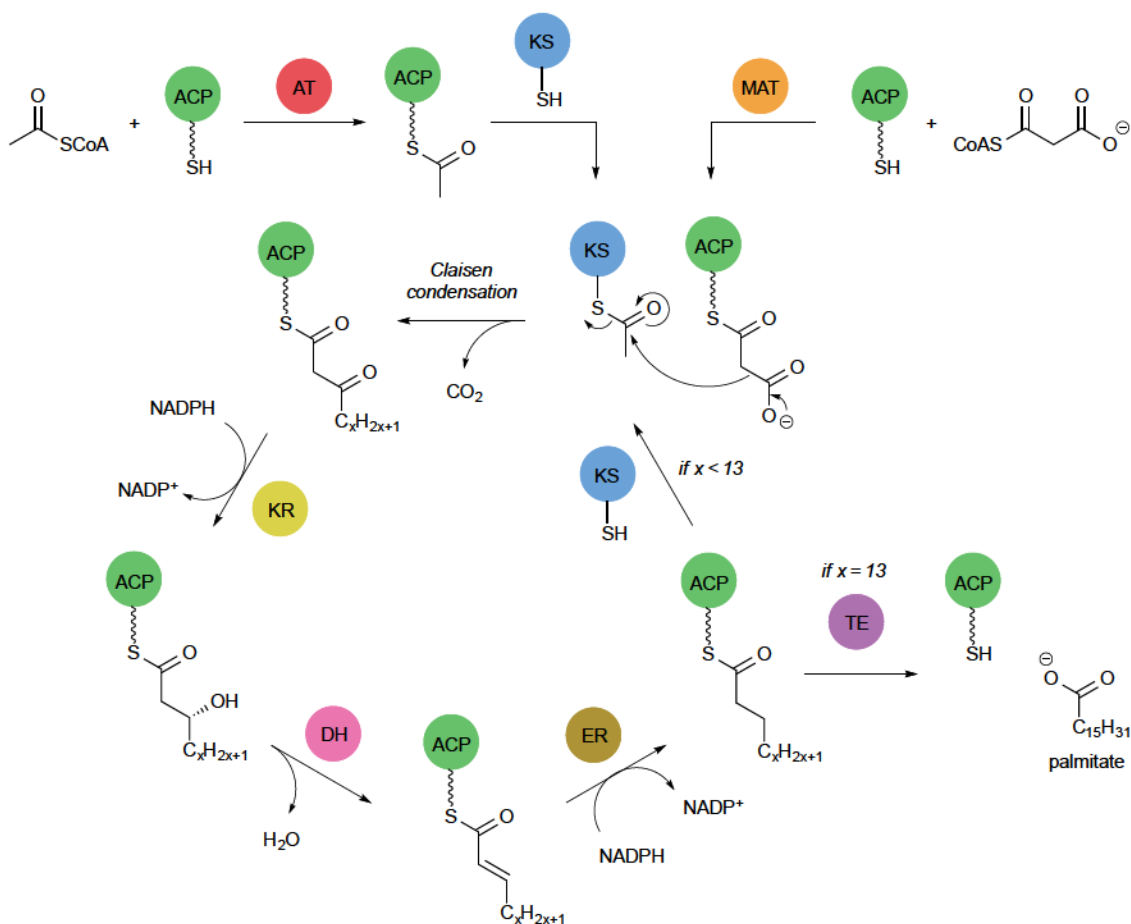


Figure 1.4 Biosynthesis of fatty acids by FAS

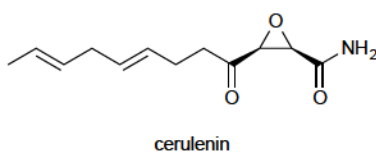


Figure 1.5 Structure of FAS inhibitor cerulenin

1.4 Glycerol-3-Phosphate Acyltransferase as an Antiobesity Drug Target

The lipolysis of dietary TAG and biosynthesis of fatty acids from acetyl- and malonyl-CoA are only two steps along the complex pathway to convert food to TAG. While disruption of any of these processes could, theoretically, prevent the formation of body fat, in reality, negative feedback loops often prevent sustained weight loss. One potential method of overcoming this negative feedback loop is to exploit both the TAG biosynthesis and fatty acid oxidation

pathways simultaneously, thereby affecting the metabolic profile. Glycerol-3-phosphate acyltransferase (GPAT) is a promising target for this approach.

Glycerol-3-phosphate acyltransferase (GPAT) catalyzes the transesterification of long chain fatty acyl-CoAs with the primary hydroxyl group of glycerol-3-phosphate (G3P) to form lysophosphatidic acid (LPA), the acylglycerol-3-phosphate shown in Fig. 1.6. This represents the first committed and rate-limiting step in the biosynthesis of TAG.³¹ An acylglycerol-3-phosphate acyltransferase (AGPAT) then catalyzes a second transesterification of fatty acyl-CoA onto the secondary hydroxyl group of LPA to afford the diacylglycerol-3-phosphate phosphatidic acid (PA). Dephosphorylation of PA, promoted by lipid phosphate phosphohydrolase (LPP), produces diacylglycerol (DAG), which undergoes a third acylation, catalyzed by diglyceride acyltransferase (DGAT) to produce TAG which can be stored as body fat.

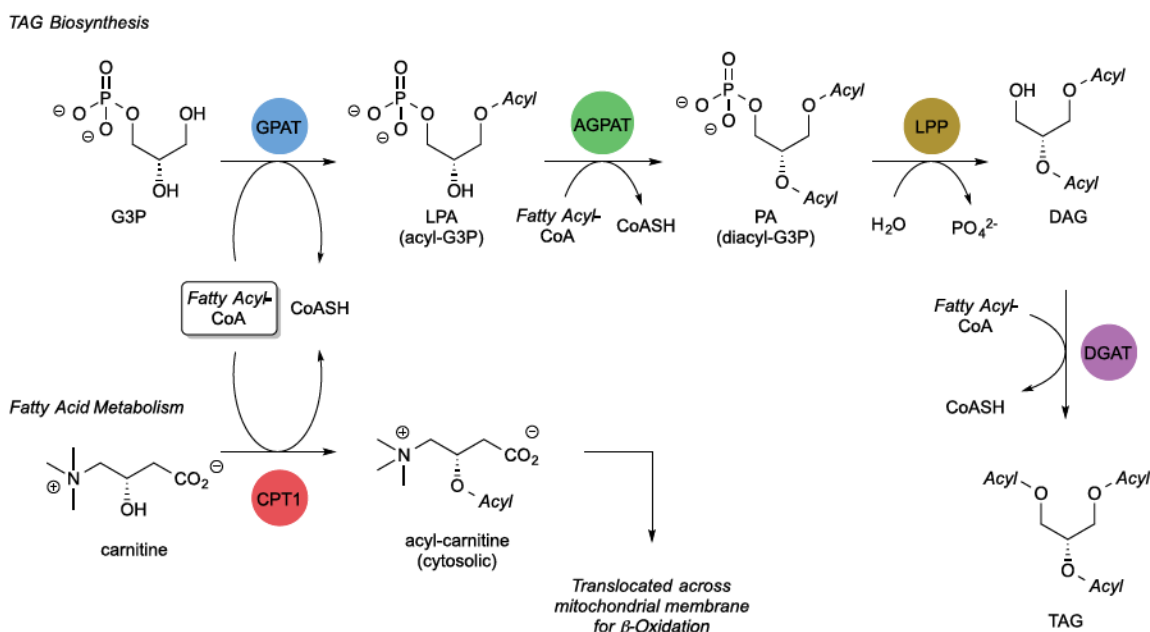


Figure 1.6 Competition of GPAT and CPT1 for fatty acyl-CoAs: biosynthesis of TAG versus fatty acid oxidation

The activity of GPAT appears to be coupled to the activity of carnitine palmitoyltransferase-1 (CPT1), the enzyme responsible for the rate-limiting step in the β -oxidation of fatty acids. CPT1 catalyzes the acylation of carnitine with long chain fatty acyl CoAs. The acylated carnitine product is then able to diffuse across the outer mitochondrial membrane where it is translocated by carnitine-acylcarnitine translocase (CACT) into the mitochondrial matrix, and the fatty acid eventually undergoes β -oxidation. GPAT and CPT1 are colocated on the outer mitochondrial membrane and compete for fatty acyl-CoA substrates.³² For example, GPAT overexpression in rat hepatocytes showed an 80% decrease in the rate of fatty acid oxidation accompanied by an increase in glycerolipid synthesis.³³ Conversely, when GPAT-knockout mice were fed a high-fat, high-sugar diet to induce obesity, elevated rates of fatty acid oxidation were observed.³⁴ These findings suggest that GPAT appears to play a major role in the partitioning of fatty acyl-CoA substrates between the glycerolipid biosynthesis and β -oxidation pathways. The decreased production of TAG and concomitant increase in β -oxidation accompanying lower GPAT activity make the enzyme an attractive target for antiobesity therapy. Inhibition of GPAT by a small molecule inhibitor has the potential to limit *de novo* synthesis of TAG while shuttling existing fatty acyl-CoA stores toward CPT1-mediated fat oxidation.

Recent work in our lab has involved the development of small molecule inhibitors of GPAT.³⁵ The initial class of inhibitors was rationally designed to mimic the enzymatic transition state (Fig. 1.7). The benzoic and phosphonic acid moieties of these compounds, which are deprotonated at physiological pH, were chosen to mimic the anionic phosphate group of the native substrate. The sulfonamide was chosen to mimic both the geometry of the tetrahedral intermediate and the charge density of the oxyanion. The relatively acidic aryl sulfonamide hydrogen is proposed to interact with the catalytic histidine responsible for deprotonating the

primary hydroxyl group of G3P prior to acylation. Finally, the long alkyl chain of the sulfonamide was designed to bind the lipophilic palmitoyl-CoA binding site.

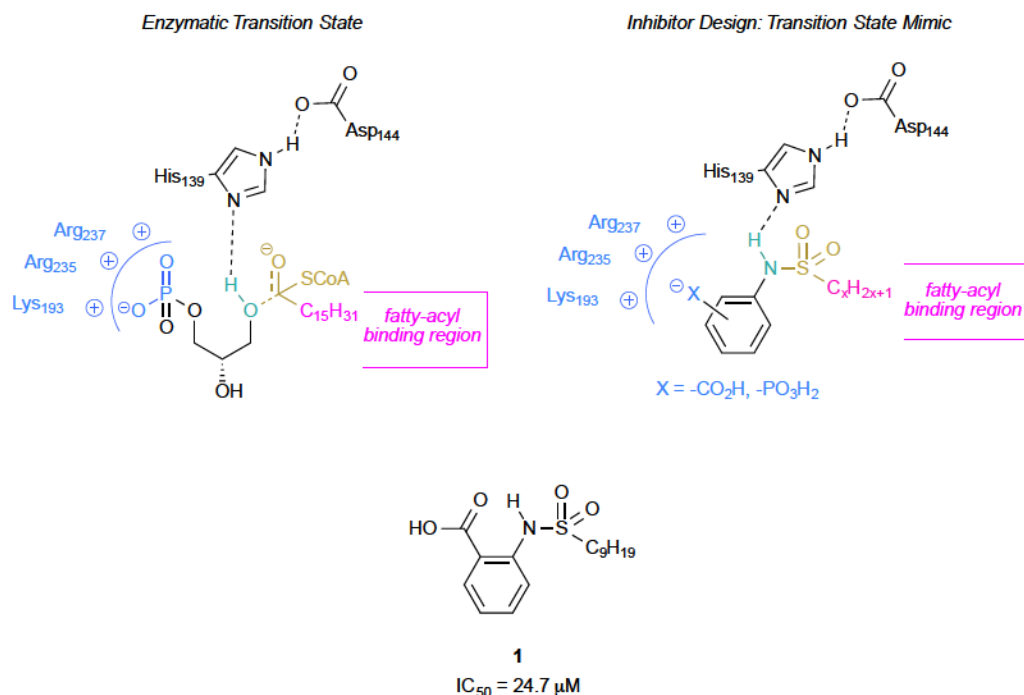


Figure 1.7 First generation GPAT inhibitors designed as mimics of enzymatic transition state

Of the compounds tested, *o*-substituted alkylsulfonamidobenzoic acids were the most active against GPAT *in vitro*. One compound, nonyl derivative **1**, possessed a modest inhibitory activity of $24.7 \pm 2.1 \mu M$ against GPAT *in vitro* and was chosen for further testing *in vivo*.³⁶ Diet-induced obese (DIO) mice injected with 5 mg/kg/d of **1** over nine days showed a $12.1 \pm 3.6\%$ decline in weight compared with the vehicle control. After cessation of treatment on day 9, the treated mice maintained a weight loss of 15.6-17.6% for the remainder of the 15-day study. The study concluded that compound **1**, in addition to the inhibition of GPAT, caused a change to the metabolic profile that allowed for significant and sustained weight loss. This observation justifies both GPAT as a target and the sulfonamidobenzoic acid transition state mimic approach for the development of antiobesity therapeutics.

1.5 Summary

Obesity and obesity-related diseases are a growing global epidemic with huge medical and economic costs. Existing methods of combating obesity have demonstrated limited efficacies while being plagued by severe side effects. By limiting *de novo* biosynthesis of TAG, inhibition of GPAT offers a new mechanistic strategy for combating the accumulation of body fat. Modest inhibition of GPAT has been shown to drastically alter the metabolic profile away from fat synthesis and toward fat metabolism, thereby demonstrating the therapeutic potential of this approach. More potent GPAT inhibitors may give us better insight into the biological processes involved and serve as therapeutic agents against obesity and related metabolic disorders.

1.6 Thesis Goals

The primary goal of this thesis is to rationally design and synthesize more potent inhibitors of GPAT for the treatment of obesity. Inhibitors containing a sulfonamidobenzoic acid motif have shown promising weight loss in mouse models despite only moderate activity *in vitro*. We would like to build from this scaffold to develop a structure-activity relationship (SAR) of the inhibitors with GPAT. SAR analysis could then aid in the drug design of future classes of inhibitors and lead to increased potency. More potent inhibitors would, in turn, promote higher fat reduction as part of a viable obesity therapy.

1.7 References

1. Flegal, K.M., Carroll, M.D., Ogden, C.L., Curtin, L.R. *J. Am. Chem. Assoc.* **2010**, 303, 235-241.
2. Poirier, P., Giles, T.D., Bray, G.A. *Arterioscler. Thromb. Vasc. Biol.* **2006**, 26, 968–976.
3. Yusuf, S., Hawken, S., Ounpuu, S. *Lancet* **2004**, 364, 937–952.

4. Haslam, D.W., James, W.P. *Lancet*, **2005**, 366, 1197–1209.
5. Hall, J.E. *Hypertension* **2003**, 41, 625–633.
6. Hammoud, A.O., Gibson, M., Peterson, C.M., Meikle, A.W., Carrell, D.T. *Fertil. Steril.* **2008**, 90, 897–904.
7. Calle, E.E., Rodriguez, C., Walker-Thurmond, K., Thun, M.J. *N. Engl. J. Med.* **2003**, 348, 1625–1638.
8. Nisoli, E.; Carruba, M. O. *Obesity Reviews* **2000**, 1, 127–139.
9. U.S. Food and Drug Administration. *Early Communication about an Ongoing Safety Review of Meridia (sibutramine hydrochloride)*. Washington, DC, United States. 2009.
10. U.S. Food and Drug Administration. *Meridia (sibutramine hydrochloride): Follow-Up to an Early Communication about an Ongoing Safety Review*. Washington, DC, United States. 2010.
11. Thomsen, W. J.; Grottick, A. J.; Menzaghi, F.; Reyes-Saldana, H.; Espitia, S.; Yuskin, D.; Whelan, K.; Martin, M.; Morgan, M.; Chen, W.; Al-Shamma, H.; Smith, B.; Chalmers, D.; Behan, D. (2008). *J. Pharmacol. Exp. Ther.* **2008**, 325, 577–587.
12. U.S. Food and Drug Administration. *FDA Briefing Information, LORQESS (Lorcaserin Hydrochloride) Tablets, for the September 16, 2010 Meeting of the Endocrinologic and Metabolic Drugs Advisory Committee*. Washington, DC, United States. 2010.
13. U.S. Food and Drug Administration. *FDA approves Belviq to treat some overweight or obese adults*. Washington, DC, United States. 2012.
14. U.S. Drug Enforcement Agency. *Schedules of Controlled Substances: Placement of Lorcaserin into Schedule IV*. Washington, DC, United States. 2013.
15. Maldonado, R.; Valverde, O.; Berrendero, F. "Involvement of the endocannabinoid system in drug addiction". *Trends Neurosci.* **2006**, 29, 225-232.

16. Pi-Sunyer, F. X.; Aronne, L. J.; Heshmati, H. M.; Devin, J.; Rosenstock, J. J. *Am. Med. Assoc.* **2006**, 295, 761-75.
17. Vinod, K. Y.; Hungund, B. L. *Trends Pharmacol. Sci.* **2006**, 27, 539-545.
18. Weintraub, M.; Hasday, J. D.; Mushlin, A. I.; Lockwood, D. H. (1984). *Arch. Intern. Med.* **144**, 6, 1143-1148.
19. Connolly, H. M.; Crary, J. L.; McGoon, M. D.; Hensrud, D. D.; Edwards, B. S.; Edwards, W. D.; Schaff, H. V. *New Engl. J. Med.* **1997**, 337, 581–588.
20. European Medical Agency. *Refusal of the marketing authorisation for Qsiva (phentermine / topiramate)*. London, United Kindgom. 2013.
21. Greenway, F.L.; Fujioka, K.; Plodkowskie, R.A.; Mudaliar, S.; Guttadauria, M.; Erickson, J.; Kim, D.D.; Dunayevich, E. *Lancet* **2010**, 376, 595-605.
22. U.S. Food and Drug Administration. *FDA approves weight-management drug Contrave*. Washington, D.C., United States. 2014.
23. Lucas, K. H.; Kaplan-Machlis, B. *Ann. Pharmacother.* **2001**, 35, 314-328.
24. Foxcroft, D. R. *Obes. Rev.* **2005**, 6, 323–328.
25. Torgerson, J. S.; Hauptman, J.; Boldrin, M. N.; Sjöström, L. *Diabetes Care* **2004**, 27, 155–161.
26. Siebenhofer, A.; Jeitler, K.; Horvath, K.; Berghold, A.; Siering, U.; Semlitsch, T. *Cochrane Database Syst. Rev.* **2013**, 3, CD007654.
27. McDuffie, J. R.; Calis, K. A.; Booth, S. L.; Uwaifo, G. I.; Yanovski, J. A. *Pharmacotherapy* **2002**, 22, 814–822.
28. Nomura, S.; Horiuchi, T.; Omura, S.; Hata, T. *J. Biochem.* **1972**, 71, 783–796.

29. Vance, D.; Goldberg, I.; Mitsuhashi, O.; Bloch, K.; Ōmura, S.; Nomura, S. *Biochem. Biophys. Res. Comm.* **1972**, *48*, 649–656.
30. Loftus, T. M.; Jaworsky, D. E.; Frehywot, G. L.; Townsend, C. A.; Ronnett, G. V.; Lane, M. D.; Kuhajda, F. P. *Science* **2000**, *288*, 2379–2381.
31. Coleman, R. A.; Lewin, T. M.; Muoio, D. M. *Annu. Rev. Nutr.* **1998**, *18*, 331–351.
32. Van der Leij, F. R.; Kram, A. M.; Bartelds, B.; Roelofsen, H.; Smid, G. B.; Takens, J.; Zammit, V. A.; Kuipers, J. R. G. *Biochem. J.* **1999**, *341*, 777–784.
33. Lindén, D.; William-Olsson, L.; Ahnmark, A.; Ekroos, K.; Hallberg, C.; Sjögren, H. P.; Becker, B.; Svensson, L.; Clapham, J. C.; Oscarsson, J.; Schreyer, S. *FASEB J.* **2006**, *20*, 434–443.
34. Hammond, L. E.; Neschen, S.; Romanelli, A. J.; Cline, G. W.; Ilkayeva, O. R.; Shulman, G. I.; Muoio, D. M.; Coleman, R. A. *J. Biol. Chem.* **2005**, *280*, 25629–25636.
35. Wydysh, E. A.; Medghalchi, S. M.; Vadlamudi, A.; Townsend, C. A. *J. Med. Chem.* **2009**, *52*, 3317–3327.
36. Kuhajda, F. P.; Aja, S.; Tu, Y.; Han, W. F.; Medghalchi, S. M.; Meskini, El, R.; Landree, L. E.; Peterson, J. M.; Daniels, K.; Wong, K.; Wydysh, E. A.; Townsend, C. A.; Ronnett, G. V. *Am. J. Physiol. Regul. Integr. Comp. Physiol.* **2011**, *301*, R116–R130.

Chapter 2

Design, Synthesis, and Evaluation of *o*-(Octanesulfonamido)benzoic Acids as Inhibitors of Glycerol-3-phosphate Acyltransferase

2.1 Introduction

Obesity, defined as having a Body Mass Index (BMI) of 30.0 or higher, has been implicated in multiple diseases, including cardiovascular disease¹, type-2 diabetes², hypertension, nonalcoholic fatty liver disease³, infertility⁴, and certain types of cancer.⁵ According to the World Health Organization, it affects approximately 500 million adults and is the fifth leading risk of deaths globally, accounting for at least 2.8 million deaths a year. Despite an increase in obesity and obesity-related diseases, few effective pharmacological therapies currently exist to combat the physiological source of obesity, the accumulation of triacylglycerol (TAG). One approach involves exploiting the mechanisms of the lipid metabolic pathway, either by decreasing the rate of fat synthesis, as shown with the small molecule fatty acid synthase (FAS) inhibitors C75⁶ and cerulenin⁷, or increasing the rate of fatty acid oxidation.⁸ GPAT catalyzes the transesterification of fatty acyl-CoAs with the primary hydroxyl group of glycerol-3-phosphate (G3P), the first committed and rate-limiting step in the biosynthesis of TAG.⁹ In mammals, mitochondrial GPAT (mtGPAT) is an integral membrane protein that co-localizes on the mitochondrion with carnitine-palmitoyl transferase I (CPT1), the rate-limiting enzyme in β -oxidation. These enzymes are co-regulated and compete for fatty acyl-CoA substrates.¹⁰ Inhibition of GPAT by a small molecule inhibitor has the potential to reduce *de novo* synthesis of TAG and to divert the

flux of fatty acyl-CoAs to β -oxidation mediated by CPT1, thus making GPAT an attractive therapeutic target against obesity.

2.2 Inhibitor Design and Molecular Modeling

Recently, it has been demonstrated that *o*-(alkanesulfonamido)benzoic acids such as **1a-b** (Fig. 2.1) possess moderate inhibitory activity against mammalian GPAT *in vitro*.¹¹ The 8-carbon derivative **1c** has also been synthesized and exhibits an inhibitory activity comparable to **1b**. The benzoic acid moiety of these compounds, which is deprotonated at physiological pH, is believed to mimic the anionic phosphate group of the native substrate. The acidic aryl sulfonamide proton is proposed to interact with the catalytic histidine responsible for deprotonating the primary hydroxyl group of G3P necessary for acylation. Finally, the long alkyl chain of the sulfonamide was designed to bind the lipophilic palmitoyl-CoA binding site.

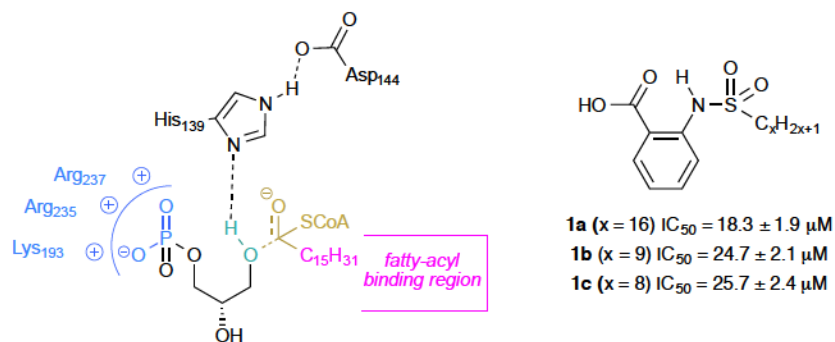


Figure 2.1 Structure of *o*-(alkanesulfonamido)benzoic acid GPAT inhibitors

While structural information regarding mammalian GPAT is limited, X-ray crystal structures of squash GPAT revealed the conserved catalytic HXXXXD motif present in all GPATs as well as a putative G3P binding site comprised of conserved cationic residues Lys193, Arg235, and Arg237.^{12a-b} A complex network of relatively hydrophobic pockets and tunnels emanating from the active site was also observed. Protein homology-based modeling of multiple human

acyltransferases, including AGPAT1, AGPAT2, and AGPAT9, with the squash GPAT crystal structure showed that, despite low sequence homology, the human enzymes are similar in predicted secondary structure and hydrophobic residue distribution.¹³ These findings suggest that, although the primary sequences of the acyltransferase homologs differ, the architectures of the active sites may be quite similar. An *in silico* docking simulation of **1c** with squash GPAT, as shown in Fig. 2.2, displayed the inhibitor bound at the putative G3P binding pocket with the carboxylate anion positioned at the phosphate binding site and the long alkyl chain residing in the putative palmitoyl-CoA binding site described by Turnbull et al.^{12a} Furthermore, the docking model showed a second hydrophobic tunnel, described previously by Tamada et al.,^{12b} extending away from the G3P binding site and presenting from C-4 and C-5 of the benzoic acid ring of the docked inhibitor. This volume was lined by hydrophobic and aromatic residues including Phe98, Gly99, Tyr102, Ile103, Ala143, Leu176, Pro179, and Phe180.

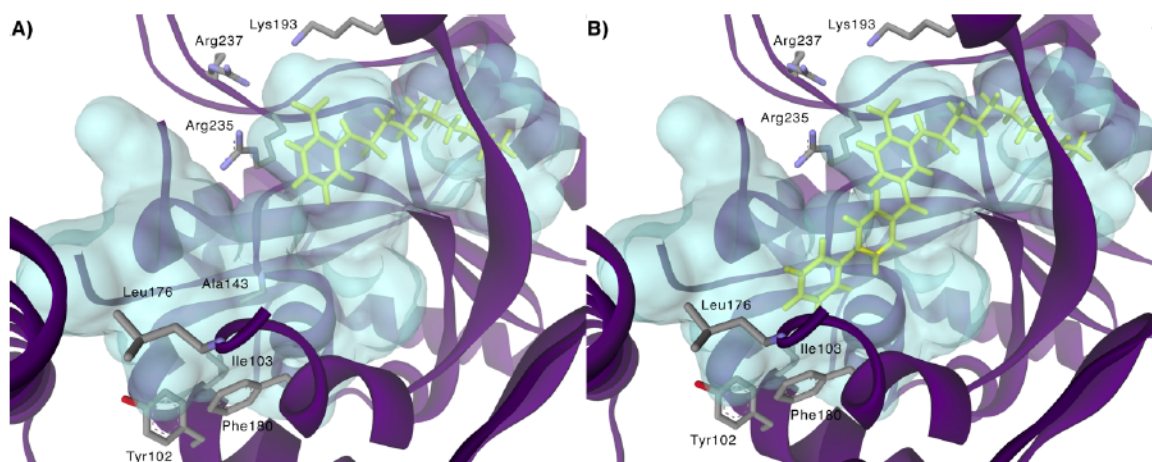


Figure 2.2 A) Compound **1c** (yellow) docked into the active site of squash GPAT; B) Compound **14b** manually docked into the binding site obtained for compound **1c**

In an attempt to improve upon the inhibitory activity of **1c**, a series of potential inhibitors, shown in Fig. 2.3, was designed and synthesized with various aryl substituents either directly-bound to the 4- or 5-positions of **1c** or coupled via one of several linkers (keto-, vinyl-, or ethyl-).

The aryl substituents were chosen to promote π -stacking with the aromatic residues in the potential hydrophobic channel as well as for synthetic accessibility. The linkers were chosen to examine the effects of pharmacophore separation and conformational rigidity versus flexibility. The 8-carbon chain of **1c** was chosen for its ready commercial availability and, within experimental error, essentially unchanged GPAT inhibitory activity compared to the 9-carbon analog reported previously.¹¹ The candidates were tested for GPAT inhibition *in vitro* to develop a structure-activity relationship and assess the validity of the docking model as a tool to direct future medicinal chemistry efforts.

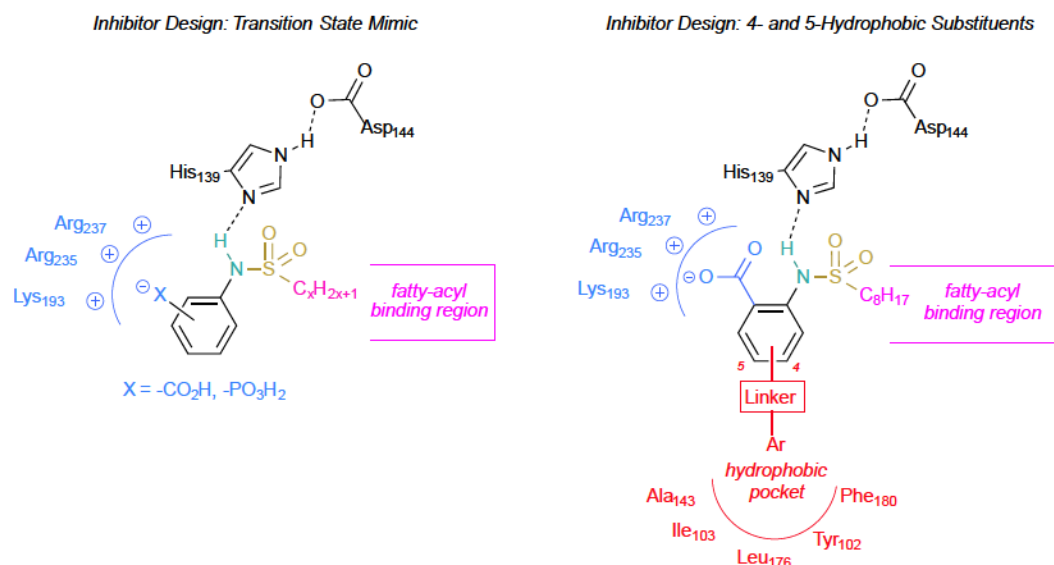


Figure 2.3 Inhibitor design for 4- and 5-substituted derivatives of **1c**

2.3 Synthesis of 4- and 5-Substituted Analogs

An efficient, divergent route was devised to access the 4- and 5-substituted derivatives of **1c** as shown in Fig. 2.4. Sulfonamide coupling of 4- and 5-bromoanthranilates **2** and **3**, respectively, with octanesulfonyl chloride generated sulfonamides **4** and **5**. Suzuki-Miyaura coupling reactions with various aryl boronic acids were then performed either under argon to afford coupling products **6a-l** and **7a-l** or under an atmosphere of carbon monoxide to afford keto-

linker precursors **8a-b** and **9a-d**. Alternatively, coupling of **4** and **5** with various *trans*-arylvinyl boronic acids under an argon atmosphere provided vinyl-linker precursors **10a-b** and **11a-b**. Each of the benzoates was then hydrolyzed, either under Gassman conditions¹⁴ or in aqueous 1 M NaOH, to afford analogs **12a-l**, **13a-l**, **14a-b**, **15a-d**, **16a-b**, and **17a-b**. Alternatively, hydrogenation of **10a-b** and **11a-b** prior to hydrolysis afforded ethyl-linked analogs **18a-b** and **19a-b**.

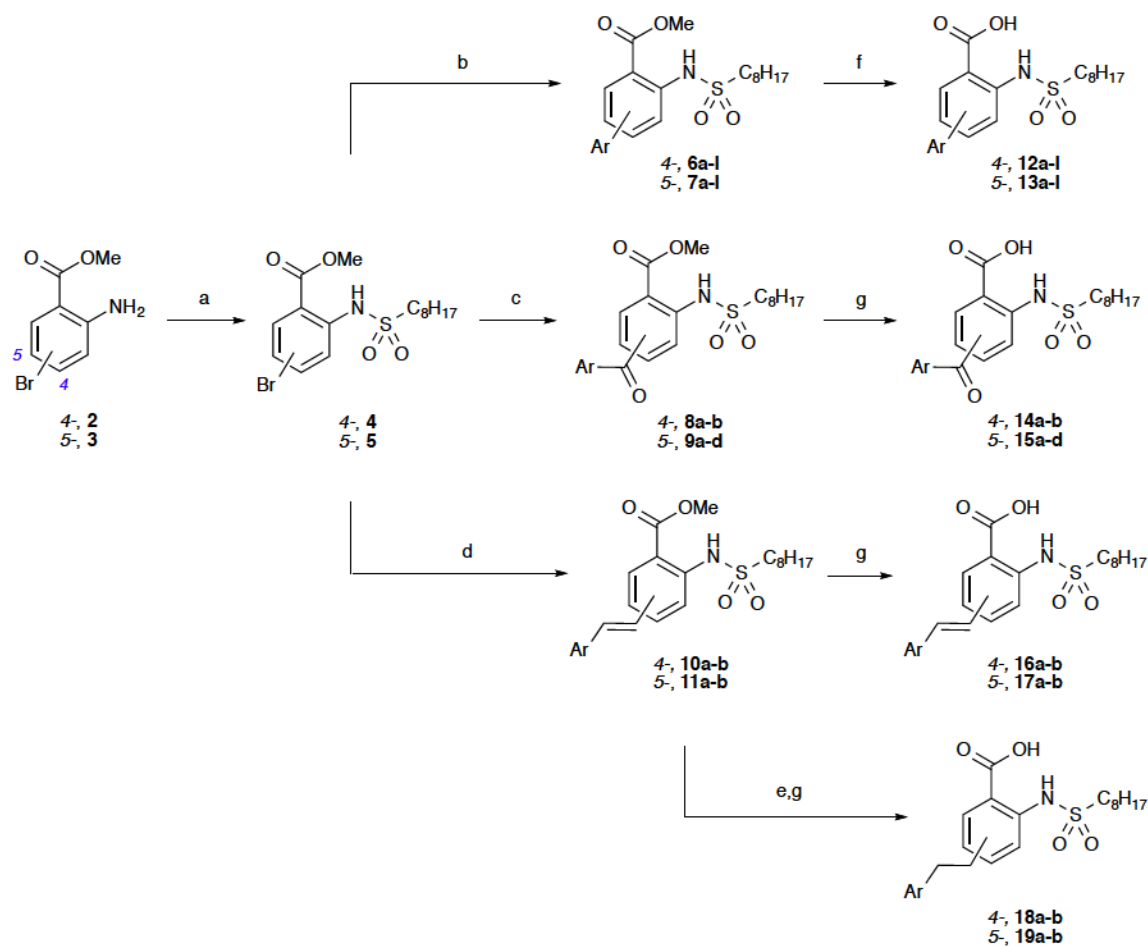


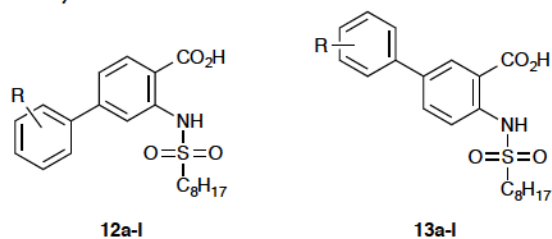
Figure 2.4 Synthesis of GPAT inhibitor analogs. Reagents and conditions: (a) $\text{ClSO}_2\text{C}_8\text{H}_{17}$, NEt_3 , CH_2Cl_2 , 62–76%; (b) $\text{Pd(PPh}_3)_4$, Ar-B(OH)_2 , Na_2CO_3 , PhMe/MeOH , 90°C , 45–80%; (c) $\text{Pd(PPh}_3)_4$, Ar-B(OH)_2 , K_2CO_3 , dioxane, 90°C , CO (1 atm), 28–46%; (d) $\text{Pd(PPh}_3)_4$, $(E)\text{-Ar-(CH}_2)_2\text{B(OH)}_2$, K_2CO_3 , PhCH_3 , 105°C , 58–83%; (e) Pd/C , H_2 (1 atm), MeOH , 80–91%; (f) KOtBu , H_2O , Et_2O , 0°C –r.t., 71–94%; (g) 1 M NaOH, THF, 40°C , 73–92%

2.4 Inhibition Data

The inhibitory data for the 4- and 5-aryl-substituted analogs are presented in Table 2.1. Several of these compounds exhibited marked improvement over **1c**. In general, hydrophobic substituents such as *p*-*n*-butylphenyl (**12d**), biphenyl (**12e,f**), and methoxyphenyl (**12g,h**) exhibited a moderate increase in inhibitory activity of up to two-fold. Chlorophenyl analogs (**12a-c**) also demonstrated markedly more potent inhibition, particularly the *m*-chloro analog which also was about 2-fold more active than **1c**. Conversely, hydroxyl- and fluoro-containing analogs (**12i-l**) caused a modest decrease in inhibitory activity. The *p*-hydroxyl analog, for instance, showed a nearly three-fold decline in inhibition.

The structure-activity relationship of 5-aryl-substituted class mirrors that of the 4-aryl derivatives. For instance, several of the compounds showed notable improvement over **1c**, particularly those containing chlorophenyl and hydrophobic substituents. Specifically, both the *m*-chloro (**13b**) and *p*-*n*-butyl (**13d**) analogs effected a 2.9-fold increase in inhibitory activity. Also similar to the 4-aryl class, hydroxyphenyl and fluorophenyl groups were not well tolerated, decreasing inhibition by nearly three-fold.

Table 2.1 GPAT Inhibition by 4- and 5-Substituted Derivatives



Entry	Compound	R	IC ₅₀ (μM) ± SD
1	12a	<i>o</i> -Cl	26.9 ± 4.1
2	12b	<i>m</i> -Cl	13.8 ± 2.5
3	12c	<i>p</i> -Cl	18.1 ± 3.5
4	12d	<i>p</i> - <i>n</i> -C ₄ H ₉	15.7 ± 1.6
5	12e	<i>o</i> -C ₆ H ₅	17.1 ± 0.8
6	12f	<i>p</i> -C ₆ H ₅	13.5 ± 3.2
7	12g	<i>o</i> -OCH ₃	16.1 ± 0.5
8	12h	<i>p</i> -OCH ₃	13.3 ± 1.1
9	12i	<i>o</i> -F	47.2 ± 2.0
10	12j	<i>m</i> -F	32.6 ± 3.6
11	12k	<i>o</i> -OH	63.1 ± 5.5
12	12l	<i>p</i> -OH	64.8 ± 3.8
13	13a	<i>o</i> -Cl	14.4 ± 1.3
14	13b	<i>m</i> -Cl	8.9 ± 0.9
15	13c	<i>p</i> -Cl	9.2 ± 0.7
16	13d	<i>p</i> - <i>n</i> -C ₄ H ₉	9.0 ± 0.4
17	13e	<i>o</i> -C ₆ H ₅	10.1 ± 0.7
18	13f	<i>p</i> -C ₆ H ₅	29.1 ± 6.3
19	13g	<i>o</i> -OCH ₃	27.6 ± 2.0
20	13h	<i>p</i> -OCH ₃	19.5 ± 5.5
21	13i	<i>o</i> -F	34.6 ± 2.0
22	13j	<i>m</i> -F	37.6 ± 9.7
23	13k	<i>o</i> -OH	61.7 ± 13.8
24	13l	<i>p</i> -OH	47.3 ± 6.4

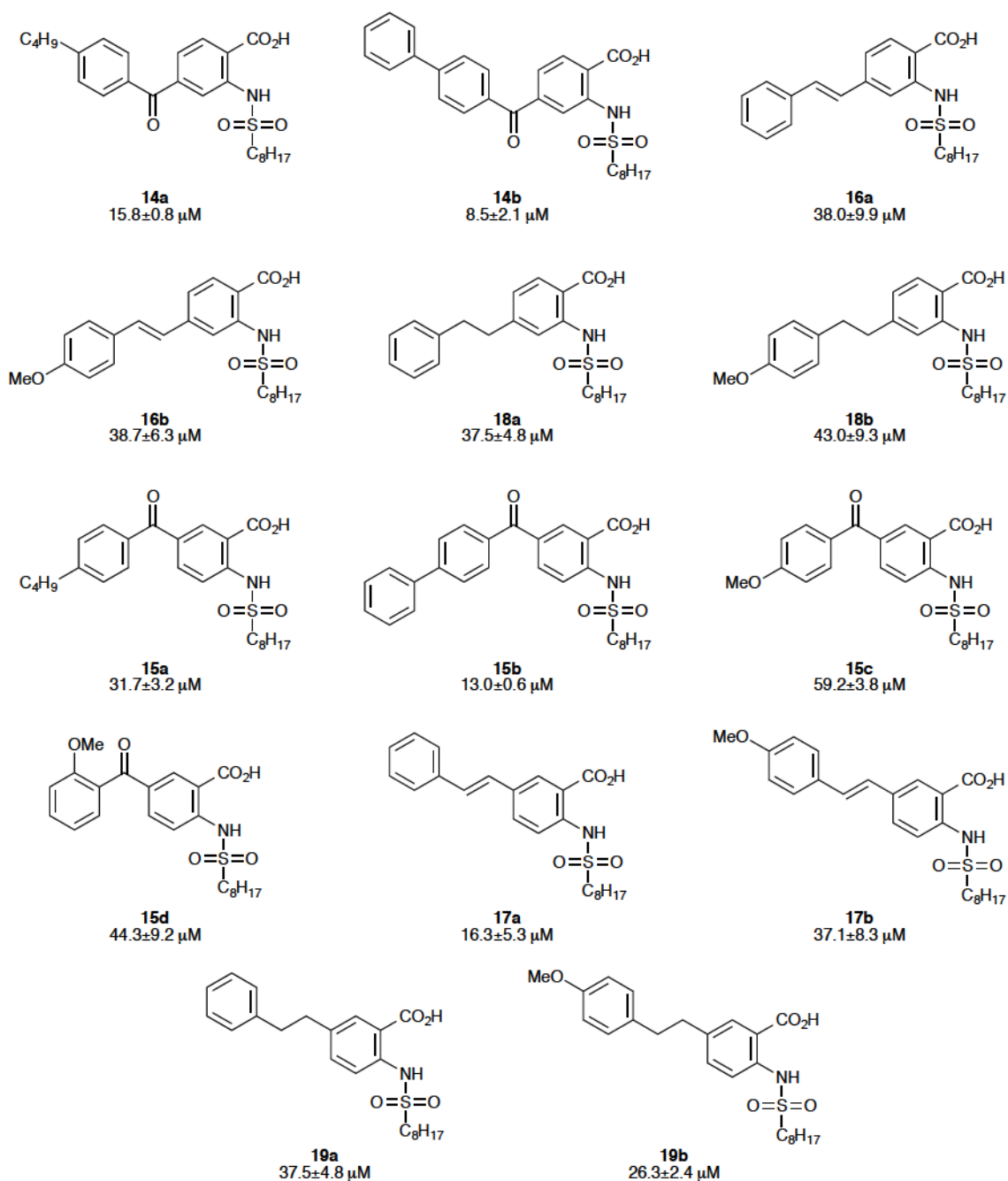


Figure 2.5 4- and 5-Substituted analogs with linkers: structures and IC_{50} data

The data for the 4- and 5-aryl analogs are consistent with the presence of a hydrophobic binding pocket extending from C-4 and C-5 of the benzoic acid of **1c**. Both steric and electronic factors may be affecting binding in this pocket. Sterically, the pocket is large enough around the 4-position of **1c** to accommodate the relatively voluminous and rigid *o*- and *p*-biphenyl analogs

12e and **12f**. The region near the 5-position, however, appears more constrained in size. Consequently, the *p*-biphenyl analog **13f** shows a large decrease in activity, possibly due to steric interactions with residues on the edge of the binding pocket. The *o*-biphenyl analog **13e**, however, may orient the terminal phenyl substituent away from the edge and back into the binding pocket resulting in a 2.5-fold increase in activity. Van der Waals and π -stacking interactions seem to be favored within the pocket as phenyl-, alkylphenyl-, and alkoxyphenyl substituents showed an increase in activity. Conversely, the more polarized fluorine-containing analogs demonstrated moderately diminished activity possibly due to binding at a site intolerant of the inhibitor's high charge density or disruption of key π - π interactions within the hydrophobic channel.

While the 3-fold increase in observed activity for the 4-aryl and 5-aryl derivatives was promising, we worried that the kinked nature of the hydrophobic tunnel observed in the docking model was preventing the analogs from extending fully into it. Therefore, we next sought to incorporate various linker regions on a subset of the more promising hydrophobic leads. Keto, vinyl, and ethyl linkers were chosen to examine the effect of separating the substituents from the pharmacophore and to explore conformational rigidity versus flexibility in extending the substituents into the hydrophobic tunnel. Inhibition data for the 4- and 5-substituted analogs are shown in Table 2.2. In general, the analogs possessing a keto linker were slightly to moderately less potent than the corresponding structures without a linker. For example, 5-keto-substituted *p*-*n*-butyl analog **15a** exhibited a 3.5-fold decrease in inhibition compared to compound **13d**. The *p*-biphenyl analogs **14b** and **15b**, however, were notable exceptions. Compound **14b** showed a 2-fold more potent inhibition compared to the linker-free analog **13f**. While the rigid linear carbon skeleton of **13f** may sterically interfere with residues on the face of

the hydrophobic pocket, the ketone linker in **15b** could potentially direct the large biphenyl moiety back towards the cavity. Compound **14b**, with an IC_{50} of 8.5 μM , was 3-fold more potent than **1c** and, to our knowledge, represents the most active GPAT inhibitor discovered to date. The benzophenone moiety present in this derivative imparts potential utility as a biochemical tool. Benzophenones have been shown to undergo a photo-induced $n \rightarrow \pi^*$ transition to form a diradical species, which can crosslink with nearby proteins.¹⁵ Photocrosslinking studies with a benzophenone-containing inhibitor could offer insight into its binding location within the GPAT enzyme. Additionally, photocrosslinking could potentially aid in identifying the off-target binding of other proteins.

The more rigid vinyl and conformationally flexible ethyl linkers were generally not well tolerated. For example, **16b**, a vinyl-linked *p*-methoxyphenyl analog, produced an activity of 37.5 μM compared to 13.3 μM for the linker-free derivative **12h**. No significant benefit was apparent from the incorporation of the conformationally flexible ethyl linkers. The same *p*-methoxyphenyl substituent with a linker region in compound **18b** demonstrated an IC_{50} of 43.0 μM or 3.2-fold lower activity than the corresponding compound **12h**.

2.5 Conclusions

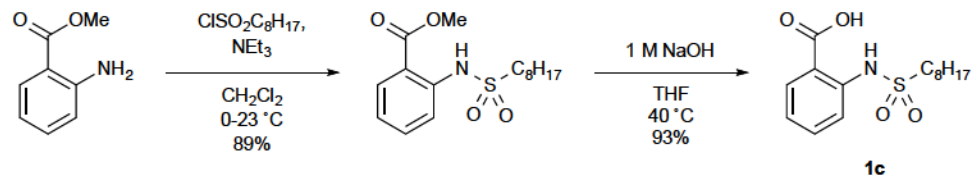
Several 4- and 5-substituted analogs of GPAT inhibitor (octanesulfonamido)benzoic acid were synthesized and analyzed for *in vitro* inhibitory activity. In general, hydrophobic substituents led to an increase in inhibitory activity while more polar and hydrogen-bonding substituents showed a decrease in inhibitory activity, consistent with the presence of a hydrophobic pocket identified by *in silico* studies. Taking advantage of the hydrophobic pocket, *p*-biphenylketone-substituted **14b** improved the inhibitory activity 3-fold to 8.5 μM ,

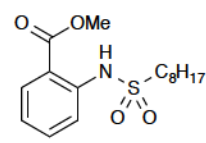
representing the most potent GPAT inhibitor to date. The benzophenone moiety in this compound lends it potential as a biochemical tool for photocrosslinking experiments. Future studies will aim to determine whether further extension of aryl and alkyl substituents into this channel confers additional inhibitory activity and if the observed increases *in vitro* correlate with *in vivo* TAG biosynthesis and overall fat metabolism in keeping with earlier studies.¹⁶

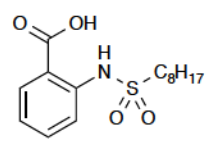
2.6 Experimental

General Information. All reagents and solvents were obtained from commercial sources, and used as supplied unless otherwise indicated. Reactions requiring anhydrous conditions were conducted under an inert atmosphere of argon using anhydrous solvents. CH₂Cl₂, toluene and MeOH were distilled over CaH₂. Et₂O and THF were distilled over Na and benzophenone. All reactions were monitored by analytical thin-layer chromatography (TLC) using indicated solvent systems on Analtech Uniplat Silica Gel TLC plates (250 microns). TLC plates were visualized using UV light (254 nm) and/or by staining in potassium permanganate, cerium ammonium molybdate, or phosphomolybdic acid followed by heating. All NMR spectra were recorded on either Bruker Advance 400 MHz or 300 MHz spectrometers as indicated. Chemical shifts (δ H) are quoted in ppm (parts per million) and referenced to residual solvent signals: ¹H δ = 7.26 (CDCl₃), 2.50 (DMSO-d₆), 3.31 (CD₃OD), ¹³C δ = 77.0 (CDCl₃), 39.43 (DMSO-d₆), 49.05 (CD₃OD). Coupling constants (*J*) are given in Hz. Elemental analyses were performed by Atlantic Microlabs, Inc.

Preparation of 2-(octanesulfonamido)benzoic acid (1c)

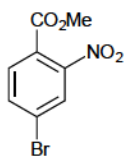
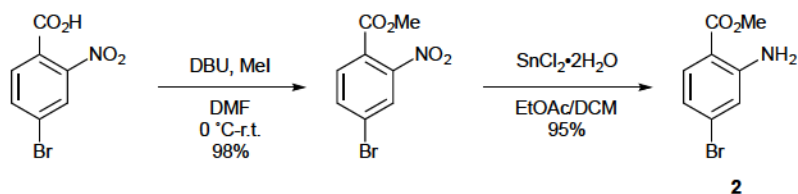


 **Methyl 2-(octanesulfonamido)benzoate.** To a stirring solution of methyl anthranilate (2.5 mL, 19.3 mmol) in CH₂Cl₂ at 0 °C was added octanesulfonyl chloride (4.5 mL, 23.2 mmol) dropwise followed by freshly distilled triethylamine (8.1 mL, 57.9 mmol). The reaction mixture was allowed to warm to room temperature and stirred for 16 h, then quenched with saturated NH₄Cl and extracted with CH₂Cl₂ (×3). The combined organic extracts were washed with brine, dried over Na₂SO₄, and concentrated *in vacuo* to provide 6.0 g of a crude off-white solid. Recrystallization from warm EtOAc/hexanes afforded the desired sulfonamide as a white solid (5.6 g, 17.1 mmol, 89%). ¹H-NMR (400 MHz; CDCl₃): δ 8.07 (ddd, *J* = 8.0, 1.7, 0.4 Hz, 1H), 7.76 (ddd, *J* = 8.4, 1.2, 0.5 Hz, 1H), 7.64 (ddd, *J* = 8.4, 7.3, 1.7 Hz, 1H), 7.19 (ddd, *J* = 8.0, 7.3, 1.2 Hz, 1H), 3.95 (s, 3H), 3.29-3.25 (m, 2H), 1.79-1.71 (m, 2H), 1.39 (s, 2H), 1.23 (s, 8H), 0.85 (t, *J* = 7.0 Hz, 3H); ¹³C-NMR (101 MHz; DMSO-*d*₆): δ 167.8, 139.8, 134.7, 131.0, 123.0, 118.5, 116.1, 52.6, 51.2, 31.0, 28.7, 28.6, 28.0, 22.8, 21.9, 13.9.

 **2-(Octanesulfonamido)benzoic acid (1c).** To a stirring solution of methyl 2-(octanesulfonamido)benzoate (5.6 g, 17.1 mmol) in THF (86 mL) at room temperature was added 1 M NaOH (171 mL, 171 mmol). The reaction mixture was stirred at 40 °C for 18 h, then the reaction was quenched with 1 M HCl and extracted with EtOAc (×3). The combined organic extracts were washed with brine, dried over Na₂SO₄, and concentrated *in vacuo* to afford 5.3 g of a crude off-white solid. Recrystallization from warm

EtOAc/hexanes afforded the desired carboxylic acid as a white solid (5.0 g, 16.0 mmol, 93%).
¹H-NMR (400 MHz; acetone-d₆): δ 10.67 (s, 1H), 8.14 (ddd, *J* = 8.0, 1.7, 0.4 Hz, 1H), 7.76 (ddd, *J* = 8.4, 1.2, 0.4 Hz, 1H), 7.65 (ddd, *J* = 8.4, 7.3, 1.7 Hz, 1H), 7.21-7.18 (m, 1H), 3.28-3.24 (m, 2H), 1.75 (m, 2H), 1.39 (m, 2H), 1.29-1.23 (m, 7H), 0.85 (t, *J* = 7.0 Hz, 3H); ¹³C-NMR (101 MHz, DMSO-d₆): δ 170.19, 141.04, 134.73, 131.85, 122.52, 117.42, 115.79, 51.26, 31.32, 28.55, 28.52, 27.42, 23.16, 22.23, 13.94; HRMS (FAB) calcd for C₁₅H₂₄NO₄S [M+H]⁺, 314.14260; found, 314.14278.

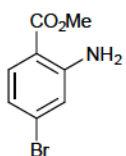
Preparation of methyl 2-amino-4-bromobenzoate (2)



Methyl 4-bromo-2-nitrobenzoate. To a stirring solution of 4-bromo-2-nitrobenzoic acid (5.0 g, 21.7 mmol) in DMF (33 mL) at 0 °C was added DBU (3.91 mL, 26.1 mmol) followed by iodomethane (2.04 mL, 32.8 mmol). The

reaction mixture was allowed to warm to room temperature and stirred for 12 h, then quenched with NaHCO₃, and extracted with Et₂O (3 × 100 mL). The combined organic layers were washed with brine, dried over Na₂SO₄, and concentrated *in vacuo*. Purification by flash chromatography (10% EtOAc in hexanes) afforded methyl 4-bromo-2-nitrobenzoate (98%).

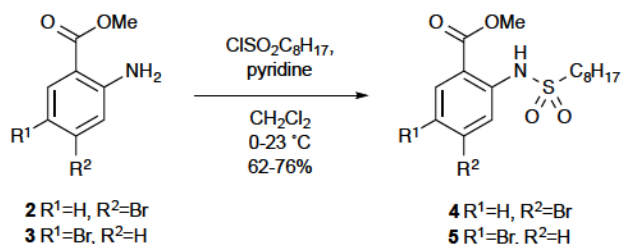
Spectral data match literature values.¹⁷



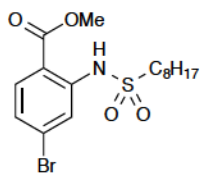
Methyl 2-amino-4-bromobenzoate 2. To a stirring solution of methyl 4-bromo-2-nitrobenzoate (4.75 g, 18.3 mmol) in 3:1 EtOAc/DCM (45 mL) at room

temperature was added $\text{SnCl}_2 \cdot 2\text{H}_2\text{O}$ (20.6 g, 91.3 mmol). The reaction mixture was stirred at room temperature for 16 h, then quenched with NaHCO_3 . The gelatinous mixture was filtered over Celite, and the filtrate was extracted with DCM (3×100 mL). The combined organic layers were washed with brine, dried over Na_2SO_4 , and concentrated *in vacuo*. Purification by flash chromatography (10% EtOAc in hexanes) afforded aniline **2** (95%). Spectral data match literature values.¹⁷

Preparation of Sulfonamides **4** and **5**.



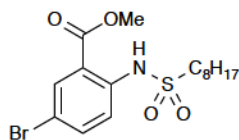
General Procedure. To a stirring solution of the starting aniline (6.6 mmol) in DCM (24 mL) at 0°C was added pyridine (4 mL). Octanesulfonyl chloride (1.2 equiv) was then added slowly via syringe. The solution was stirred and allowed to warm to room temperature. Reaction progress was monitored by TLC (20 % EtOAc in hexanes). Upon completion, the reaction was poured into saturated NaHCO_3 solution (50 mL), extracted with DCM (3×30 mL), and washed with 1 M HCl (50 mL). The combined organic layers were concentrated *in vacuo* and purified by flash chromatography (10% EtOAc in hexanes).



Methyl 4-bromo-2-(octanesulfonamido)benzoate (4). (62% yield from aniline **2**). $^1\text{H-NMR}$ (400 MHz; CDCl_3): δ 10.47 (s, 1H), 7.94 (d, $J = 2.0$ Hz, 1H), 7.89 (d, $J = 8.4$ Hz, 1H), 7.23 (dd, $J = 2.0, 8.4$ Hz, 1H), 3.93 (s, 3H),

3.15 (t, $J = 8.0$ Hz, 2H), 1.79 (m, 2H), 1.37 (m, 2H), 1.23 (m, 8H), 0.86 (t, $J = 6.8$ Hz, 3H); $^{13}\text{C-}$

NMR (100 MHz; CDCl₃): δ 167.8, 142.0, 132.5, 129.7, 125.7, 120.4, 113.5, 52.6, 52.4, 31.5, 28.8, 28.7, 27.9, 23.2, 22.5, 13.9.



Methyl-5-bromo-2-(octanesulfonamido)benzoate (5). (76% yield

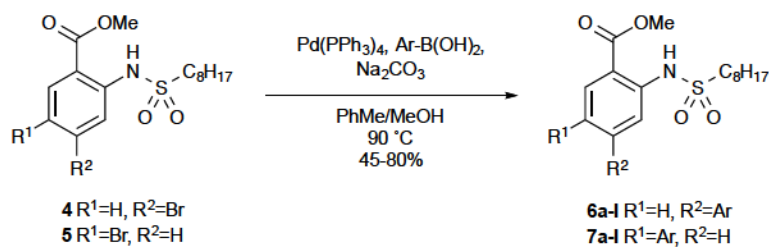
from aniline **3** (>99%, TCI America)). ¹H-NMR (400 MHz; CDCl₃): δ

10.33 (s, 1H), 8.17 (d, J = 2.4 Hz, 1H), 7.66 (m, 2H), 3.95 (s, 3H), 3.11 (t, J = 8.0 Hz, 2H),

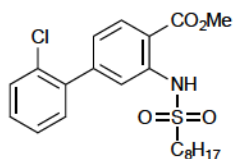
1.78 (m, 2H), 1.26 (m, J = 10 Hz), 0.89 (t, J = 6.8 Hz, 3H); ¹³C-NMR (100 MHz; CDCl₃): δ 167.2,

140.1, 137.5, 134.0, 119.5, 116.5, 115.0, 52.8, 52.3, 31.6, 28.8, 28.8, 28.0, 23.3, 22.5, 14.0.

Preparation of Suzuki Coupling Products 6a-l and 7a-l



General Procedure. Aryl bromide **4** or **5** (0.247 mmol) was placed into a vial flushed with argon, and a solution of 10 mg Pd(PPh₃)₄ in 0.40 mL toluene was added, followed by 0.25 mL 2 M Na₂SO₃ solution. The solution was stirred at room temperature for 5 min, and then a solution of the boronic acid (0.318 mmol, 1.25 equiv.) in 0.40 mL MeOH was added. The vial was capped and heated to 90 °C for 24 h. The reaction was then cooled to room temperature and diluted with CH₂Cl₂, the organic phase was separated from the aqueous phase, and the organic phase was concentrated *in vacuo*. The crude product was purified by column chromatography (EtOAc/hexanes) to yield the desired Suzuki coupling product.



2-Chloro-3-(octanesulfonamido)-biphenyl-4-carboxylic acid methyl

ester (6a). 76% yield; $^1\text{H-NMR}$ (400 MHz; CDCl_3): δ 10.46 (s, 1H), 8.04

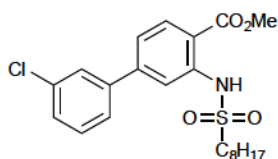
(d, J = 8.4 Hz, 1H), 7.77 (s, 1H), 7.41 (m, 1H), 7.27 (m, 3H), 7.09 (d, J =

8.4 Hz, 1H), 3.85 (s, 3H), 3.14 (t, J = 8.0 Hz, 2H), 1.75 (m, 2H), 1.31 (m, 2H), 1.18 (m, 8H),

0.80 (t, J = 6.8 Hz, 3H); $^{13}\text{C-NMR}$ (100 MHz; CDCl_3): δ 168.1, 145.8, 140.7, 138.6, 132.0,

131.2, 130.9, 130.0, 129.4, 127.0, 123.4, 118.4, 113.8, 52.5, 52.0, 31.5, 28.7, 28.7, 27.9, 23.2,

22.4, 13.9.



3-Chloro-3-(octanesulfonamido)-biphenyl-4-carboxylic acid

methyl ester (6b). 74% yield; $^1\text{H-NMR}$ (400 MHz; CDCl_3): δ 10.51

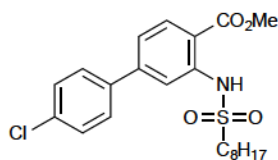
(s, 1H), 8.11 (d, J = 8.4 Hz, 1H), 7.97 (d, J = 1.6 Hz, 1H), 7.59 (s,

1H), 7.51 (m, 1H), 7.39 (m, 2H), 7.29 (dd, J = 1.6, 8.4 Hz, 1H), 3.97 (s, 3H), 3.18 (t, J = 8.0 Hz,

2H), 1.82 (m, 2H), 1.37 (m, 2H), 1.25 (m, 8H), 0.86 (t, J = 6.8 Hz, 3H); $^{13}\text{C-NMR}$ (100 MHz;

CDCl_3): δ 168.1, 145.9, 141.5, 140.9, 134.8, 132.0, 130.2, 128.6, 127.2, 125.4, 121.1, 116.1,

114.1, 52.5, 52.2, 31.5, 28.8, 28.7, 27.9, 23.3, 22.4, 13.9.



4-Chloro-3-(octanesulfonamido)-biphenyl-4-carboxylic acid

methyl ester (6c). 74% yield; $^1\text{H-NMR}$ (400 MHz; CDCl_3): δ 10.49

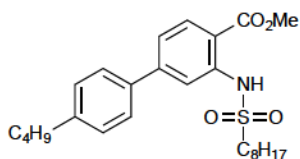
(s, 1H), 8.10 (d, J = 8.4 Hz, 1H), 7.97 (s, 1H), 7.56 (d, J = 6.8 Hz,

2H), 7.43 (d, J = 6.8 Hz, 2H), 7.29 (d, J = 8.4 Hz, 1H), 3.96 (s, 3H), 3.16 (t, J = 8.0 Hz, 2H),

1.82 (m, 2H), 1.36 (m, 2H), 1.22 (m, 8H), 0.84 (t, J = 6.8 Hz, 3H); $^{13}\text{C-NMR}$ (100 MHz;

CDCl_3): δ 168.1, 146.1, 141.5, 137.4, 134.9, 132.0, 129.1, 128.5, 120.9, 115.9, 113.9, 52.5, 52.2,

31.5, 28.8, 28.7, 27.9, 23.3, 22.4, 13.9.



4-n-Butyl-3-(octanesulfonamido)-biphenyl-4-carboxylic acid

methyl ester (6d). 72% yield; $^1\text{H-NMR}$ (400 MHz; CDCl_3): δ 10.65

(s, 1H), 8.22 (d, J = 8.3 Hz, 1H), 8.16 (d, J = 1.7 Hz, 1H), 7.70 (d, J

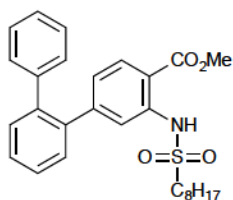
= 8.2 Hz, 2H), 7.46 (dd, J = 8.3, 1.7 Hz, 1H), 7.42 (d, J = 8.2 Hz, 2H), 4.08 (s, 3H), 3.33-3.29

(m, 2H), 2.81 (t, J = 7.7 Hz, 2H), 2.00-1.90 (m, 2H), 1.80-1.76 (m, 2H), 1.59-1.45 (m, 4H),

1.45-1.30 (m, 8H), 1.10 (t, J = 7.3 Hz, 3H), 1.00 (t, J = 6.9 Hz, 3H).; $^{13}\text{C-NMR}$ (101 MHz,

CDCl_3): δ 168.54, 147.68, 144.00, 141.67, 136.55, 132.07, 129.25, 127.31, 121.14, 115.94,

113.57, 52.63, 52.31, 35.51, 33.72, 31.83, 29.08, 29.00, 28.20, 23.55, 22.73, 22.53, 14.20, 14.12.



2-Phenyl-3-(octanesulfonamido)-biphenyl-4-carboxylic acid methyl

ester (6e). 67% yield; $^1\text{H-NMR}$ (400 MHz; CDCl_3): δ 10.41 (s, 1H), 8.00

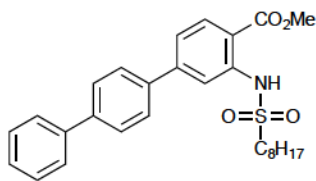
(d, J = 8.0 Hz, 1H), 7.45 (m, 5H), 7.25 (m, 5H), 7.03 (dd, J = 8.4, 1.6 Hz,

1H), 3.93 (s, 3H), 2.67 (t, J = 7.6 Hz, 2H), 1.67 (m, 2H), 1.32 (m, 2H), 0.92 (t, J = 6.8 Hz, 3H);

$^{13}\text{C-NMR}$ (100 MHz; CDCl_3): δ 168.2, 148.6, 141.0, 140.5, 140.3, 138.7, 131.2, 130.8, 130.2,

129.8, 128.3, 128.0, 127.5, 126.6, 123.6, 118.9, 112.7, 52.3, 51.2, 31.6, 28.9, 28.8, 27.8, 23.3,

22.5, 13.9.



4-Phenyl-3-(octanesulfonamido)-biphenyl-4-carboxylic acid

methyl ester (6f). 71% yield; $^1\text{H-NMR}$ (400 MHz; DMSO-d_6): δ

10.28 (s, 1H), 8.06 (d, J = 8.4 Hz, 1H), 7.90 (s, 1H), 7.81 (q, J =

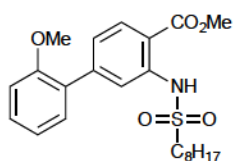
8.4 Hz, 4H), 7.73 (d, J = 8.4 Hz, 2H), 7.57 (d, J = 8.4 Hz, 1H), 7.49 (t, J = 7.6 Hz, 2H), 7.40 (t, J

= 7.2 Hz, 1H), 3.91 (s, 3H), 3.37 (t, J = 8.0 Hz, 2H), 1.64 (m, 2H), 1.32 (m, 2H), 1.20 (m, 8H),

0.80 (t, J = 6.8 Hz, 3H); $^{13}\text{C-NMR}$ (100 MHz; DMSO-d_6): δ 167.7, 145.5, 140.5, 140.4, 139.2,

137.2, 131.8, 128.9, 127.7, 127.5, 127.3, 126.6, 121.2, 116.0, 114.8, 52.7, 51.4, 31.0, 28.2, 28.2,

27.0, 22.9, 21.9, 13.8.



2-Methoxy-3-(octanesulfonamido)-biphenyl-4-carboxylic acid methyl

ester (6g). 70% yield; $^1\text{H-NMR}$ (400 MHz; CDCl_3): δ 10.48 (s, 1H), 8.07

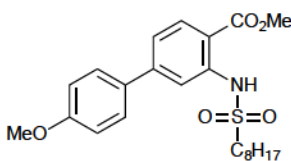
(d, $J = 8.4$ Hz, 1H), 7.98 (s, 1H), 7.37 (m, 2H), 7.28 (d, $J = 8.4$ Hz, 1H),

7.05 (m, 2H), 3.95 (s, 3H), 3.84 (s, 3H), 3.20 (t, $J = 8.0$ Hz, 2H), 1.82 (m, 2H), 1.40 (m, 2H),

1.23 (m, 8H), 0.86 (t, $J = 7.2$ Hz, 3H); $^{13}\text{C-NMR}$ (100 MHz; CDCl_3): δ 168.3, 156.3, 145.2,

140.6, 130.9, 130.5, 129.8, 128.6, 123.6, 120.9, 118.6, 113.1, 111.3, 55.5, 52.3, 51.8, 31.5, 28.8,

28.7, 27.9, 23.2, 22.4, 13.9.



4-Methoxy-3-(octanesulfonamido)-biphenyl-4-carboxylic acid

methyl ester (6h). 71% yield; $^1\text{H-NMR}$ (400 MHz; CDCl_3): δ 10.47

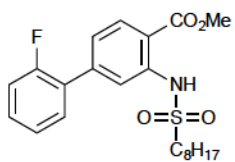
(s, 1H), 8.04 (d, $J = 8.4$ Hz, 1H), 7.96 (d, $J = 1.6$ Hz, 1H), 7.57 (dd, J

= 6.8, 2.0 Hz, 2H), 7.28 (dd, $J = 8.4, 1.6$ Hz, 1H), 6.97 (dd, $J = 6.8, 2.0$ Hz, 2H), 3.93 (s, 3H),

3.84 (s, 3H), 3.14 (t, $J = 8.0$ Hz, 2H), 1.80 (m, 2H), 1.23 (m, 10H), 0.86 (t, $J = 7.2$ Hz, 3H); $^{13}\text{C-}$

NMR (100 MHz; CDCl_3): δ 168.3, 160.2, 147.0, 141.4, 131.8, 131.3, 128.4, 120.5, 115.4, 114.3,

113.0, 55.3, 52.4, 52.0, 31.5, 28.8, 28.7, 27.9, 23.2, 22.4, 13.9.



2-Fluoro-3-(octanesulfonamido)-biphenyl-4-carboxylic acid methyl

ester (6i). 69% yield; $^1\text{H-NMR}$ (400 MHz; CDCl_3): δ 10.51 (s, 1H), 8.12

(d, $J = 8.4$ Hz, 1H), 7.96 (d, $J = 1.6$ Hz, 1H), 7.48 (dt, $J = 7.6, 2.0$ Hz, 1H),

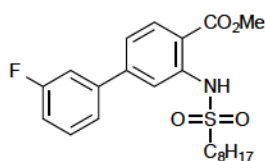
7.40 (m, 1H), 7.28 (m, 1H), 7.19 (m, 1H), 3.97 (s, 3H), 3.21 (t, $J = 8.0$ Hz, 2H), 1.83 (m, 2H),

1.37 (m, 2H), 1.25 (m, 8H), 0.87 (t, $J = 6.8$ Hz, 3H); $^{13}\text{C-NMR}$ (100 MHz; CDCl_3): δ 168.1,

159.6 (d, $J = 249$ Hz), 142.3 (d, $J = 1.4$ Hz), 141.1, 131.4, 130.5 (d, $J = 2.9$ Hz), 130.2 (d, $J = 8.4$

Hz), 127.3, 124.6 (d, $J = 3.7$ Hz), 123.0 (d, $J = 3.6$ Hz), 117.9 (d, $J = 3.5$ Hz), 116.2 (d, $J = 22.5$

Hz), 113.8, 52.5, 52.1, 31.5, 28.8, 28.7, 27.9, 23.2, 22.4, 13.9.



3-Fluoro-3-(octanesulfonamido)-biphenyl-4-carboxylic acid methyl

ester (6j). 70% yield; $^1\text{H-NMR}$ (400 MHz; CDCl_3): δ 10.49 (s, 1H),

8.10 (d, $J = 8.4$ Hz, 1H), 7.98 (d, $J = 1.6$ Hz, 1H), 7.41 (m, 2H), 7.30

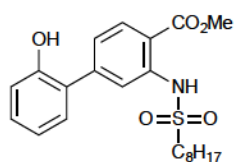
(m, 2H), 7.10 (m, 1H), 3.96 (s, 3H), 3.16 (t, $J = 8.0$ Hz, 2H), 1.81 (m, 2H), 1.36 (m, 2H), 1.21

(m, 8H), 0.86 (t, $J = 6.8$ Hz, 3H); $^{13}\text{C-NMR}$ (100 MHz; CDCl_3): δ 168.1, 163.0 (d, $J = 246$ Hz),

146.0 (d, $J = 2.2$ Hz), 141.5, 141.3 (d, $J = 7.3$ Hz), 132.0, 130.5 (d, $J = 8.0$ Hz), 122.9 (d, $J = 2.9$

Hz), 121.0, 116.1, 115.4 (d, $J = 21.1$ Hz), 114.1, 114.1 (d, $J = 22.4$ Hz), 52.5, 52.2, 31.5, 28.8,

28.7, 27.9, 23.3, 22.4, 13.9.



2-Hydroxy-3-(octanesulfonamido)-biphenyl-4-carboxylic acid methyl

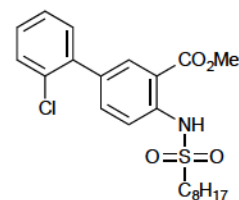
ester (6k). 45% yield; $^1\text{H-NMR}$ (400 MHz; CDCl_3): δ 10.50 (s, 1H), 8.11

(d, $J = 8.4$ Hz, 1H), 7.94 (d, $J = 1.6$ Hz, 1H), 7.29 (m, 3H), 6.99 (m, 2H),

5.90 (br s, 1H), 3.96 (s, 3H), 3.20 (t, $J = 8.0$ Hz, 2H), 1.80 (m, 2H), 1.33 (m, 10H), 0.88 (t, $J =$

6.8 Hz, 3H); $^{13}\text{C-NMR}$ (100 MHz; CDCl_3): δ 168.2, 152.7, 144.6, 141.1, 131.7, 130.2, 129.9,

126.4, 123.1, 121.0, 118.2, 116.4, 113.5, 52.5, 52.2, 31.6, 28.8, 28.7, 27.9, 23.3, 22.5, 13.9.



2-Chloro-4-(octanesulfonamido)-biphenyl-3-carboxylic acid methyl

ester (7a). 74% yield; $^1\text{H-NMR}$ (400 MHz; CDCl_3): δ 10.51 (s, 1H),

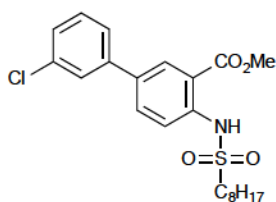
8.15 (d, $J = 2.0$ Hz, 1H), 7.82 (d, $J = 8.8$ Hz, 1H), 7.64 (dd, $J = 8.8, 2.4$ Hz,

1H), 7.48 (m, 1H), 7.33 (m, 3H), 3.94 (s, 3H), 3.20 (t, $J = 8.0$ Hz, 2H), 1.85 (m, 2H), 1.26 (m,

10H), 0.87 (t, $J = 6.8$ Hz, 3H); $^{13}\text{C-NMR}$ (100 MHz; CDCl_3): δ 168.2, 140.4, 138.4, 135.8,

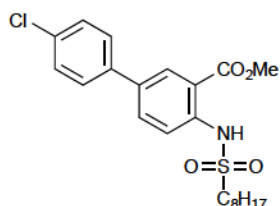
133.5, 132.3, 132.3, 131.0, 130.0, 128.9, 127.0, 117.2, 114.6, 52.5, 52.3, 31.5, 28.8, 28.7, 27.9,

23.3, 22.4, 13.9.



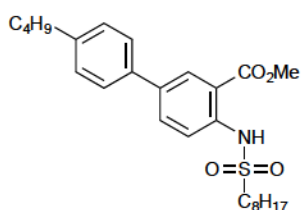
3-Chloro-4-(octanesulfonamido)-biphenyl-3-carboxylic acid methyl ester (7b). 78% yield; $^1\text{H-NMR}$ (400 MHz; CDCl_3): δ 10.45

(s, 1H), 8.23 (d, $J = 2.4$ Hz, 1H), 7.83 (d, $J = 8.4$ Hz, 1H), 7.71 (dd, $J = 2.4, 8.8$ Hz, 1H), 7.53 (m, 1H), 7.43 (m, 1H), 7.35 (m, 2H), 3.98 (s, 3H), 3.17 (t, $J = 8.0$ Hz, 2H), 1.82 (m, 2H), 1.37 (m, 2H), 1.24 (m, 8H), 0.85 (t, $J = 6.8$ Hz, 3H); $^{13}\text{C-NMR}$ (100 MHz; CDCl_3): δ 168.0, 140.8, 140.5, 134.7, 133.8, 133.0, 130.1, 129.7, 127.5, 126.6, 124.7, 118.1, 115.2, 52.5, 52.2, 31.5, 28.7, 28.7, 27.9, 23.2, 22.4, 13.8.



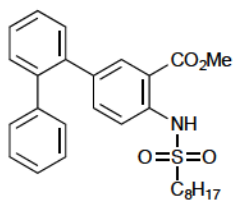
4-Chloro-4-(octanesulfonamido)-biphenyl-3-carboxylic acid methyl ester (7c). 80% yield; $^1\text{H-NMR}$ (400 MHz; CDCl_3): δ 10.43

(s, 1H), 8.24 (d, $J = 2.4$ Hz, 1H), 7.84 (d, $J = 8.4$ Hz, 1H), 7.72 (dd, $J = 2.4, 8.8$ Hz, 1H), 7.50 (d, $J = 8.8$ Hz, 2H), 7.42 (d, $J = 8.8$ Hz, 2H), 3.97 (s, 3H), 3.17 (t, $J = 8.0$ Hz, 2H), 1.82 (m, 2H), 1.36 (m, 2H), 1.23 (m, 8H), 0.85 (t, $J = 6.8$ Hz, 3H); $^{13}\text{C-NMR}$ (100 MHz; CDCl_3): δ 168.1, 140.3, 137.5, 134.2, 133.7, 133.0, 129.6, 129.0, 127.8, 118.3, 115.4, 52.6, 52.2, 31.5, 28.8, 28.7, 27.9, 23.3, 22.5, 13.9.



4'-Butyl-4-(octanesulfonamido)-[1,1'-biphenyl]-3-carboxylic acid methyl ester (7d). 74% yield; 74% yield; $^1\text{H-NMR}$ (400 MHz,

CDCl_3): δ 0.87 (t, 3H, $J = 6.8$), 0.96 (t, 3H, $J = 7.2$), 1.24 (m, 8H), 1.39 (m, 4H), 1.65 (m, 2H), 1.83 (m, 2H), 2.66 (t, 2H, $J = 8.0$), 3.18 (t, 2H, $J = 8.0$), 3.97 (s, 3H), 7.27 (d, 2H, $J = 8.4$), 7.49 (d, 2H, $J = 8.0$), 7.75 (d, 1H, $J = 8.4$), 7.83 (d, 1H, $J = 8.8$), 8.28 (s, 1H), 10.42 (s, 1H); $^{13}\text{C-NMR}$ (100 MHz, CDCl_3): δ 14.0, 14.1, 22.4, 22.6, 23.4, 28.1, 28.9, 29.0, 31.7, 33.3, 33.6, 35.3, 52.2, 52.6, 115.5, 118.4, 126.6, 129.1, 129.6, 133.2, 135.7, 136.5, 139.9, 142.6, 168.4.



2-Phenyl-4-(octanesulfonamido)-biphenyl-3-carboxylic acid methyl

ester (7e). 65% yield; ¹H-NMR (400 MHz; CDCl₃): δ 10.37 (s, 1H), 7.93

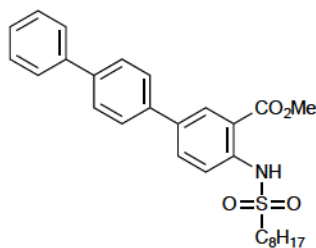
(d, *J* = 2.0 Hz, 1H), 7.55 (d, *J* = 8.8 Hz, 1H), 7.43 (m, 4H), 7.22 (m, 4H),

7.13 (m, 2H), 3.87 (s, 3H), 3.11 (t, *J* = 8.0 Hz, 2H), 1.77 (m, 2H), 1.36 (m, 2H), 1.25 (m, 8H),

0.88 (t, *J* = 6.8 Hz, 3H); ¹³C-NMR (100 MHz; CDCl₃): δ 168.2, 140.9, 140.6, 139.4, 138.4,

136.2, 135.8, 132.5, 130.6, 130.0, 129.8, 128.0, 127.9, 127.6, 126.7, 117.1, 114.6, 52.3, 52.0, 31.6,

28.8, 28.8, 28.0, 23.2, 22.5, 14.0.



4-Phenyl-4-(octanesulfonamido)-biphenyl-3-carboxylic acid

methyl ester (7f). 72% yield; ¹H-NMR (400 MHz; CDCl₃): δ

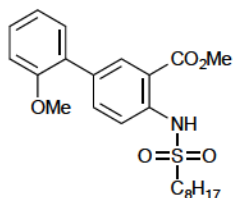
10.45 (s, 1H), 8.34 (d, *J* = 2.4 Hz, 1H), 7.85 (m, 2H), 7.67 (m,

6H), 7.48 (t, *J* = 7.6 Hz, 2H), 7.40 (m, 1H), 3.99 (s, 3H), 3.19 (t, *J*

= 8.0 Hz, 2H), 1.84 (m, 2H), 1.39 (m, 2H), 1.24 (m, 8H), 0.87 (t, *J* = 6.8 Hz, 3H); ¹³C-NMR

(100 MHz; CDCl₃): δ 168.3, 140.5, 140.3, 140.1, 138.0, 135.0, 133.1, 129.6, 128.8, 127.6, 127.5,

127.0, 126.9, 118.3, 115.4, 52.6, 52.2, 31.6, 28.9, 28.8, 28.0, 23.3, 22.5, 14.0.



2-Methoxy-4-(octanesulfonamido)-biphenyl-3-carboxylic acid methyl

ester (7g). 67% yield; ¹H-NMR (400 MHz; CDCl₃): δ 10.46 (s, 1H), 8.22

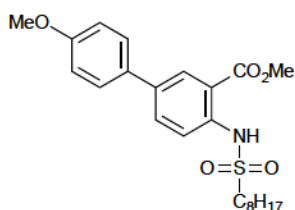
(d, *J* = 2.8 Hz, 1H), 7.80 (d, *J* = 8.8 Hz, 1H), 7.74 (dd, *J* = 2.0, 8.8 Hz, 1H),

7.32 (m, 2H), 7.03 (m, 2H), 3.94 (s, 3H), 3.83 (s, 3H), 3.19 (t, *J* = 8.0 Hz, 2H), 1.84 (m, 2H),

1.36 (m, 2H), 1.26 (m, 8H), 0.87 (t, *J* = 7.2 Hz, 3H); ¹³C-NMR (100 MHz; CDCl₃): δ 168.4,

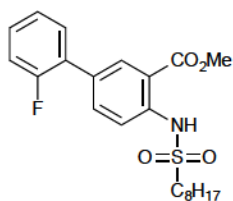
156.2, 139.6, 135.9, 132.9, 132.1, 130.3, 129.0, 128.4, 120.8, 117.2, 114.7, 111.1, 55.4, 52.4, 52.1,

31.5, 28.8, 28.7, 27.9, 23.2, 22.4, 13.9.



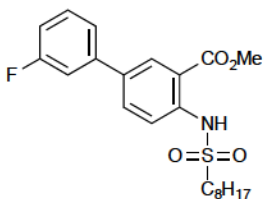
4-Methoxy-4-(octanesulfonamido)-biphenyl-3-carboxylic acid methyl ester (7h). 71% yield; $^1\text{H-NMR}$ (400 MHz; CDCl_3): δ 10.37

(s, 1H), 8.22 (d, $J = 2.4$ Hz, 1H), 7.81 (d, $J = 8.8$ Hz, 1H), 7.71 (dd, $J = 2.4, 8.8$ Hz, 1H), 7.50 (d, $J = 8.8$ Hz, 2H), 6.99 (d, $J = 8.8$ Hz, 2H), 3.96 (s, 3H), 3.85 (s, 3H), 3.16 (t, $J = 8.0$ Hz, 2H), 1.81 (m, 2H), 1.37 (m, 2H), 1.23 (m, 8H), 0.85 (t, $J = 6.8$ Hz, 3H); $^{13}\text{C-NMR}$ (100 MHz; CDCl_3): δ 168.3, 159.3, 139.5, 135.3, 132.8, 131.6, 129.2, 127.7, 118.4, 115.4, 114.3, 55.3, 52.5, 52.1, 31.6, 28.8, 28.8, 28.0, 23.3, 22.5, 13.9.



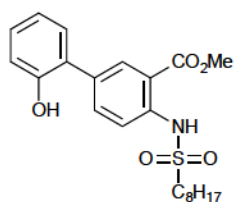
2-Fluoro-4-(octanesulfonamido)-biphenyl-3-carboxylic acid methyl ester (7i). 73% yield; $^1\text{H-NMR}$ (400 MHz; CDCl_3): δ 10.48 (s, 1H), 8.24

(s, 1H), 7.83 (d, $J = 8.8$ Hz, 1H), 7.72 (td, $J = 8.8, 2.0$ Hz, 1H), 7.41 (dt, $J = 7.6, 2.0$ Hz, 1H), 7.32 (m, 1H), 7.22 (m, 1H), 7.15 (m, 1H), 3.94 (s, 3H), 3.18 (t, $J = 8.0$ Hz, 2H), 1.82 (m, 2H), 1.38 (m, 2H), 1.24 (m, 8H), 0.86 (t, $J = 7.2$ Hz, 3H); $^{13}\text{C-NMR}$ (100 MHz; CDCl_3): δ 168.1, 159.5 (d, $J = 248$ Hz), 140.3, 135.1 (d, $J = 3.3$ Hz), 131.7 (d, $J = 3.0$ Hz), 130.2 (d, $J = 3.0$ Hz), 130.0, 129.3 (d, $J = 8.1$ Hz), 127.0 (d, $J = 13.0$ Hz), 124.5 (d, $J = 3.7$ Hz), 117.7, 116.1 (d, $J = 22.6$ Hz), 115.0, 52.5, 52.2, 31.5, 28.8, 28.7, 27.9, 23.2, 22.4, 13.9.



3-Fluoro-4-(octanesulfonamido)-biphenyl-3-carboxylic acid methyl ester (7j). 77% yield; $^1\text{H-NMR}$ (400 MHz; CDCl_3): δ 10.46 (s, 1H),

8.27 (d, $J = 2.4$ Hz, 1H), 7.85 (d, $J = 8.8$ Hz, 1H), 7.74 (dd, $J = 8.4, 2.4$ Hz, 1H), 7.41 (dd, $J = 8.0, 6.0$ Hz, 1H), 7.35 (d, 7.6 Hz, 1H), 7.26 (d, $J = 8.8$ Hz, 1H), 7.06 (m, 1H), 3.99 (s, 3H), 3.19 (t, $J = 8.0$ Hz, 2H), 1.83 (m, 2H), 1.39 (m, 2H), 1.24 (m, 8H), 0.86 (t, $J = 7.6$ Hz, 3H); $^{13}\text{C-NMR}$ (100 MHz; CDCl_3): δ 168.1, 163.1 (d, $J = 246$ Hz), 141.2 (d, $J = 7.3$ Hz), 140.5, 134.0, 133.0, 130.4 (d, $J = 8.2$ Hz), 129.7, 122.2 (d, $J = 2.8$ Hz), 118.2, 115.3, 114.3 (d, $J = 21.0$ Hz), 113.4 (d, $J = 22.3$ Hz), 52.6, 52.2, 31.5, 28.8, 28.7, 27.9, 23.2, 22.4, 13.9.



2-Hydroxy-4-(octanesulfonamido)-biphenyl-3-carboxylic acid methyl

ester (7k). 48% yield; $^1\text{H-NMR}$ (400 MHz; CDCl_3): δ 10.47 (s, 1H), 8.22

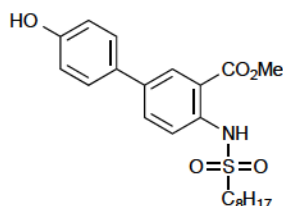
(d, J = 2.0 Hz, 1H), 7.83 (d, J = 8.4 Hz, 1H), 7.71 (dd, J = 8.4, 2.0 Hz, 1H),

7.26 (m, 2H), 7.01 (t, J = 7.6 Hz, 1H), 6.96 (d, J = 8.0 Hz, 1H), 5.31 (s, 1H), 3.94 (s, 3H), 3.19

(t, J = 8.0 Hz, 2H), 1.82 (m, 2H), 1.27 (m, 2H), 1.25 (m, 8H), 0.88 (t, J = 6.8 Hz, 3H); $^{13}\text{C-}$

NMR (100 MHz; CDCl_3): δ 168.2, 152.4, 140.2, 135.6, 132.0, 131.8, 130.3, 129.3, 126.4, 121.1,

118.0, 116.1, 115.2, 52.6, 52.4, 31.6, 28.9, 28.8, 28.0, 23.3, 22.5, 14.0.



4-Hydroxy-4-(octanesulfonamido)-biphenyl-3-carboxylic acid

methyl ester (7l). 51% yield; $^1\text{H-NMR}$ (400 MHz; CDCl_3): δ 10.37

(s, 1H), 8.21 (d, J = 2.4 Hz, 1H), 7.80 (d, J = 8.8 Hz, 1H), 7.70 (dd, J

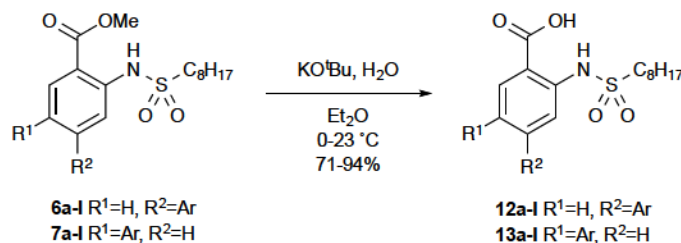
= 8.4, 2.4 Hz, 1H), 7.44 (d, J = 8.4 Hz, 2H), 6.93 (d, J = 8.4 Hz, 2H), 3.96 (s, 3H), 3.16 (t, J =

8.0 Hz, 2H), 1.81 (m, 2H), 1.36 (m, 2H), 1.21 (m, 8H), 0.84 (t, J = 7.2 Hz, 3H); $^{13}\text{C-NMR}$ (100

MHz; CDCl_3): δ 168.3, 155.7, 139.4, 135.4, 132.8, 131.6, 129.2, 127.9, 118.4, 115.8, 115.5, 52.6,

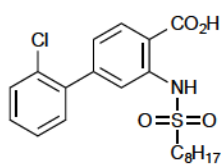
52.2, 31.6, 28.8, 28.8, 28.0, 23.3, 22.5, 13.9.

Preparation of Carboxylic Acids 12a-l and 13a-l



General Procedure. To a stirring suspension of potassium *tert*-butoxide (5.88 mmol) in Et_2O (15 mL) cooled to 0 °C, was added water (1.4 mmol) via syringe. The slurry was stirred for 5 min, and **6a-l** or **7a-l** (0.67 mmol) was added. The mixture was stirred at room temperature until

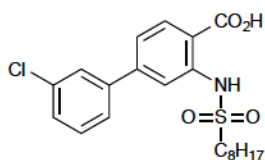
starting material disappeared by TLC analysis (20% EtOAc in hexanes). Ice water was added until 2 clear layers formed. The aqueous layer was separated and acidified with 1 M HCl. The product was then extracted with EtOAc (3 × 20 mL), evaporated *in vacuo*, and recrystallized (EtOAc/hexanes) or purified by column chromatography (3:17:80 AcOH:EtOAc:hexanes).



2-Chloro-3-(octanesulfonamido)-biphenyl-4-carboxylic acid (12a).

89% yield; mp = 200-201 °C; ¹H-NMR (400 MHz; DMSO-*d*₆): δ 8.00 (d, *J* = 8.0 Hz, 1H), 7.56 (d, *J* = 8.0 Hz, 1H), 7.48 (s, 1H), 7.42 (m, 3H), 6.96

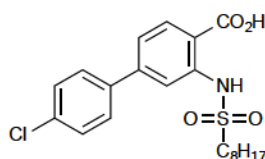
(d, *J* = 8.0 Hz, 1H), 3.08 (t, *J* = 7.6 Hz, 2H), 1.62 (m, 2H), 1.20 (m, 10H), 0.80 (t, *J* = 7.2 Hz, 3H); ¹³C-NMR (100 MHz; MeOD): δ 171.1, 146.8, 142.0, 140.0, 133.0, 133.0, 132.1, 131.1, 130.7, 128.4, 124.7, 119.6, 115.9, 52.3, 32.7, 29.8, 29.8, 28.7, 24.3, 23.5, 14.4. Anal. (C₂₁H₂₆ClNO₄S) C, H, N.



3-Chloro-3-(octylsulfonamido)-biphenyl-4-carboxylic acid (12b).

90% yield; mp = 120-121 °C; ¹H-NMR (400 MHz; MeOD): δ 8.21 (d, *J* = 8.4 Hz, 1H), 7.98 (s, 1H), 7.68 (s, 1H), 7.62 (d, *J* = 7.6 Hz, 1H),

7.46 (m, 3H), 3.25 (t, *J* = 7.6 Hz, 2H), 1.78 (m, 2H), 1.38 (m, 2H), 1.23 (m, 8H), 0.87 (t, *J* = 7.2 Hz, 3H); ¹³C-NMR (100 MHz; MeOD): δ 171.2, 146.7, 142.9, 142.6, 135.9, 133.8, 131.6, 129.6, 128.0, 126.6, 122.3, 117.1, 116.7, 52.5, 32.8, 29.9, 29.8, 28.8, 24.4, 23.6, 14.4. Anal. (C₂₁H₂₆ClNO₄S) C, H, N.

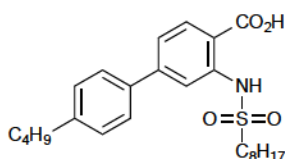


4-Chloro-3-(octanesulfonamido)-biphenyl-4-carboxylic acid (12c).

86% yield; mp = 162-163 °C; ¹H-NMR (400 MHz; MeOD): δ 8.15 (d, *J* = 8.0 Hz, 1H), 7.89 (d, *J* = 1.6 Hz, 1H), 7.65 (d, *J* = 6.8 Hz, 2H), 7.48

(d, *J* = 6.8 Hz, 2H), 7.35 (dd, *J* = 2.0, 8.0 Hz, 1H), 3.14 (t, *J* = 8.0 Hz, 2H), 1.76 (m, 2H), 1.35 (m, 2H), 1.22 (m, 8H), 0.86 (t, *J* = 6.8 Hz, 3H); ¹³C-NMR (100 MHz; MeOD): δ 165.9, 147.0,

142.9, 139.3, 135.9, 133.8, 130.2, 129.7, 122.3, 117.0, 115.2, 52.5, 32.8, 29.9, 29.8, 28.8, 24.5, 23.6, 14.3. Anal. (C₂₁H₂₆ClNO₄S) C, H, N.

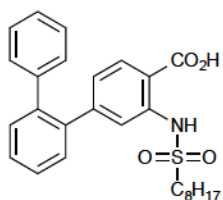


4'-Butyl-4-(octanesulfonamido)-[1,1'-biphenyl]-3-carboxylic acid

(12d). 85% yield; mp = 134-135 °C; ¹H-NMR (400 MHz; CDCl₃): δ

10.23 (s, 1H), 8.19 (d, *J* = 8.4 Hz, 1H), 8.03 (d, *J* = 1.6 Hz, 1H), 7.58

(d, *J* = 8.1 Hz, 2H), 7.39 (dd, *J* = 8.4, 1.6 Hz, 1H), 7.30 (d, *J* = 8.1 Hz, 2H), 3.22 (t, *J* = 7.9 Hz, 2H), 2.68 (t, *J* = 7.7 Hz, 2H), 1.87-1.83 (m, 2H), 1.68-1.61 (m, 2H), 1.42-1.35 (m, 4H), 1.23 (s, 9H), 0.96 (t, *J* = 7.3 Hz, 3H), 0.84 (t, *J* = 6.8 Hz, 3H); ¹³C-NMR (101 MHz, CDCl₃): δ 172.82, 148.92, 144.30, 142.16, 136.30, 133.16, 129.27, 127.33, 121.37, 115.83, 112.26, 52.45, 35.47, 33.65, 31.76, 29.03, 28.96, 28.16, 23.50, 22.66, 22.47, 14.14, 14.05; Anal. (C₂₅H₃₅NO₄S) C, H, N.

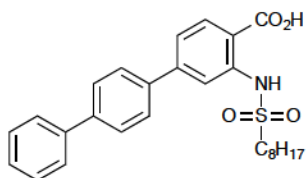


2-Phenyl-3-(octanesulfonamido)-biphenyl-4-carboxylic acid (12e).

84% yield; mp = 110-111 °C; ¹H-NMR (400 MHz; MeOD): δ 8.06 (d, *J* =

8.4 Hz, 1H), 7.45 (m, 5H), 7.23 (m, 5H), 7.12 (dd, *J* = 8.0, 1.2 Hz, 1H),

2.61 (t, *J* = 8.0 Hz, 2H), 1.56 (m, 2H), 1.26 (m, 10H), 0.91 (t, *J* = 7.2 Hz, 3H); ¹³C-NMR (100 MHz; MeOD): δ 171.3, 149.8, 142.6, 141.8, 141.8, 140.4, 133.1, 131.8, 131.2, 130.9, 129.5, 129.3, 128.7, 127.9, 124.9, 120.1, 114.9, 51.5, 32.8, 30.0, 29.9, 28.7, 24.5, 23.6, 14.4. Anal. (C₂₇H₃₁NO₄S) C, H, N.



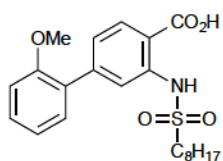
4-Phenyl-3-(octanesulfonamido)-biphenyl-4-carboxylic acid

(12f). 83% yield; mp = 220-221 °C; ¹H-NMR (400 MHz; DMSO-

d₆): δ 8.08 (d, *J* = 8.4 Hz, 1H), 7.81 (m, 7H), 7.49 (m, 3H), 7.39 (t, *J*

= 7.2 Hz, 1H), 3.31 (t, *J* = 8.0 Hz, 2H), 1.64 (m, 2H), 1.31 (m, 2H), 1.18 (m, 8H), 0.79 (t, *J* = 6.8 Hz, 3H); ¹³C-NMR (100 MHz; DMSO-d₆): δ 169.8, 145.0, 141.5, 140.3, 139.3, 137.6,

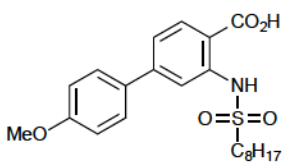
132.3, 128.9, 127.7, 127.4, 127.3, 126.6, 120.5, 115.3, 114.9, 51.0, 31.0, 28.2, 28.1, 27.0, 23.0, 21.9, 13.8. HRMS (FAB) calcd for $C_{27}H_{31}NO_4S$ $[M]^+$, 465.19738; found, 465.19692.



2-Methoxy-3-(octanesulfonamido)-biphenyl-4-carboxylic acid (12g).

89% yield; mp = 100-101 °C; 1H -NMR (400 MHz; MeOD): δ 8.12 (d, J = 8.4 Hz, 1H), 7.93 (s, 1H), 7.40 (m, 2H), 7.28 (d, J = 8.4 Hz, 1H), 7.11 (m,

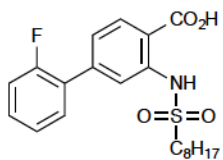
2H), 3.85 (s, 3H), 3.25 (t, J = 7.8 Hz, 2H), 1.71 (m, 2H), 1.22 (m, 10H), 0.87 (t, J = 6.9 Hz, 3H); ^{13}C -NMR (100 MHz; MeOD): δ 173.9, 157.9, 146.4, 132.7, 131.4, 131.0, 130.0, 124.8, 122.0, 119.9, 119.2, 112.8, 112.3, 56.1, 51.8, 32.8, 29.8, 29.8, 28.8, 24.4, 23.5, 14.3. Anal. ($C_{22}H_{28}NNaO_5S$) C, H, N.



4-Methoxy-3-(octanesulfonamido)-biphenyl-4-carboxylic acid

(12h). 94% yield; mp = 144 °C; 1H -NMR (400 MHz; MeOD): δ 8.12 (d, J = 8.4 Hz, 1H), 7.94 (d, J = 1.6 Hz, 1H), 7.60 (d, J = 6.8 Hz, 2H),

7.37 (dd, J = 1.6, 8.4 Hz, 1H), 7.02 (dd, J = 2.0, 6.8 Hz, 2H), 3.84 (s, 3H), 3.20 (t, J = 7.6 Hz, 2H), 1.73 (m, 2H), 1.34 (m, 2H), 1.20 (m, 8H), 0.86 (t, J = 6.8 Hz, 3H); ^{13}C -NMR (100 MHz; MeOD): δ 171.4, 161.8, 148.2, 142.9, 133.6, 132.7, 129.3, 121.8, 116.3, 115.5, 115.2, 55.8, 52.3, 32.8, 29.9, 29.8, 28.8, 24.4, 23.6, 14.4. Anal. ($C_{22}H_{29}NO_5S$) C, H, N.

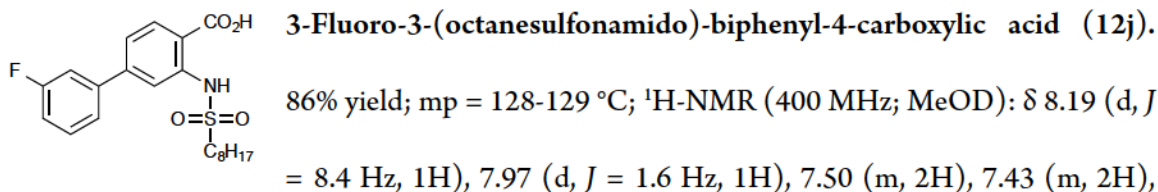


2-Fluoro-3-(octanesulfonamido)-biphenyl-4-carboxylic acid (12i). 91%

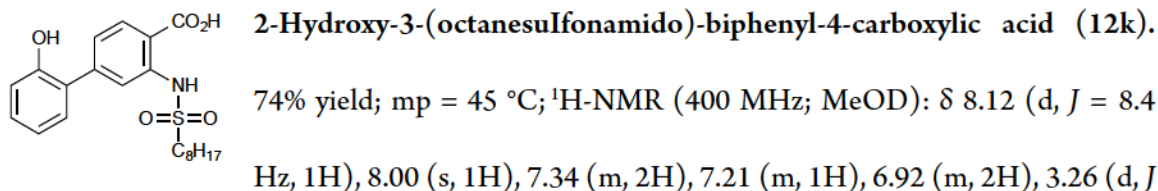
yield; mp = 117-118 °C; 1H -NMR (400 MHz; MeOD): δ 8.16 (dd, J = 2.8, 8.4 Hz, 1H), 7.92 (d, J = 1.6 Hz, 1H), 7.53 (m, 1H), 7.42 (m, 1H), 7.31 (m,

2H), 7.24 (m, 1H), 3.21 (t, J = 7.6 Hz, 2H), 1.73 (m, 2H), 1.33 (m, 2H), 1.24 (m, 8H), 0.85 (t, J = 7.2 Hz, 3H); ^{13}C -NMR (100 MHz; MeOD): δ 171.2, 161.0 (d, J = 250 Hz), 143.3, 142.5, 133.3, 131.6 (d, J = 2.7 Hz), 131.5, 128.6 (d, J = 13.0 Hz), 125.9 (d, 2.6 Hz), 124.2 (d, J = 2.9

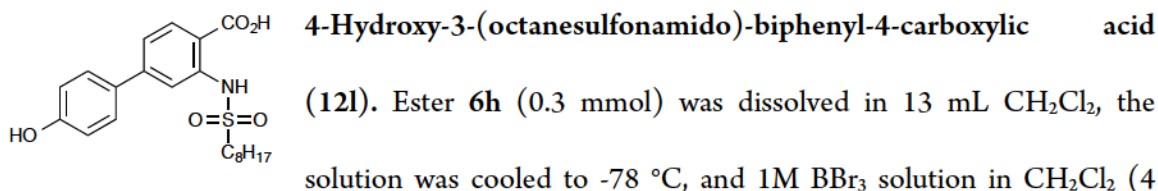
Hz), 119.1 (d, $J = 3.5$ Hz), 117.2 (d, $J = 22.4$ Hz), 116.1, 52.3, 32.7, 29.8, 29.8, 28.8, 24.4, 23.5, 14.3. Anal. ($C_{21}H_{26}FNO_4S$) C, H, N.



7.16 (m, 1H), 3.22 (t, $J = 7.6$ Hz, 2H), 1.76 (m, 2H), 1.39 (m, 2H), 1.23 (m, 8H), 0.87 (t, $J = 7.2$ Hz, 3H); ^{13}C -NMR (100 MHz; MeOD): δ 171.7, 164.5 (d, $J = 243.8$ Hz), 146.3 (d, $J = 2.0$ Hz), 143.1, 142.7, 133.7, 131.8 (d, $J = 8.6$ Hz), 124.0 (d, $J = 2.7$ Hz), 122.2, 118.2, 117.1, 116.1 (d, $J = 21.3$ Hz), 114.8 (d, $J = 22.5$ Hz), 52.4, 32.7, 29.9, 29.8, 28.8, 24.4, 23.5, 14.3. Anal. ($(C_{21}H_{26}FNO_4S) \cdot 0.5(AcOH)$) C, H, N.

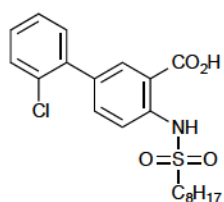


(100 MHz; MeOD): δ 175.2, 155.7, 146.5, 141.8, 132.7, 131.3, 130.6, 128.0, 124.5, 121.0, 119.5, 117.1, 116.4, 51.7, 32.7, 29.8, 29.8, 28.8, 24.3, 23.5, 14.3. Anal. ($(C_{21}H_{27}NO_5S) \cdot (H_2O)$) C, H, N.



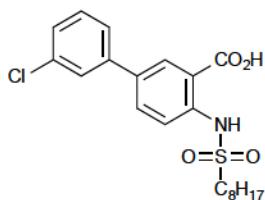
equiv) was added slowly. The solution was stirred and warmed to room temperature, and when complete by TLC (30% EtOAc in hexanes), the solution was acidified with 1M HCl and extracted with EtOAc (3 \times 20 mL). The product was then evaporated *in vacuo*, and

recrystallized (EtOAc/hexanes) or purified by column chromatography (3:17:80 AcOH:EtOAc:hexanes). 69% yield; mp = 61-62 °C; ¹H-NMR (400 MHz; MeOD): δ 8.11 (d, *J* = 8.0 Hz, 1H), 7.92 (s, 1H), 7.52 (d, *J* = 8.8 Hz, 2H), 7.37 (m, 1H), 6.89 (d, *J* = 8.8 Hz, 2H), 3.19 (t, *J* = 7.6 Hz, 2H), 1.72 (m, 2H), 1.34 (m, 2H), 1.19 (m, 8H), 0.86 (t, *J* = 6.8 Hz, 3H); ¹³C-NMR (100 MHz; MeOD): δ 171.5, 159.5, 148.4, 142.8, 133.6, 131.6, 129.3, 121.6, 116.9, 116.2, 110.7, 52.2, 32.8, 29.9, 29.8, 28.8, 24.4, 23.5, 14.3. Anal. ((C₂₁H₂₇NO₅S)·0.3(AcOH)) C, H, N.



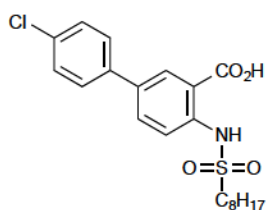
2-Chloro-4-(octanesulfonamido)-biphenyl-3-carboxylic acid (13a).

85% yield; mp = 74-75 °C; ¹H-NMR (400 MHz; MeOD): δ 8.17 (d, *J* = 2.4 Hz, 1H), 7.76 (d, *J* = 8.4 Hz, 1H), 7.60 (dd, *J* = 8.4, 2.4 Hz, 1H), 7.49 (d, *J* = 8.0 Hz, 1H), 7.37 (m, 3H), 3.21 (t, *J* = 8.0 Hz, 2H), 1.76 (m, 2H), 1.20 (m, 10H), 0.86 (t, *J* = 7.2 Hz, 3H); ¹³C-NMR (100 MHz; MeOD): δ 172.1, 141.6, 140.3, 135.6, 135.0, 133.9, 133.4, 132.3, 131.0, 130.0, 128.3, 118.4, 115.4, 52.2, 32.8, 29.9, 29.9, 28.9, 24.4, 23.6, 14.3. Anal. ((C₂₁H₂₆ClNO₄S)·0.3(AcOH)) C, H, N.



3-Chloro-4-(octanesulfonamido)-biphenyl-3-carboxylic acid (13b).

89% yield; mp = 133-134 °C; ¹H-NMR (400 MHz; MeOD): δ 8.29 (s, 1H), 7.81 (m, 2H), 7.57 (m, 1H), 7.52 (d, *J* = 7.6 Hz, 1H), 7.42 (t, *J* = 8.0 Hz, 1H), 7.34 (d, *J* = 8.0 Hz, 1H), 3.22 (t, *J* = 8.0 Hz, 2H), 1.72 (m, 2H), 1.23 (m, 10H), 0.83 (t, 7.2 Hz, 3H); ¹³C-NMR (100 MHz; MeOD): δ 171.1, 142.4, 142.1, 135.9, 135.2, 134.0, 131.5, 131.2, 128.5, 127.5, 126.0, 119.4, 117.4, 52.4, 32.8, 29.9, 29.9, 28.8, 24.4, 23.6, 14.3. Anal. (C₂₁H₂₆ClNO₄S) C, H, N.



4-Chloro-4-(octanesulfonamido)-biphenyl-3-carboxylic acid (13c).

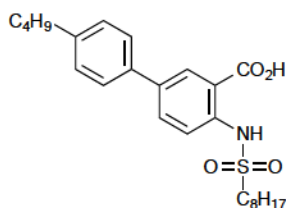
91% yield; mp = 143-144 °C; ¹H-NMR (400 MHz; MeOD): δ 8.31 (d,

J = 2.0 Hz, 1H), 7.81 (m, 2H), 7.58 (d, *J* = 8.8 Hz, 2H), 7.43 (d, *J* = 8.4

Hz, 2H), 3.22 (t, *J* = 7.6 Hz, 2H), 1.73 (m, 2H), 1.35 (m, 2H), 1.22 (m, 8H), 0.86 (t, *J* = 7.2 Hz,

3H); ¹³C-NMR (100 MHz; MeOD): δ 171.1, 141.8, 139.1, 135.5, 134.7, 133.8, 131.0, 130.1,

129.1, 119.5, 117.5, 52.4, 32.8, 29.9, 29.9, 28.8, 24.5, 23.6, 14.4. Anal. (C₂₁H₂₆ClNO₄S) C, H, N.



4'-Butyl-4-(octanesulfonamido)-biphenyl-3-carboxylic acid

(13d). 93% yield; mp = 103-104 °C; ¹H-NMR (300 MHz, CDCl₃): δ

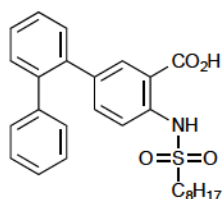
0.85 (t, 3H, *J* = 6.8), 0.97 (t, 3H, *J* = 7.2), 1.25 (m, 8H), 1.41 (m, 4H),

1.66 (m, 2H), 1.87 (m, 2H), 2.68 (t, 2H, *J* = 7.8), 3.24 (t, 2H, *J* = 7.5), 7.30 (d, 2H, *J* = 7.5), 7.52

(d, 2H, *J* = 7.8), 7.86 (m, 2H), 8.41 (s, 1H), 10.22 (s, 1H); ¹³C-NMR (75 MHz, CDCl₃): δ 14.0,

14.0, 22.4, 22.6, 23.4, 28.1, 28.9, 28.9, 31.7, 33.6, 35.3, 52.4, 114.5, 118.3, 126.5, 129.1, 130.6,

134.2, 135.9, 136.1, 140.3, 142.8, 172.4; Anal. (C₂₅H₃₅NO₄S) C, H, N.



2-Phenyl-4-(octanesulfonamido)-biphenyl-3-carboxylic acid (13e).

88% yield; mp = 114-115 °C; ¹H-NMR (400 MHz; MeOD): δ 7.89 (d, *J* =

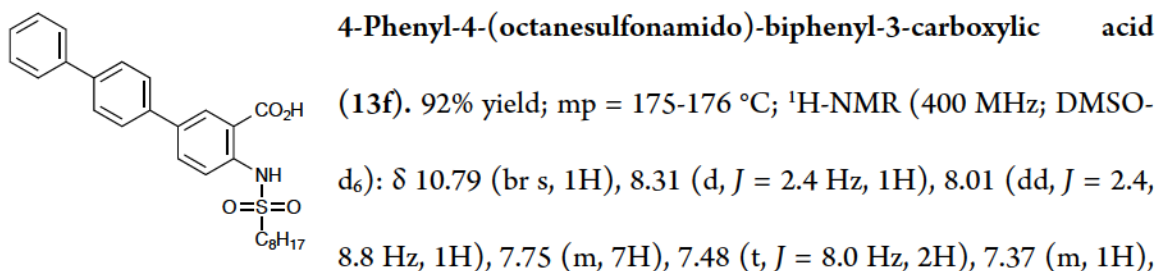
2.0 Hz, 1H), 7.51 (d, *J* = 8.8 Hz, 1H), 7.38 (m, 4H), 7.19 (m, 4H), 7.09 (m,

2H), 3.10 (t, *J* = 8.0 Hz, 2H), 1.65 (m, 2H), 1.21 (m, 10H), 0.86 (t, *J* = 6.8 Hz, 3H); ¹³C-NMR

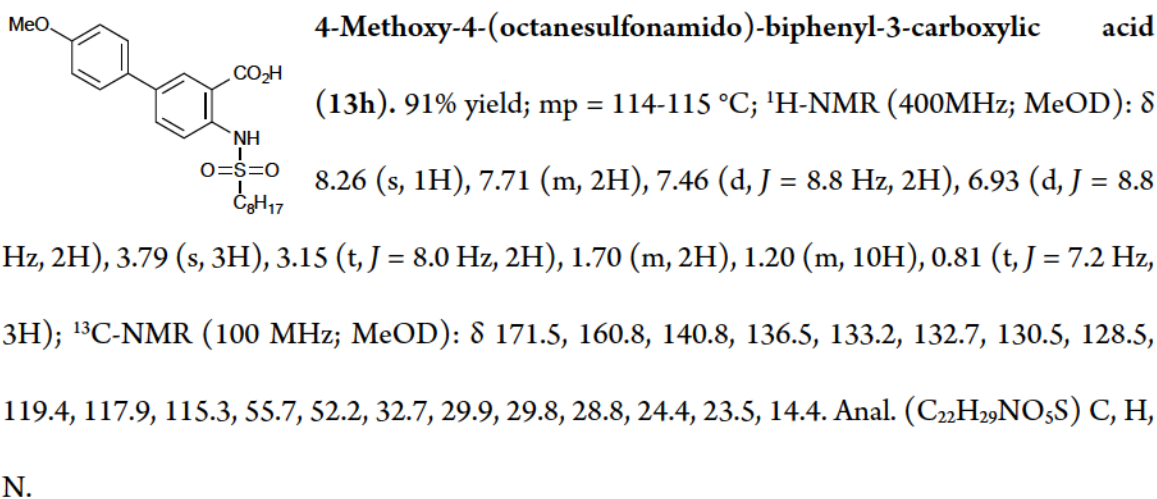
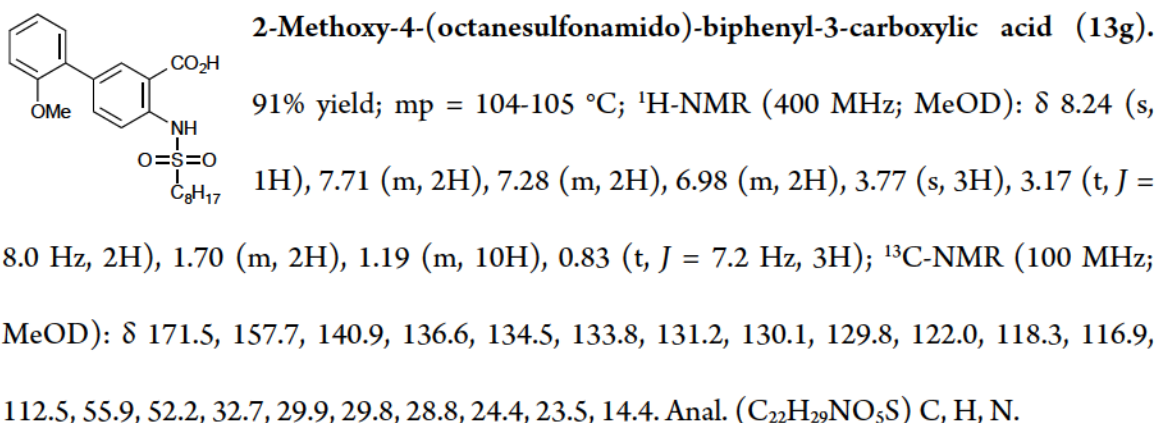
(100 MHz; MeOD): δ 171.3, 142.5, 141.9, 140.8, 139.9, 137.5, 137.0, 134.3, 131.2, 130.9,

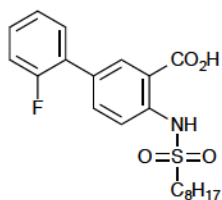
129.0, 129.0, 128.8, 127.7, 118.4, 116.9, 52.2, 32.8, 29.9, 29.9, 28.9, 24.4, 23.6, 14.4; Anal.

(C₂₇H₃₁NO₄S) C, H, N.



3.33 (t, *J* = 7.6 Hz, 2H), 1.65 (m, 2H), 1.33 (m, 2H), 1.20 (m, 8H), 0.81 (t, *J* = 7.2 Hz, 3H); ¹³C-NMR (100 MHz; DMSO-*d*₆): δ 169.8, 139.9, 139.4, 139.2, 137.3, 133.7, 132.6, 129.1, 128.9, 127.5, 127.3, 126.8, 126.5, 118.2, 116.4, 51.0, 31.0, 28.2, 28.2, 27.0, 22.9, 21.9, 13.8; HRMS (FAB) calcd for C₂₇H₃₁NO₄S [M]⁺, 465.19738; found, 465.19766.





2-Fluoro-4-(octanesulfonamido)-biphenyl-3-carboxylic acid (13i). 90%

yield; mp = 91-92 °C; ¹H-NMR (400 MHz; MeOD): δ 8.27 (s, 1H), 7.78

(d, *J* = 8.4 Hz, 1H), 7.70 (d, *J* = 8.4 Hz, 1H), 7.42 (t, *J* = 8.0 Hz, 1H), 7.32

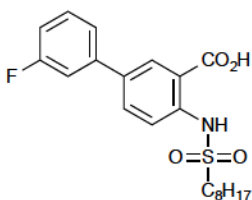
(m, 1H), 7.21 (t, *J* = 7.6 Hz, 1H), 7.15 (m, 1H), 3.19 (t, *J* = 7.6 Hz, 2H), 1.73 (m, 2H), 1.32 (m,

2H), 1.17 (m, 8H), 0.81 (t, *J* = 7.2 Hz, 3H); ¹³C-NMR (100 MHz; MeOD): δ 171.3, 160.9 (d, *J*

= 245 Hz), 141.7, 135.7 (d, *J* = 3.4 Hz), 133.3 (d, *J* = 3.3 Hz), 131.3 (d, *J* = 3.0 Hz), 130.5 (d, *J*

= 8.4 Hz), 128.4, 128.2, 125.7 (d, *J* = 3.6 Hz), 118.7, 117.5, 117.0 (d, *J* = 22.8 Hz), 52.4, 32.7, 29.8,

29.8, 28.8, 24.4, 23.5, 14.3. Anal. (C₂₁H₂₆FNO₄S) C, H, N.



3-Fluoro-4-(octanesulfonamido)-biphenyl-3-carboxylic acid (13j).

82% yield; mp = 102-103 °C; ¹H-NMR (400 MHz; MeOD): δ 8.31 (s,

1H), 7.79 (s, 2H), 7.41 (m, 2H), 7.30 (d, *J* = 10.4 Hz, 1H), 7.05 (m,

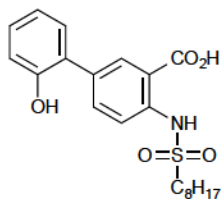
1H), 3.20 (t, *J* = 7.6 Hz, 2H), 1.73 (m, 2H), 1.33 (m, 2H), 1.21 (m, 8H), 0.82 (t, *J* = 6.8 Hz,

3H); ¹³C-NMR (100 MHz; MeOD): δ 171.3, 164.6 (d, *J* = 243 Hz), 142.9 (d, *J* = 7.4 Hz),

141.9, 135.2, 133.6, 131.7 (d, *J* = 8.4 Hz), 131.2, 123.3 (d, *J* = 2.9 Hz), 119.3, 118.1, 115.1 (d, *J*

= 21.1 Hz), 114.2 (d, *J* = 22.3 Hz), 52.4, 32.8, 29.9, 29.9, 28.8, 24.4, 23.5, 14.3. Anal.

(C₂₁H₂₆FNO₄S) C, H, N.



2-Hydroxy-4-(octanesulfonamido)-biphenyl-3-carboxylic acid (13k).

71% yield; mp = 59 °C; ¹H-NMR (400 MHz; MeOD): δ 8.33 (s, 1H), 7.75

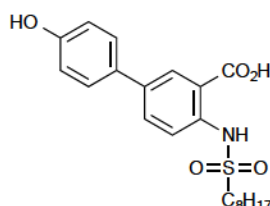
(dd, *J* = 8.4, 2.4 Hz, 1H), 7.69 (d, *J* = 8.4 Hz, 1H), 7.28 (dd, *J* = 8.0, 1.6 Hz,

1H), 7.15 (dt, *J* = 7.6, 1.6 Hz, 1H), 6.90 (m, 2H), 3.17 (t, *J* = 8.0 Hz, 2H), 1.75 (m, 2H), 1.23

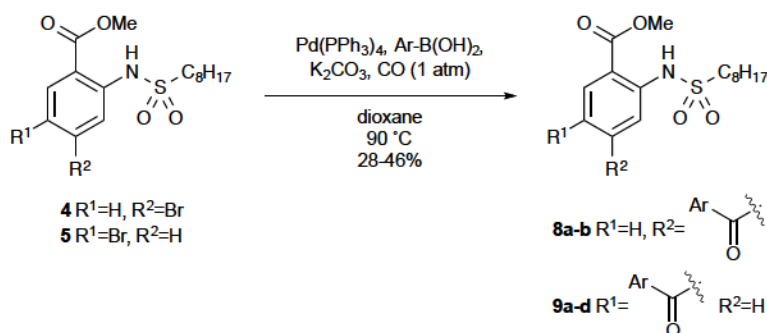
(m, 10H), 0.86 (t, *J* = 7.2 Hz, 3H); ¹³C-NMR (100 MHz; MeOD): δ 173.0, 155.4, 140.3, 135.1,

134.8, 133.6, 131.2, 129.6, 128.4, 120.9, 120.8, 118.4, 116.9, 51.9, 32.7, 29.9, 29.9, 28.9, 24.4,

23.5, 14.3. Anal. ((C₂₁H₂₇NO₅S)·0.3(AcOH)) C, H, N.

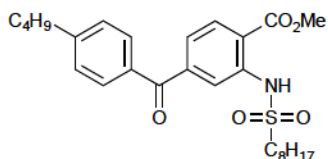

4-Hydroxy-4-(octanesulfonamido)-biphenyl-3-carboxylic acid
(13l). 71% yield; mp = 142 °C; ¹H-NMR (400 MHz; MeOD): δ 8.26 (s, 1H), 7.73 (m, 2H), 7.43 (d, *J* = 8.7 Hz, 2H), 6.87 (d, *J* = 8.7 Hz, 2H), 3.17 (t, *J* = 8.0 Hz, 2H), 1.69 (m, 2H), 1.34 (m, 2H), 1.24 (m, 8H), 0.82 (t, *J* = 7.2 Hz, 3H); ¹³C-NMR (100 MHz; MeOD): δ 175.2, 158.3, 140.5, 137.0, 133.2, 131.7, 130.3, 128.6, 119.4, 117.7, 116.7, 52.1, 32.7, 29.8, 29.8, 28.7, 24.3, 23.5, 14.3. Anal. (C₂₁H₂₇NO₅S) C, H, N.

Preparation of Suzuki Coupling products 8a-b and 9a-d



General Procedure. To an round bottom flask flushed with carbon monoxide was added 1.23 mmol of aryl bromide **4** or **5**, dioxane (9 mL), Pd(PPh₃)₄ (10 mol%), K₂CO₃ (3.0 equiv), and boronic acid (1.1 eq). The catalyst was loaded by bubbling CO through the solution, and the reaction mixture was heated to 90 °C and stirred under 1 atm of carbon monoxide. Reaction progress was monitored by TLC (10% EtOAc in hexanes) until disappearance of starting material was observed (approx. 24 h). Upon completion, the reaction was quenched with 1 M HCl solution, and the crude product was extracted with EtOAc (3 × 20 mL). The combined organic extracts were washed with brine, dried with MgSO₄, and concentrated *in vacuo*. Purification by flash chromatography (10% EtOAc in hexanes) afforded carbonyl insertion

Suzuki products **8a-b** or **9a-d** as well as directly-coupled Suzuki side products without carbonyl insertion.



Methyl 4-(4-n-butylbenzoyl)-2-(octanesulfonamido)benzoate

(8a). 25% yield (48% directly-coupled product); ¹H-NMR (400

MHz; CDCl₃): δ 10.46 (s, 1H), 8.15 (d, *J* = 8.2 Hz, 1H), 8.03 (d, *J*

= 1.5 Hz, 1H), 7.75 (d, *J* = 8.3 Hz, 2H), 7.43 (dd, *J* = 8.2, 1.5 Hz, 1H), 7.30 (d, *J* = 8.3 Hz, 2H),

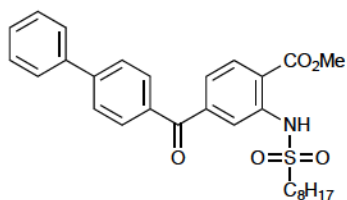
3.98 (s, 3H), 3.17-3.14 (m, 2H), 2.69 (t, *J* = 7.8 Hz, 2H), 1.84-1.77 (m, 2H), 1.65-1.50 (m, 2H),

1.40-1.35 (m, 4H), 1.28-1.22 (m, 8H), 0.94 (t, *J* = 7.3 Hz, 3H), 0.85 (t, *J* = 6.9 Hz, 3H); ¹³C-

NMR (101 MHz, CDCl₃): δ 194.89, 167.90, 149.35, 143.67, 140.99, 133.75, 131.59, 130.47,

128.65, 122.94, 121.12, 118.61, 52.91, 52.83, 35.81, 33.22, 31.68, 28.96, 28.89, 28.06, 23.42,

22.59, 22.39, 14.07, 13.93.



Methyl

4-([1,1'-biphenyl]-4-carbonyl)-2-

(octanesulfonamido)benzoate (8b). 35% yield (44% directly-

coupled product); ¹H-NMR (400 MHz; CDCl₃): δ 10.48 (s,

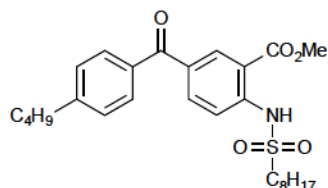
1H), 8.18 (d, *J* = 8.2 Hz, 1H), 8.09 (d, *J* = 1.5 Hz, 1H), 7.93-7.90 (m, 2H), 7.73-7.71 (m, 2H),

7.66-7.64 (m, 2H), 7.55-7.40 (m, 4H), 3.99 (s, 3H), 3.20-3.16 (m, 2H), 1.86-1.78 (m, 2H),

1.39-1.35 (m, 2H), 1.28-1.22 (m, 8H), 0.86 (t, *J* = 6.9 Hz, 3H); ¹³C-NMR (101 MHz, CDCl₃): δ

194.94, 168.01, 146.31, 143.48, 141.19, 139.81, 134.94, 131.04, 129.14, 127.47, 127.36, 123.13,

118.85, 117.52, 53.08, 53.06, 31.81, 29.10, 29.02, 28.22, 23.57, 22.72, 14.20.



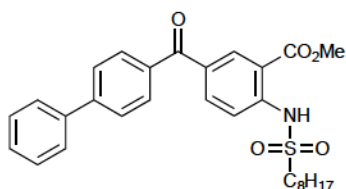
Methyl 5-(4-n-butylbenzoyl)-2-(octanesulfonamido)benzoate

(9a). 40% yield (37% directly-coupled product); ¹H-NMR (300

MHz, CDCl₃): δ 0.85 (t, 3H, *J* = 6.3), 0.94 (t, 3H, *J* = 7.2), 1.23

(m, 8H), 1.37 (m, 4H), 1.65 (m, 2H), 1.84 (m, 2H), 2.70 (t, 2H, *J* = 7.5), 3.21 (t, 2H, *J* = 7.8),

3.94 (s, 3H), 7.30 (d, 2H, $J = 8.1$), 7.70 (d, 2H, $J = 7.8$), 7.83 (d, 1H, $J = 8.7$), 7.97 (d, 1H, $J = 8.7$), 8.55 (s, 1H), 10.76 (s, 1H); ^{13}C -NMR (75 MHz, CDCl_3): δ 13.9, 14.0, 22.4, 22.6, 23.4, 28.0, 28.9, 28.9, 31.7, 33.3, 35.7, 52.8, 52.8, 114.3, 116.6, 128.6, 130.1, 131.7, 133.8, 134.5, 136.3, 144.3, 148.6, 168.0, 194.1.

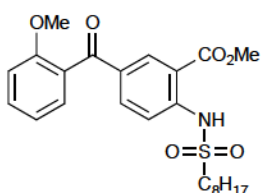


Methyl

5-([1,1'-biphenyl]-4-carbonyl)-2-

(octanesulfonamido)benzoate (9b). 32% yield (42% directly-coupled product); ^1H -NMR (400 MHz, CDCl_3): δ 0.87 (t, 3H, J

= 6.8), 1.15-1.30 (m, 8H), 1.35-1.45 (m, 2H), 1.80-1.90 (m, 2H), 3.24 (t, 2H, $J = 8.0$), 3.95 (s, 3H), 7.38-7.55 (m, 3H), 7.66 (d, 2H, $J = 8.0$), 7.73 (d, 2H, $J = 8.0$), 7.84-7.89 (m, 3H), 8.03 (d, 1H, $J = 8.8$), 8.59 (s, 1H); ^{13}C -NMR (100 MHz, CDCl_3): δ 14.0, 22.5, 23.3, 28.0, 28.8, 28.9, 31.6, 52.8, 52.8, 114.2, 116.7, 127.1, 127.2, 128.3, 129.0, 130.5, 131.4, 133.9, 135.6, 136.3, 139.7, 144.5, 145.5, 167.9, 194.1.

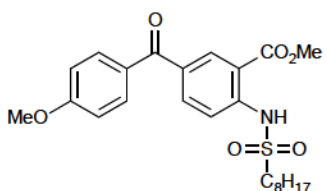


Methyl

5-(2-methoxybenzoyl)-2-(octanesulfonamido)benzoate

(9c). 28% yield (57% directly-coupled product); ^1H -NMR (400 MHz, CDCl_3): δ 0.82 (t, 3H, $J = 6.8$), 1.20 (m, 8H), 1.34 (m, 2H), 1.79 (m,

2H), 3.18 (t, 2H, $J = 8.0$), 3.69 (s, 3H), 3.89 (s, 3H), 6.98 (t, 1H, $J = 8.0$), 7.04 (d, 1H, $J = 7.6$), 7.33 (d, 1H, $J = 7.6$), 7.47 (t, 1H, $J = 7.6$), 7.74 (d, 1H, $J = 7.2$), 7.89 (dd, 1H, $J_1=8.8$, $J_2=2.0$), 8.53 (d, 1H, $J = 2.0$), 10.77 (s, 1H); ^{13}C -NMR (100 MHz, CDCl_3): δ 14.0, 22.5, 23.4, 28.0, 28.8, 28.9, 31.6, 52.7, 52.8, 55.6, 111.6, 114.2, 116.4, 120.8, 128.0, 129.7, 129.7, 132.4, 133.5, 136.3, 144.7, 157.2, 168.1, 194.1.

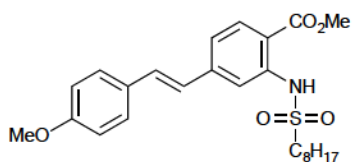


Methyl

5-(4-methoxybenzoyl)-2-

(octanesulfonamido)benzoate (9d). 46% yield (28% directly-

6H), 7.55 (d, 2H, $J = 8.0$), 7.88 (s, 1H), 8.02 (d, 1H, $J = 8.0$), 10.52 (s, 1H); ^{13}C -NMR (100 MHz, CDCl_3): δ 13.9, 22.4, 23.2, 27.9, 28.7, 28.8, 31.5, 51.9, 52.3, 113.5, 115.5, 120.0, 126.8, 126.9, 128.4, 128.7, 131.6, 132.5, 136.2, 141.3, 143.7, 168.1.



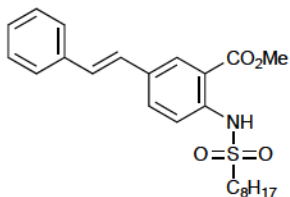
(*E*)-Methyl

4-(4-methoxystyryl)-2-

(octanesulfonamido)benzoate (**10b**). 58% yield; ^1H -NMR

(300 MHz, CDCl_3): δ 0.87 (t, 3H, $J = 7.2$), 1.33 (m, 10H), 1.80

(m, 2H), 3.15 (t, 2H, $J = 8.1$), 3.82 (s, 3H), 3.91 (s, 3H), 6.88 (m, 3H), 7.20 (m, 2H), 7.46 (d, 2H, $J = 8.7$), 7.82 (s, 1H), 7.97 (d, 1H, $J = 8.4$), 10.48 (s, 1H); ^{13}C -NMR (75 MHz, CDCl_3): δ 13.9, 22.5, 23.2, 27.9, 28.7, 28.8, 31.4, 51.8, 52.2, 55.1, 113.1, 114.1, 115.2, 119.8, 124.7, 128.2, 128.9, 131.6, 132.1, 141.4, 144.2, 159.9, 168.1.

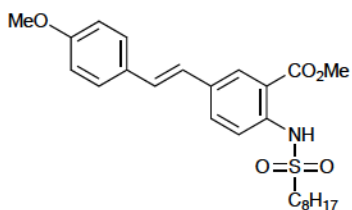


(*E*)-Methyl 2-(octanesulfonamido)-5-styrylbenzoate (**11a**). 83%

yield; ^1H -NMR (300 MHz, CDCl_3): δ 0.87 (t, 3H, $J = 7.2$), 1.23 (m,

10H), 1.81 (m, 2H), 3.16 (t, 2H, $J = 8.1$), 3.97 (s, 3H), 7.04 (d, 2H, J

= 2.1), 7.28 (m, 1H), 7.37 (t, 2H, $J = 7.5$), 7.51 (d, 2H, $J = 7.2$), 7.66 (dd, 1H, $J = 2.1, 8.7$), 7.76 (d, 1H, $J = 8.7$), 8.15 (d, 1H, $J = 2.1$), 10.43; ^{13}C -NMR (75 MHz, CDCl_3): δ 13.9, 22.4, 23.1, 27.8, 28.6, 28.7, 31.4, 52.0, 52.4, 115.1, 117.9, 126.3, 126.3, 127.7, 128.5, 128.8, 129.3, 131.8, 132.1, 136.6, 139.8, 168.0.



(*E*)-Methyl

5-(4-methoxystyryl)-2-

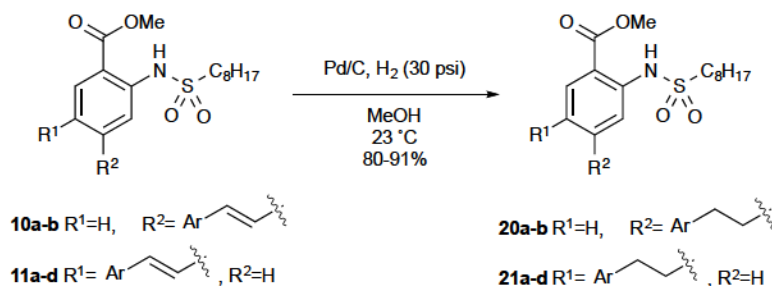
(octanesulfonamido)benzoate (**11b**). 73% yield; ^1H -NMR

(400 MHz, CDCl_3): δ 0.85 (t, 2H, $J = 7.2$), 1.26 (m, 10H), 1.77

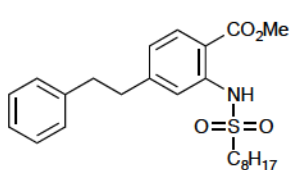
(m, 2H), 3.14 (t, 2H, $J = 7.8$), 3.77 (s, 3H), 3.94 (s, 3H), 6.82-7.01 (m, 4H), 7.42 (d, 2H, $J = 8.7$), 7.61 (d, 1H, $J = 8.7$), 7.73 (d, 1H, $J = 8.7$), 8.09 (s, 1H), 10.40 (s, 1H); ^{13}C -NMR (100

MHz, CDCl₃): δ 13.8, 22.3, 23.1, 27.8, 28.6, 28.7, 31.4, 51.9, 52.4, 55, 113.9, 115.0, 117.9, 124.1, 127.5, 128.3, 128.9, 129.3, 131.8, 132.2, 139.4, 159.3, 168.3.

Preparation of Compounds 20a-b and 21a-b.

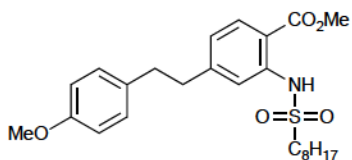


General Procedure. The alkene (0.5 mmol) was dissolved in anhydrous MeOH (5 mL), 10% Pd/C catalyst (30 mg) was added, and the solution was hydrogenated at 30 psi for 5h. When complete, the catalyst was removed by filtration and the reduced product was purified by column chromatography (10% EtOAc in hexanes).



Methyl 2-(octanesulfonamido)-4-phenethylbenzoate (20a). 89% yield; ¹H-NMR (400 MHz; CDCl₃): δ 10.43 (s, 1H), 7.95 (d, J = 8.1 Hz, 1H), 7.54 (s, 1H), 7.31-7.15 (m, 5H), 6.92 (d, J = 8.1 Hz, 1H),

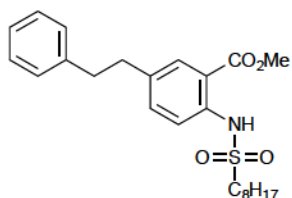
3.93 (s, 3H), 2.99 (m, 6H), 1.77 (m, 2H), 1.30 (m, 10H), 0.88 (t, J = 7.2 Hz, 3H); ¹³C-NMR (100 MHz; CDCl₃): δ 168.2, 149.5, 141.0, 140.6, 131.3, 128.3, 128.2, 126.0, 122.8, 117.5, 112.7, 52.2, 51.7, 37.7, 36.8, 31.5, 28.8, 28.7, 27.9, 23.2, 22.4, 13.9.



Methyl 4-(4-methoxyphenethyl)-2-(octanesulfonamido)benzoate (20b). 87% yield; ¹H-NMR (400 MHz; CDCl₃): δ 10.42 (s, 1H), 7.93 (d, J = 8.1 Hz, 1H),

7.53 (s, 1H), 7.05 (d, J = 8.4 Hz, 2H), 6.89 (d, J = 8.1 Hz, 1H), 6.80 (d, J = 8.4 Hz, 2H), 3.91 (s,

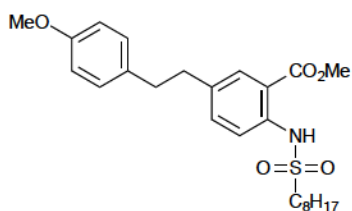
3H), 3.77 (s, 3H), 3.01 (t, $J = 8.1$ Hz, 2H), 2.92 (m, 4H), 1.75 (m, 2H), 1.26 (m, 10H), 0.86 (t, $J = 7.2$ Hz, 3H); ^{13}C -NMR (100 MHz; CDCl_3): δ 168.2, 157.7, 149.5, 140.9, 132.5, 131.3, 129.2, 122.9, 117.5, 113.6, 112.6, 55.0, 52.2, 51.5, 37.9, 35.9, 31.5, 28.7, 28.6, 27.8, 23.1, 22.4, 13.8.



Methyl 2-(octanesulfonamido)-5-phenethylbenzoate (21a). 91%

yield; ^1H -NMR (400 MHz; CDCl_3): δ 10.32 (s, 1H), 7.88 (d, $J = 2.1$ Hz, 1H), 7.69 (d, $J = 8.4$ Hz, 1H), 7.31 (m, 3H), 7.20 (m, 3H), 3.95

(s, 3H), 3.14 (t, $J = 7.8$ Hz, 2H), 2.93 (s, 4H), 1.80 (m, 2H), 1.32 (m, 10H), 0.89 (t, $J = 7.2$ Hz, 3H); ^{13}C -NMR (100 MHz; CDCl_3): δ 168.2, 140.8, 138.8, 136.0, 134.9, 130.9, 128.2, 128.2, 125.9, 117.9, 115.0, 52.3, 51.8, 37.4, 36.7, 31.5, 28.7, 28.6, 27.8, 23.1, 22.4, 13.9.



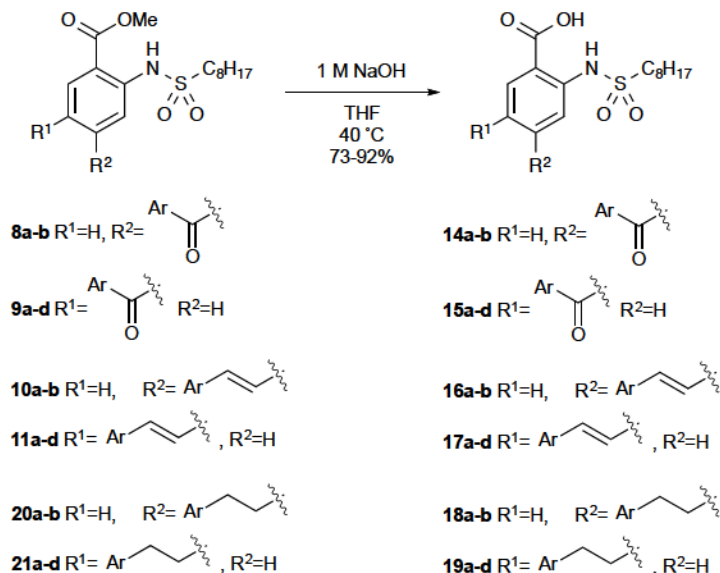
Methyl 5-(4-methoxyphenethyl)-2-

(octanesulfonamido)benzoate (21b). 80% yield; ^1H -NMR

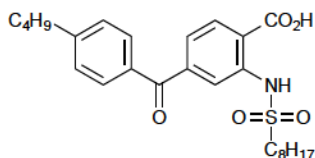
(400 MHz; CDCl_3): δ 10.29 (s, 1H), 7.84 (d, $J = 1.8$ Hz, 1H),

7.65 (d, $J = 8.4$ Hz, 1H), 7.30 (dd, $J = 2.1, 8.7$ Hz, 1H), 7.07 (d, $J = 8.4$ Hz, 2H), 6.82 (d, $J = 8.4$ Hz, 2H), 3.93 (s, 3H), 3.79 (s, 3H), 3.11 (t, $J = 8.0$ Hz, 2H), 2.85 (s, 4H), 1.77 (m, 2H), 1.30 (m, 10H), 0.85 (t, $J = 7.2$ Hz, 3H); ^{13}C -NMR (100 MHz; CDCl_3): δ 168.3, 157.8, 138.9, 136.1, 135.0, 133.0, 131.0, 129.2, 117.9, 115.0, 113.7, 55.1, 52.4, 51.8, 37.0, 36.6, 31.5, 28.8, 28.7, 27.9, 23.2, 22.4, 13.9.

Preparation of Benzoic Acids 14a-b, 15a-d, 16a-b, 17a-b, 18a-b, and 19a-b



General Procedure. To the starting ester (0.5 mmol) dissolved in THF (3 mL) at room temperature was added 1 M NaOH (3 mL). The reaction mixture was heated to 40 °C until the starting material had disappeared by TLC (20% EtOAc in hexanes). When complete, the solution was acidified with 1 M HCl and extracted with 3 × 10 mL EtOAc. The combined organic extracts were dried over Na₂SO₄, concentrated *in vacuo*, and the resulting product was purified by recrystallization (EtOAc/hexanes) or column chromatography (3:7:90 AcOH:EtOAc:hexanes).



4-(4-*n*-Butylbenzoyl)-2-(octanesulfonamido)benzoic acid

(14a). 85% yield; mp = 149-150 °C; ¹H-NMR (400 MHz, CDCl₃):

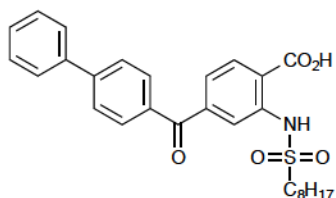
δ 10.27 (s, 1H), 8.23 (d, *J* = 8.2 Hz, 1H), 8.04 (d, *J* = 1.5 Hz, 1H),

7.76-7.74 (m, 2H), 7.45 (dd, *J* = 8.2, 1.5 Hz, 1H), 7.30 (d, *J* = 8.3 Hz, 2H), 3.21-3.17 (m, 2H),

2.69 (t, *J* = 7.7 Hz, 2H), 1.85-1.77 (m, 2H), 1.67-1.60 (m, 2H), 1.40-1.35 (m, 4H), 1.32-1.20

(m, 8H), 0.94 (t, *J* = 7.3 Hz, 3H), 0.85 (t, *J* = 6.9 Hz, 3H); ¹³C-NMR (101 MHz, CDCl₃): δ

195.11, 178.03, 172.12, 149.64, 144.50, 141.52, 133.71, 132.72, 130.63, 128.79, 123.15, 118.54, 116.61, 52.99, 35.91, 33.30, 31.78, 29.05, 28.99, 28.18, 23.50, 22.68, 22.48, 14.16, 14.02; Anal. ($C_{26}H_{35}NO_5S$) C, H, N.



4-([1,1'-Biphenyl]-4-carbonyl)-2-

(octanesulfonamido)benzoic acid (**14b**). 87% yield; mp = 188-

189 °C; 1H -NMR (400 MHz; $CDCl_3$): δ 8.27 (d, J = 8.2 Hz, 1H),

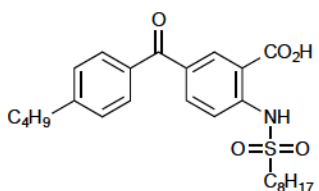
8.10 (d, J = 1.4 Hz, 1H), 7.92 (d, J = 8.3 Hz, 2H), 7.73 (d, J = 8.3 Hz, 2H), 7.67-7.64 (m, 2H),

7.51-7.42 (m, 4H), 3.21 (t, J = 7.9 Hz, 2H), 1.87-1.79 (m, 2H), 1.40-1.35 (m, 2H), 1.27-1.22

(m, 8H), 0.85 (t, J = 6.9 Hz, 3H); ^{13}C -NMR (101 MHz, $CDCl_3$): δ 194.73, 146.30, 144.17,

141.53, 139.64, 134.68, 132.69, 130.92, 129.01, 128.44, 127.34, 127.25, 123.08, 118.48, 52.98,

31.65, 28.95, 28.86, 28.08, 23.42, 22.57, 14.05; Anal. ($C_{28}H_{31}NO_5S$) C, H, N.



5-(4-*n*-Butylbenzoyl)-2-(octanesulfonamido)benzoic acid

(**15a**). 90% yield; mp = 149-150 °C; 1H -NMR (400 MHz,

$CDCl_3$): δ 0.84 (t, 3H, J = 6.8), 0.95 (t, 3H, J = 7.2), 1.24 (m, 8H),

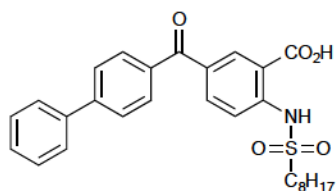
1.40 (m, 4H), 1.65 (m, 2H), 1.85 (m, 2H), 2.71 (t, 2H, J = 7.6), 3.25 (t, 2H, J = 8.0), 7.32 (d,

2H, J = 8.0), 7.72 (d, 2H, J = 8.0), 7.85 (d, 1H, J = 7.2), 8.05 (d, 1H, J = 7.2), 8.64 (s, 1H), 10.61

(s, 1H); ^{13}C -NMR (100 MHz, $CDCl_3$): δ 13.9, 14.0, 22.4, 22.6, 23.4, 28.1, 28.9, 28.9, 31.6, 33.2,

35.8, 53.0, 113.3, 116.8, 128.7, 130.2, 131.7, 134.3, 135.0, 137.2, 144.9, 148.9, 171.1, 194.5;

Anal. ($C_{26}H_{35}NO_5S$) C, H, N.

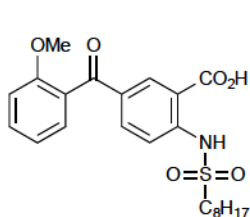


5-([1,1'-Biphenyl]-4-carbonyl)-2-

(octanesulfonamido)benzoate (**15b**). 91% yield; mp = 210-211

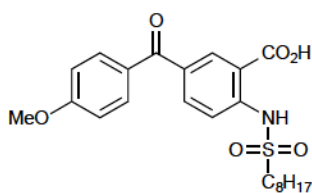
°C; 1H -NMR (400 MHz, $DMSO-d_6$): δ 0.87 (t, 3H, J = 6.8),

1.15-1.30 (m, 8H), 1.35-1.45 (m, 2H), 1.80-1.90 (m, 2H), 3.24 (t, 2H, $J = 8.0$), 3.95 (s, 3H), 7.40-7.55 (m, 3H), 7.70-7.90 (m, 7H), 8.06 (d, 1H, $J = 8.8$), 8.41 (s, 1H); ^{13}C -NMR (100 MHz, DMSO- d_6): δ 13.9, 22.0, 22.9, 27.1, 28.2, 28.3, 29.9, 31.1, 51.5, 115.1, 116.9, 126.8, 127.0, 128.4, 129.1, 130.3, 130.5, 133.6, 135.6, 135.8, 138.8, 144.2, 144.4; Anal. ($\text{C}_{28}\text{H}_{31}\text{NO}_5\text{S}$) C, H, N.



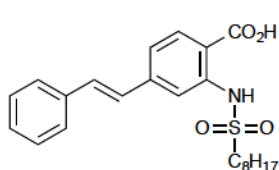
5-(2-methoxybenzoyl)-2-(octanesulfonamido)benzoic acid (15c).

81% yield; mp = 125-126 °C; ^1H -NMR (400 MHz, CDCl_3): δ 0.83 (t, 3H, $J = 6.8$), 1.22 (m, 8H), 1.40 (m, 2H), 1.78 (m, 2H), 3.37 (t, 2H, $J = 8.0$), 3.74 (s, 3H), 7.11 (t, 1H, $J = 7.2$), 7.18 (d, 1H, $J = 7.6$), 7.37 (dd, 1H, $J_1=7.6$, $J_2=2.0$), 7.55 (t, 1H, $J = 7.6$), 7.82 (d, 1H, $J = 7.2$), 7.99 (dd, 1H, $J_1=8.8$, $J_2=2.0$), 8.51 (d, 1H, $J = 2.0$), 11.00 (s, 1H); ^{13}C -NMR (100 MHz, CDCl_3): δ 13.4, 22.3, 23.3, 27.6, 28.7, 28.8, 31.5, 51.9, 55.1, 111.8, 114.1, 116.6, 120.8, 128.5, 129.2, 131.6, 132.2, 133.7, 135.6, 145.3, 157.2, 169.2, 193.3; Anal. ($\text{C}_{23}\text{H}_{29}\text{NO}_6\text{S}$) C, H, N.



5-(4-Methoxybenzoyl)-2-(octanesulfonamido)benzoic acid (15d).

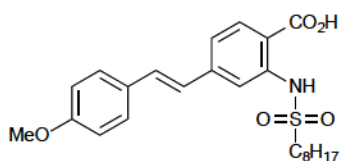
83% yield; mp = 132-133 °C; ^1H -NMR (400 MHz, CDCl_3): δ 0.84 (t, 3H, $J = 6.8$), 1.10-1.30 (m, 8H), 1.35-1.40 (m, 2H), 1.75-1.90 (m, 2H), 3.23 (t, 2H, $J = 8.0$), 3.90 (s, 3H), 6.98 (d, 2H, $J = 8.0$), 7.79 (d, 2H, $J = 8.4$), 7.83 (d, 1H, $J = 8.8$), 8.00 (d, 1H, $J = 8.8$), 8.58 (s, 1H), 10.63 (s, 1H); ^{13}C -NMR (100 MHz, CDCl_3): δ 14.0, 22.5, 23.3, 28.0, 28.8, 28.9, 31.6, 52.9, 55.5, 113.5, 113.8, 116.7, 129.4, 131.9, 132.4, 134.7, 136.8, 144.6, 163.6, 171.3, 193.5; Anal. ($\text{C}_{23}\text{H}_{28}\text{NNaO}_6\text{S} \cdot \frac{1}{4}(\text{H}_2\text{O})$) C, H, N.



(E)-2-(octanesulfonamido)-4-styrylbenzoic acid (16a).

80% yield; mp = 91-92 °C; ^1H -NMR (400 MHz, CDCl_3): δ 0.86 (t, 3H, $J = 7.2$), 1.20-1.30 (m, 8H), 1.35-1.48 (m, 2H), 1.80-1.90 (m, 2H), 3.24 (t, 2H,

$J = 8.0$), 7.10-7.44 (m, 7H), 7.57 (d, 2H, $J = 11.2$), 7.89 (s, 1H), 8.13 (d, 1H, $J = 8.4$), 10.28 (s, 1H); ^{13}C -NMR (100 MHz, CDCl_3): δ 14.0, 22.5, 23.3, 28.0, 28.8, 28.9, 31.6, 52.2, 112.5, 115.6, 120.3, 126.8, 127.0, 128.7, 128.8, 132.9, 133.3, 136.2, 142.0, 145.0, 172.5; Anal. ($\text{C}_{23}\text{H}_{29}\text{NO}_4\text{S}$) C, H, N.



(E)-4-(4-methoxystyryl)-2-(octanesulfonamido)benzoic acid

(16b). 91% yield; mp = 98-98 °C; ^1H -NMR (400 MHz, CDCl_3):

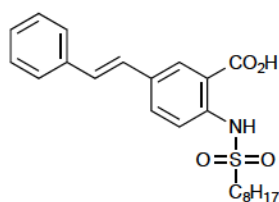
δ 0.84 (t, 3H, $J = 7.2$), 1.10-1.30 (m, 8H), 1.30-1.40 (m, 2H),

1.75-1.85 (m, 2H), 3.20 (t, 2H, $J = 8.0$), 3.85 (s, 3H), 6.90-7.00 (m, 3H), 7.20-7.30 (m, 3H),

7.49 (d, 2H, $J = 8.8$), 7.84 (s, 1H), 8.08 (d, 1H, $J = 8.4$), 10.25; ^{13}C -NMR (100 MHz, CDCl_3): δ

14.0, 22.5, 23.4, 28.0, 28.8, 28.9, 31.6, 52.1, 55.4, 112.0, 114.3, 115.2, 120.1, 124.7, 128.5, 129.0,

132.8, 132.9, 142.1, 145.4, 160.2, 172.2; Anal. ($\text{C}_{24}\text{H}_{30}\text{NNaO}_5\text{S} \cdot 1(\text{H}_2\text{O})$) C, H, N.



(E)-2-(Octanesulfonamido)-5-styrylbenzoic acid (17a). 92% yield;

mp = 94-95 °C; ^1H -NMR (400 MHz, CDCl_3): δ 0.86 (t, 3H, $J = 7.2$),

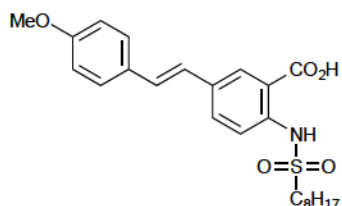
1.15-1.30 (m, 8H), 1.30-1.45 (m, 2H), 1.80-1.90 (m, 2H), 3.20 (t, 2H,

$J = 8.0$), 7.00-7.10 (m, 2H), 7.20-7.40 (m, 3H), 7.52 (d, 2H, $J = 8.4$), 7.70-7.80 (m, 2H), 8.25 (s,

1H), 10.25 (s, 1H); ^{13}C -NMR (100 MHz, CDCl_3): δ 14.0, 22.5, 23.3, 28.0, 28.8, 28.9, 31.6, 52.3,

114.6, 118.1, 126.3, 126.5, 128.0, 128.7, 129.3, 130.4, 132.3, 133.2, 136.7, 140.4, 169.1; Anal.

($\text{C}_{23}\text{H}_{29}\text{NO}_4\text{S} \cdot 1/4(\text{H}_2\text{O})$) C, H, N.



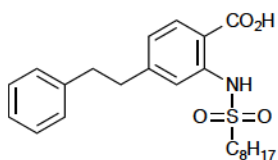
(E)-5-(4-methoxystyryl)-2-(octanesulfonamido)benzoic acid

(17b). 90% yield; mp = 98-99 °C; ^1H -NMR (400 MHz, MeOD):

δ 0.84 (t, 3H, $J = 7.2$), 1.15-1.25 (m, 8H), 1.30-1.40 (m, 2H),

1.65-1.75 (m, 2H), 3.17 (t, 2H, $J = 8.0$), 3.79 (s, 3H), 6.89 (d, 2H, $J = 8.8$), 6.95-7.10 (m, 2H),

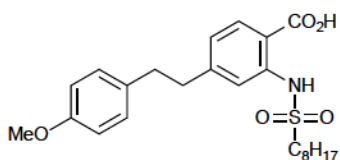
7.46 (d, 2H, $J = 8.8$), 7.65-7.75 (m, 2H), 8.19 (s, 1H); ^{13}C -NMR (100 MHz, MeOD): δ 14.4, 23.6, 24.5, 28.8, 28.9, 29.9, 32.9, 52.3, 55.7, 115.2, 119.4, 121.1, 125.5, 128.9, 130.0, 130.8, 131.2, 132.8, 134.3, 141.0, 161.0, 172.3; Anal. ($\text{C}_{24}\text{H}_{31}\text{NO}_5\text{S}$) C, H, N.



2-(Octanesulfonamido)-4-phenethylbenzoic acid (18a). 85% yield;

mp = 94-95 °C; ^1H -NMR (400 MHz; MeOD): δ 7.97 (d, $J = 8.1$ Hz, 1H), 7.46 (s, 1H), 7.22 (m, 2H), 7.13 (m, 3H), 6.97 (d, $J = 8.1$ Hz, 1H), 2.94 (m, 6H), 1.64 (m, 2H), 1.23 (m, 10H), 0.89 (t, $J = 7.2$ Hz, 3H); ^{13}C -NMR (100 MHz;

MeOD): δ 171.3, 150.7, 142.3, 142.0, 133.1, 129.4, 129.3, 127.0, 124.3, 118.7, 114.6, 51.9, 38.6, 37.8, 32.7, 29.9, 28.7, 24.4, 23.6, 14.4. Anal. ($\text{C}_{23}\text{H}_{31}\text{NO}_4\text{S}$) C, H, N.

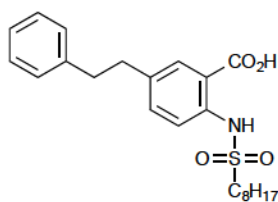


4-(4-Methoxyphenethyl)-2-(octanesulfonamido)benzoic acid

(18b). 87% yield; mp = 106-107 °C; ^1H -NMR (400 MHz;

MeOD): δ 7.95 (d, $J = 8.1$ Hz, 1H), 7.42 (s, 1H), 7.00 (d, $J = 8.1$

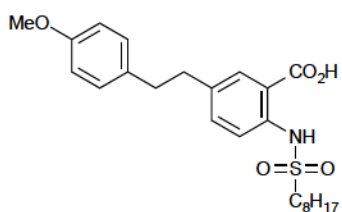
Hz, 2H), 6.93 (d, $J = 8.1$ Hz, 1H), 6.75 (d, $J = 8.1$ Hz, 2H), 3.70 (s, 3H), 2.89 (m, 6H), 1.61 (m, 2H), 1.17 (m, 10H), 0.85 (t, $J = 7.2$ Hz, 3H); ^{13}C -NMR (100 MHz; MeOD): δ 171.3, 159.3, 150.8, 142.3, 133.9, 133.0, 130.4, 124.2, 118.7, 114.7, 114.5, 55.5, 51.8, 38.8, 36.9, 32.7, 29.9, 29.8, 28.7, 24.3, 23.5, 14.4. Anal. ($\text{C}_{24}\text{H}_{33}\text{NO}_5\text{S}$) C, H, N.



2-(Octanesulfonamido)-5-phenethylbenzoic acid (19a). 89% yield;

mp = 92-93 °C; ^1H -NMR (400 MHz; MeOD): δ 7.89 (d, $J = 2.1$ Hz, 1H), 7.60 (d, $J = 8.7$ Hz, 1H), 7.34 (dd, $J = 2.1, 8.7$ Hz, 1H), 7.23 (m,

2H), 7.13 (m, 3H), 3.11 (t, $J = 8.0$ Hz, 2H), 2.88 (s, 4H), 1.68 (m, 2H), 1.23 (m, 10H), 0.86 (t, $J = 7.2$ Hz, 3H); ^{13}C -NMR (100 MHz; MeOD): δ 171.3, 142.3, 140.3, 137.6, 135.9, 132.8, 129.4, 129.2, 126.9, 119.0, 116.9, 52.0, 38.6, 37.9, 32.7, 29.8, 29.8, 28.8, 24.3, 23.5, 14.4. Anal. ($\text{C}_{23}\text{H}_{31}\text{NO}_4\text{S}$) C, H, N.



5-(4-Methoxyphenethyl)-2-(octanesulfonamido)benzoic acid

(19b). 89% yield; mp = 102-103 °C; ¹H-NMR (400 MHz;

MeOD): δ 7.87 (d, *J* = 2.1 Hz, 1H), 6.60 (d, *J* = 8.4 Hz, 1H), 7.33

(dd, *J* = 2.4, 8.4 Hz, 1H), 7.04 (d, *J* = 8.7 Hz, 2H), 6.78 (d, *J* = 8.7 Hz, 2H), 3.73 (s, 3H), 3.12 (t,

J = 8.0 Hz, 2H), 2.84 (s, 4H), 1.68 (m, 2H), 1.28 (m, 10H), 0.88 (t, *J* = 7.2 Hz, 3H); ¹³C-NMR

(100 MHz; MeOD): δ 171.3, 159.3, 140.2, 137.8, 135.9, 134.3, 132.8, 130.4, 119.8, 117.0,

114.6, 55.5, 52.0, 38.1, 37.7, 32.7, 29.8, 29.8, 28.7, 24.3, 23.5, 14.3. Anal. (C₂₄H₃₃NO₅S) C, H, N.

Protein-Ligand Docking

The squash glycerol-3-phosphate acyltransferase coordinates used were from the PDB entry 1IUQ.^{12b} The resolution of the structure was 1.55 Å. Both *in silico* viewing and manipulation were carried out using Accelrys Discovery Studio, version 2.1. Glycerol, sulfate, and water molecules were removed prior to ligand docking experiments. The A chain was then designated as the receptor and typed with the CHARMM forcefield. A model of compound **1** was then created as the input ligand and docked into the active site of the receptor using the CDOCKER protocol. The docked ligand in Figure 2.2A in was one of the resulting poses. Figure 2.2B was created by manually docking compound **14b** into the binding site obtained for compound **1** in Figure 2.2A.

Biological Testing

Mitochondrial Preparation. The mtGPAT assay has been reported previously.¹⁸ The mitochondrial preparation was performed with the Mitochondria Isolation Kit (Sigma-Aldrich, Catalog # MITOISO1) according to the provided instructions. Specifically, the liver from a

freshly-sacrificed BALB/c mouse was homogenized in 12 mL extraction buffer (isotonic solution, 10 mM HEPES, pH 7.5, containing 200 mM mannitol, 70 mM sucrose, 1 mM EGTA, 24 mg albumin), transferred to a 2 mL microcentrifuge tube, and centrifuged at $1000 \times \text{RPM}$. The pellet was discarded and the supernatant was centrifuged at $3500 \times \text{RPM}$. The pellet was resuspended in extraction buffer, and the previous two centrifugation steps were repeated. After the final $3500 \times \text{RPM}$ spin, the pellet was resuspended in storage buffer (10 mM HEPES, pH 7.4, containing 250 mM sucrose, 1mM ATP, 0.08 mM ADP, 5 mM sodium succinate, 2 mM K_2HPO_4 , and 1 mM DTT) and used as the mitochondrial preparation in the GPAT Assay

GPAT Assay. The mitochondrial preparation (3 μL) including mtGPAT was added to 200 μL of an incubation mixture containing 75 mM Tris/HCl, pH 7.4; 4 mM MgCl_2 ; 2 mg/mL bovine serum albumin; 7.6 mCi/mmol ^{14}C -labeled glycerol-3-phosphate, 50 μM palmitoyl-CoA, and 1 μL of varying inhibitor concentrations (0, 0.625, 2.5, 10, 40 $\mu\text{g}/\text{mL}$ in DMSO) to initiate the reaction. After 10 min, the reaction was terminated by adding 3 mL $\text{CHCl}_3\text{:MeOH}$ (1:2) and 600 μL of 1% perchloric acid. After an additional 5 min, 1 mL CHCl_3 and 1 mL 1% perchloric acid were added, and the upper aqueous layer was removed. After washing three times with 2 mL of 1% perchloric acid, the organic layer was evaporated under nitrogen, and the amount of ^{14}C present was measured by scintillation counting to determine the extent of reaction inhibition. Data points were recorded in triplicate, and IC_{50} values were calculated based on the amount of test inhibitor required to produce 50% of mtGPAT activity observed in the absence of inhibitor but in the presence of DMSO vehicle control.

2.7 References

1. a) Poirier, P.; Giles, T. D.; Bray, G. A., et al. *Arterioscler. Thromb. Vasc. Biol.* **2006**, 26, 968–976. b) Bastien, M.; Poirier, P.; Lemieux, I.; Després, J.-P. *Prog. Cardiovasc. Dis.* **2014**, 56, 369–381.
2. Haslam, D. W.; James, W. P.T. *Lancet* **2005**, 366, 1197–1209.
3. a) Hall, J.E. *Hypertension* **2003**, 41, 625–633. b) Adams, S. T., Salhab, M., Hussain, Z. I.; Miller, G. V.; Leveson, S. H. *Blood Pressure* **2013**, 22, 131-137.
4. Hammoud, A.O., Gibson, M., Peterson, C.M., Meikle, A.W., Carrell, D.T. *Fertil. Steril.* **2008**, 90, 897–904.
5. a) Calle, E. E.; Rodriguez, C.; Walker-Thurmond, K.; Thun, M. J. N. *Engl. J. Med.* **2003**, 348, 1625–1638. b) Pantasri, T.; Norman, R. J. *Gynecol. Endocrinol.* **2014**, 30, 90–94.
6. a) Loftus, T.M.; Jaworski, D.E.; Frehywot, G.L.; Townsend, C.A.; Ronnett, G.V.; Lane, M.D.; Kuhajda, F.P. *Science* 2000, 288, 2379-2381. b) Gilbert, C. A.; Slingerland, J. M. *Annu. Rev. Med.* **2013**, 64, 45–57.
7. Makimura, H.; Mizuno, T.M.; Yang, X.J.; Silverstein, J.; Beasley, J.; Mobbs, C.V. *Diabetes* **2001**, 50, 733-739.
8. Thupari, J. N.; Landree, L. E.; Ronnett, G. V.; Kuhajda, F. P. *Proc. Natl. Acad. Sci. U.S.A.* **2002**, 99, 9498–9502.
9. Coleman, R.A.; Lewin, T.M.; Muoio, D.M. *Annu. Rev. Nutr.* **1998**, 18, 331-351.
10. Muoio, D. M.; Seefeld, K.; Witters, L. A.; Coleman, R. A. *Biochem. J.* **1999**, 338 (Pt 3), 783–791.
11. Wydysh, E.A.; Medghalchi, S.M.; Vadlamudi, A.; Townsend, C.A. *J. Med. Chem.* **2009**, 52, 3317-3327.

12. a) Turnbull, A. P.; Rafferty, J. B.; Sedelnikova, S. E.; Slabas, A. R.; Schierer, T. P.; Kroon, J. T.; Simon, J. W.; Fawcett, T.; Nishida, I.; Murata, N.; Rice, D. W. *Structure* 2001, 9, 347–353. b) Tamada, T.; Feese, M. D.; Ferri, S. R.; Kato, Y.; Yajima, R.; Toguri, T.; Kuroki, R. *Acta Crystallogr. D. Biol. Crystallogr.* **2003**, 60, 13–21.
13. Agarwal, A. K.; Sukumaran, S.; Bartz, R.; Barnes, R. I.; Garg, A. *Journal of Endocrinology* **2007**, 193, 445–457.
14. Gassman, P. G.; Schenk, W. N. *J. Org. Chem.* **1977**, 42, 918–920.
15. Gubbens, J.; Ruijter, E.; de Fays, L. E. V.; Damen, J. M. A.; Ben de Kruijff; Slijper, M.; Rijkers, D. T. S.; Liskamp, R. M. J.; de Kroon, A. I. P. M. *Chem. Biol.* **2009**, 16, 3–14.
16. Kuhajda, F. P.; Aja, S.; Tu, Y.; Han, W. F.; Medghalchi, S. M.; Meskini, El, R.; Landree, L. E.; Peterson, J. M.; Daniels, K.; Wong, K.; Wydysh, E. A.; Townsend, C. A.; Ronnett, G. V. *Am. J. Physiol. Regul. Integr. Comp. Physiol.* **2011**, 301, R116–R130.
17. Allison, B.D.; Phuong, V.K.; McAtee, L.C.; Rosen, M.; Morton, M.; Prendergast, C.; Barrett, T.; Lagaud, G.; Freedman, J.; Li, L.; Wu, X.; Venkatesan, H.; Pippel, M.; Woods, C.; Rizzolio, M.C.; Hack, M.; Hoey, K.; Deng, X.; King, C.; Shankley, N.P.; Rabinowitz, M.H. *J. Med. Chem.* **2006**, 49, 6371–6390.
18. Schlossman, D. M.; Bell, R. M. *J. Biol. Chem.* **1976**, 251, 5738–5744.

Chapter 3

A Practical Route to Substituted 7-Aminoindoles from Pyrrole-3-carboxaldehydes

3.1 Introduction

Glycerol-3-phosphate acyltransferase (GPAT) catalyzes the first committed and rate-limiting step in the biosynthesis of glycerolipids. Moderate inhibition of GPAT has previously been achieved *in vitro* using a variety of sulfonamidobenzoic acids.¹ Additionally, diet-induced obese (DIO) mice treated with these inhibitors demonstrated significant weight loss, which was sustained after cessation of treatment validating GPAT as a target for antiobesity therapy.² Utilizing an energy-minimized docking model of these inhibitors in the active site of a GPAT homolog, several inhibitor analogs have been synthesized to bind an observed hydrophobic pocket.³ These analogs increased the inhibitory activity *in vitro* by up to three-fold, but low solubility precluded *in vivo* analysis. In order to overcome poor solubility as well as to probe new scaffolds for GPAT inhibition, we chose a series of heteroaromatic bicycles, shown in Fig. 3.1, to replace the simple benzene ring of the first generation of inhibitors. The possible locations of the nitrogen within the heteroaromatic system provide potential H-bond donating and accepting capabilities to interact with the enzyme and aid with solubility. In addition, each unique scaffold confers perturbations to the electronic structure of the inhibitors, which will affect binding within GPAT. Because no suitable methods exist for the rapid generation of libraries of these polysubstituted heteroaromatic bicyclic scaffolds, we elected to develop a method for their

synthesis. In this chapter, strategies for the synthesis of indoles are discussed and a new general method is developed.

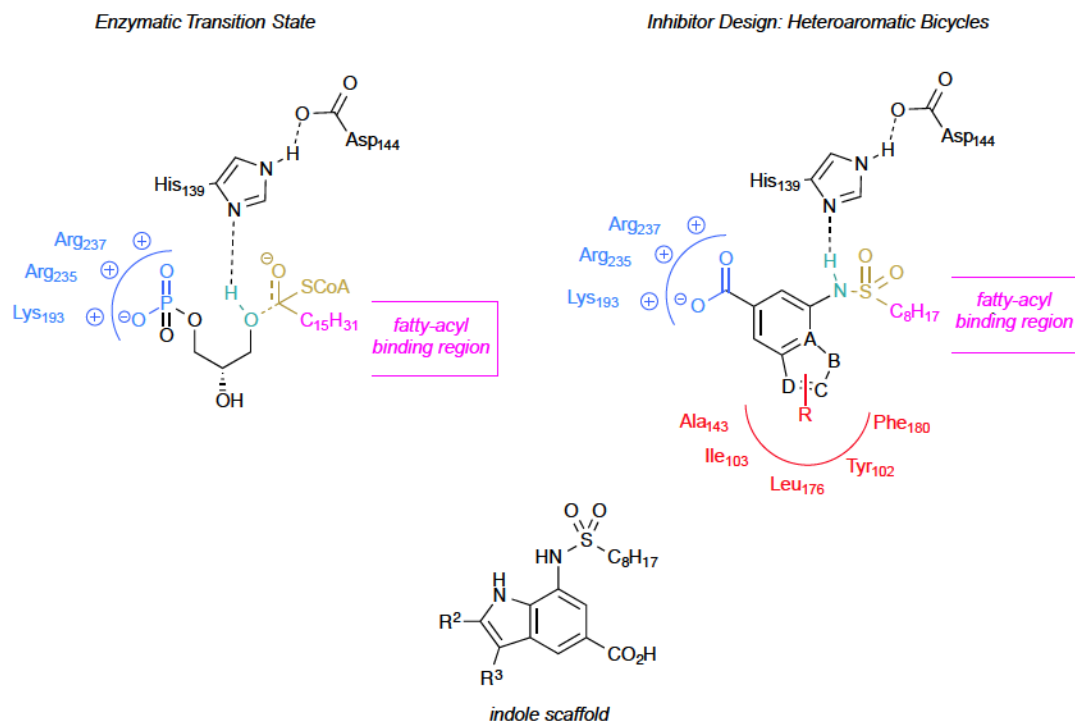


Figure 3.1 Design of heteroaromatic bicyclic inhibitors and general structure of indole scaffold

Synthetic routes to indoles have long been prized owing to the prevalence of the aromatic heterocycles in natural products as well as synthetic medicinal agents.⁴ Classical indole syntheses, including the work of Fischer⁵, Bischler⁶, Sugasawa⁷, Larock⁸, Hegedus⁹, Mori¹⁰, Reissert¹¹, Bartoli¹², and many others¹³, remain benchmarks in the development of heterocyclic methodology. The majority of these approaches utilize an aza-functionalized benzene ring to annulate the 5-membered pyrrolic portion of the indole as shown in Fig. 3.2. The Fischer indole synthesis, for example, involves acid-catalyzed hydrazone formation from a ketone with phenylhydrazine, followed by [3,3]-sigmatropic rearrangement and cyclization with extrusion of ammonia.⁵ Other acidic methods of annulation include the Bischler⁶ and Sugasawa⁷ methods, which commence with alkylation of aniline with an α -halo ketone or nitrile, respectively,

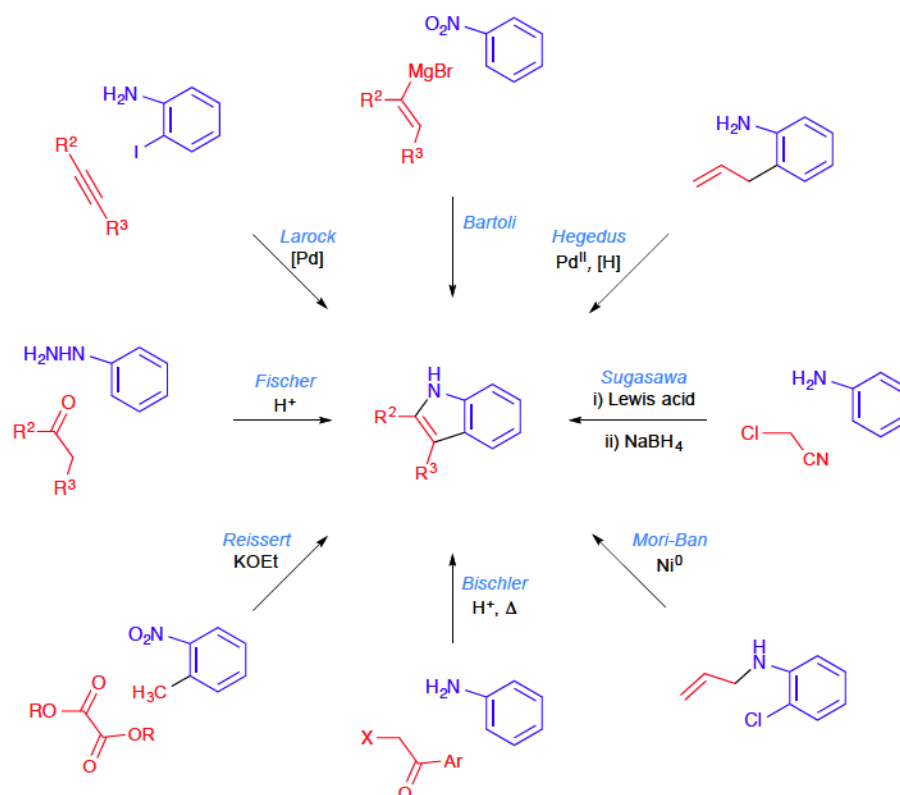


Figure 3.2 Prominent indole syntheses from benzenoid precursors

followed by annulation. Both of these methods require harshly acidic conditions of $\text{BCl}_3/\text{AlCl}_3$ for the Bischler method and $\text{HBr}/200\text{ }^\circ\text{C}$ for the Sugasawa method. Also using aniline starting materials, the Larock⁸, Hegedus⁹, and Mori-Ban¹⁰ methods utilize palladium or nickel complexes to promote annulation with a pendant alkynyl or allyl moiety. Other methods start with *o*-substituted nitrobenzenes. The Reissert method, for example, involves the condensation of *o*-nitrotoluene with a dialkyl oxalate, followed by reductive cyclization with zinc in acetic acid and decarboxylation to the indole.¹¹ Also using nitrobenzene, the Bartoli method begins with addition of a Grignard reagent into the nitro moiety and elimination to a nitrosobenzene intermediate.¹² Addition of another equivalent of the Grignard reagent, followed by [3,3]-sigmatropic rearrangement, cyclization, and elimination of water affords the indole.

In contrast to the indole-forming methods starting from functionalized benzenes, few synthetic strategies exist that originate from a substituted pyrrole to build up the benzenoid

portion of the indole.¹⁴ The latter strategy can benefit from the unique chemistry of pyrroles, which react with electrophiles preferentially at C-2 but exclusively at C-3 when *N*-protected with the sterically cumbersome triisopropylsilyl group as shown in Fig. 3.3.¹⁵ This tunable reactivity allows for ready introduction of the would-be C-2 and C-3 substituents of the indole prior to annulation. Further, the intrinsic reactivity of pyrroles at C-2 introduces a disconnection optimal for the indole-forming cyclization itself. Tactical issues of symmetry and regiochemistry inherent to routes from substituted benzene rings are avoided.

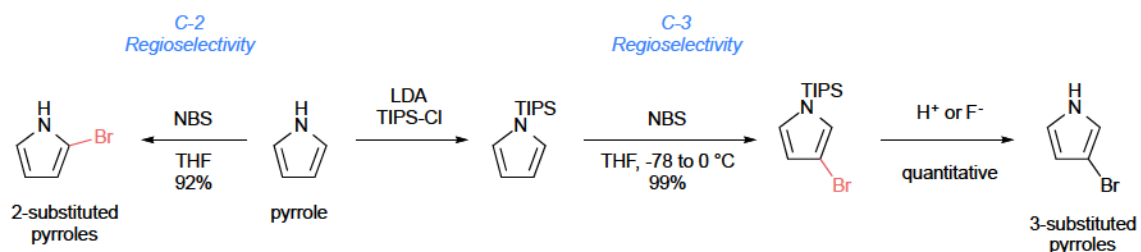


Figure 3.3 Tunable regioselectivity for electrophilic reactions of pyrroles

Our strategy, shown in Fig. 3.4, utilizes a three-component Wittig reaction of pyrrole-3-carboxaldehydes with fumaronitrile and a trialkylphosphine to generate predominantly *E*-alkenes. These allylic nitriles are positioned for intramolecular cyclization under Houben-Hoesch conditions to furnish, after aromatization, substituted 7-aminoindoles. An optional tailoring step to install C-6 substituents prior to ring closure can also be envisioned. This scheme would allow for control of the C-2, C-3, and C-6 indole substituents on the resulting 7-amino-5-cyanoindoles that are not readily accessible using existing methods. The amine (e.g., by sulfonylation, diazotization, acylation) and the nitrile (e.g., by hydration, hydrolysis, reduction, etc.) can be differentially modified for rapid structural diversification. In addition to the analogs of GPAT discussed previously, accessible medicinal drug targets, shown in Fig. 3.5, include a

class of potent β -secretase 1 (BACE1) inhibitors¹⁶ as well as a class of nicotinic acetylcholine receptor (nAChR) allosteric modulators.¹⁷

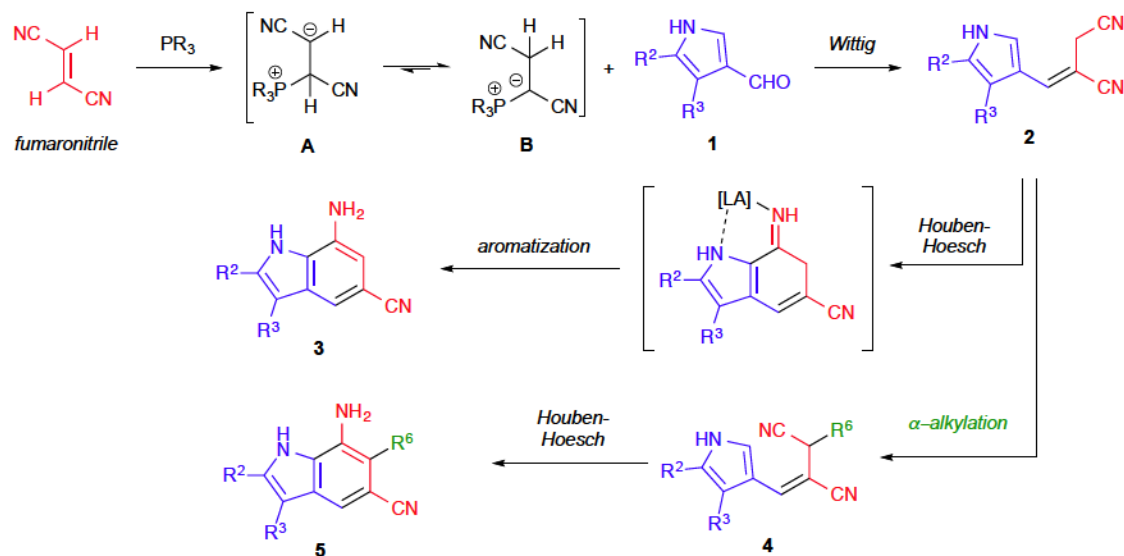


Figure 3.4 Proposed route to substituted 7-aminoindoles

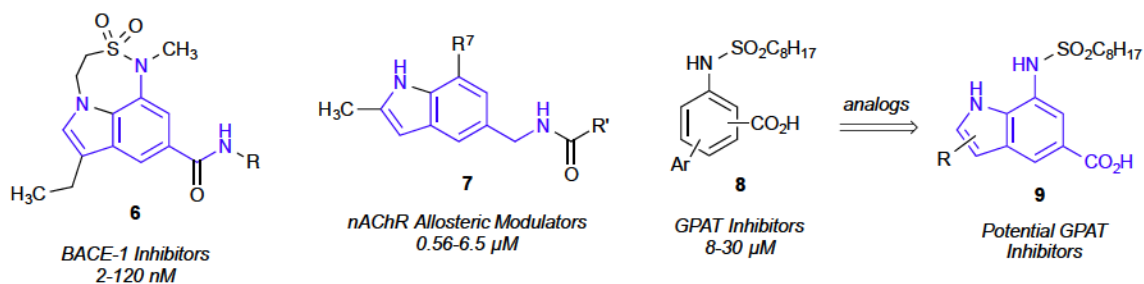


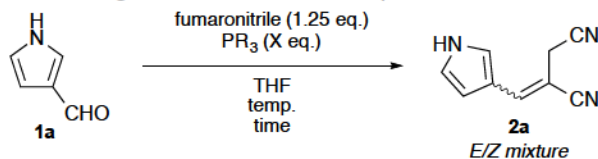
Figure 3.5 Representative medicinal chemistry targets

3.2 One-Pot, Three-Component Wittig Reaction: Optimization

Of fundamental importance to the planned synthesis was the acquisition of *E*-alkenes such as **2** (Fig. 3.4). The *E*-selective olefination of aldehydes with esters of fumarate and maleate, maleic anhydride, or maleimide and tributyl- or triphenylphosphine has been previously described.¹⁸ We envisioned a similar 1,4-addition of a phosphine to fumaronitrile followed by rapid prototropic rearrangement of the initially formed zwitterion **A** to the thermodynamically favored phosphonium ylide **B**, which is poised for *in situ* Wittig olefination with pyrrole-3-carboxaldehydes such as **1**. Trimethyl-, triethyl-, tributyl-, and triphenylphosphine, as well as trimethylphosphite, were evaluated for the efficiency of their reactions with fumaronitrile and aldehyde **1a** as shown in Table 3.1. PPh₃ and P(OMe)₃ were unreactive under the reaction conditions. PMe₃, PEt₃, and PBu₃, when used in excess, exhibited understandably similar reactivity, converting aldehyde **1a** to alkene **2a** in moderate yield (72-80%) but with only slight *E*-selectivity (4:3) after extended reaction time (48 h). Concerned that the excess phosphine was adding into the product, itself an α,β -unsaturated nitrile, and causing isomerization of the alkene, we next attempted the reaction with limiting phosphine. At room temperature, these reactions gave the desired alkene **2a** in high yield (91-99%) and good *E/Z*-ratio (3:1) suggesting that the excess phosphine was indeed causing alkene isomerization. To ameliorate the sluggish reaction rate, we heated the reaction with PEt₃ to 65 °C. These improved conditions cut the reaction time 6-fold while maintaining the favorable yield (97%) and *E/Z*-ratio (3:1) of the room temperature reaction. There are distinct advantages to each of the phosphines tested. The volatility of PMe₃ (bp 38 °C) allows for easy removal upon workup but prohibits heating of the reaction without a sealed vessel. PBu₃ (bp 240 °C) requires an additional oxidative workup step

but is the most economical choice. Finally, PEt_3 (bp 126 °C) afforded the highest yield and allows for heating to reflux while maintaining the option of low-pressure removal.

Table 3.1 Optimization of Wittig Reaction with Aldehyde **1a**

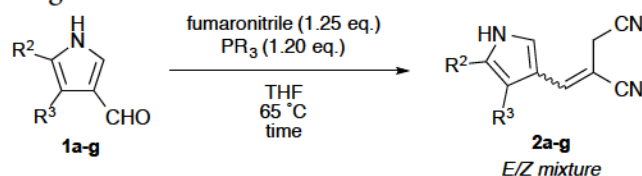


entry	PR_3	X	temp (°C)	time (h)	yield of 2a (%)	E/Z
1	PMe_3	1.4	23	48	76	4:3
2	PEt_3	1.4	23	48	80	4:3
3	PBu_3	1.4	23	48	72	4:3
4	PPh_3	1.4	23	48	0	
5	P(OMe)_3	1.4	23	48	0	
6	PEt_3	1.2	23	48	95	3:1
7	PEt_3	1.2	23	48	99	3:1
8	PEt_3	1.2	23	48	91	3:1
9	PEt_3	1.2	65	8	97	3:1

3.3 One-Pot, Three-Component Wittig Reaction: Scope

To demonstrate scope, the optimized conditions using PEt_3 at 65 °C were applied to various 4- and 5-substituted pyrrole-3-carboxaldehydes **1a-g**. Alkenes **2a-g** were obtained in generally good to excellent yield and moderate diastereoselectivity (Table 3.2). The reaction conditions were tolerant of a wide range of substituents including alkyl, aryl, halogen, and ester moieties. Electron-withdrawing substituents at the pyrrolic α -position led to slower conversion. Additionally, minor substituent effects were observed for the diastereoselectivity of the reactions.

Table 3.2 Scope of Wittig Reaction

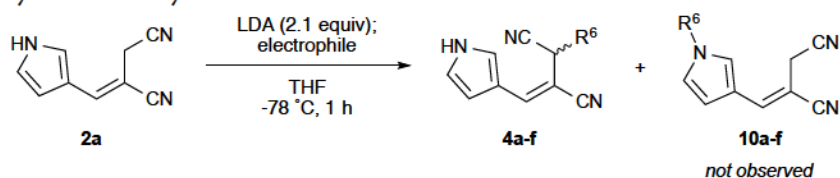


entry	aldehyde	R ²	R ³	time (h)	product	yield (%)	<i>E/Z</i>
1	1a	-H	-H	8	2a	97	3:1
2	1b	-Br	-H	10	2b	97	3:1
3	1c	-CO ₂ Et	-H	8	2c	96	5:1
4	1d	-Ph	-H	8	2d	88	3:1
5	1e	-H	-Me	8	2e	85	4:1
6	1f	-H	-Et	8	2f	85	4:1
7	1g	-H	-Br	8	2g	93	5:3

3.4 Alkylation of C-6

To further diversify the library of *E*-alkenes, we next sought to functionalize the allylic nitrile. To accomplish this task without the use of protecting groups, we elected to exploit the relatively more acidic pyrrole N-H and developed a dianion approach to alkylate the allylic position chemoselectively (Table 3.3). Addition of 2.1 equivalents of LDA followed by the addition of various electrophiles, effected selective α -alkylation of nitrile **2a** to afford **4a-f** without detection of *N*-alkylated pyrrole side products **10a-f**. Analogous attempts with the electrophiles ethyl chloroformate, methyl acrylate, Br₂, and NBS showed no desired reaction.

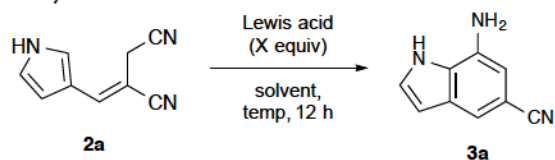
Table 3.3 Alkylation of Allylic Nitrile 3a



entry	electrophile	product	R ⁶	yield (%)
1	MeI	4a	-CH ₃	77
2	EtI	4b	-CH ₂ CH ₃	80
3	BnBr	4c	-CH ₂ Ph	75
4	allyl-Br	4d	-CH ₂ CH=CH	67
5	propargyl-Br	4e	-CH ₂ C≡CH	72
6	BrCH ₂ CO ₂ Et	4f	-CH ₂ CO ₂ Et	80

3.5 Lewis Acid-Mediated Annulation: Optimization

With reaction conditions established to *E*-olefinic precursors **2a-g** and **4a-f**, we next sought to optimize indole cyclization conditions as shown in Table 3.4. Of the Lewis acids tested, only BF₃•OEt₂ successfully effected cyclization. Initial attempts to use a catalytic amount of BF₃•OEt₂ gave only stoichiometric yield. Presumably, this is due to chelation of the Lewis acid by the 7-aminoindole product thereby preventing catalytic turnover. Similarly, using THF as the solvent afforded no reaction, likely owing to association of the Lewis acid with the ethereal solvent. The optimized conditions used 2.5 equivalents of BF₃•OEt₂ in 1,2-dichloroethane at 90 °C for 12 h, which gave efficient annulation of alkene **2a** to indole **3a**.

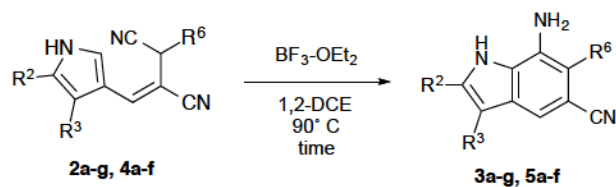
Table 3.4 Optimization of Cyclization to Indole **3a**

entry	Lewis acid	X	solvent	temp (°C)	yield of 3a (%)
1	none		CH ₂ Cl ₂	45	0
2	AlCl ₃	0.2	CH ₂ Cl ₂	45	0
3	Sc(OTf) ₃	0.2	CH ₂ Cl ₂	45	0
4	TiCl ₄	0.2	CH ₂ Cl ₂	45	0
5	BF ₃ •OEt ₂	0.2	CH ₂ Cl ₂	45	19
6	BF ₃ •OEt ₂	1.1	THF	70	0
7	BF ₃ •OEt ₂	1.1	PhCH ₃	85	61
8	BF ₃ •OEt ₂	2.5	DCE	90	91

3.6 Lewis Acid-Mediated Annulation: Scope

Application of the annulation conditions to the *E*-alkenes **2a-g** and **4a-f** gave indoles **3a-g** and **5a-f** in good to excellent yields (Table 3.5). The reaction conditions were amenable to a wide scope of substituents. Of particular interest to us, the bromo- and propargyl-substituted indoles can be further functionalized through coupling reactions or click chemistry, respectively, to rapidly generate large libraries of compounds. The more electron-deficient pyrroles (e.g. **2c**, **2g**) demonstrated lower yields, typical of electrophilic aromatic substitution with an electron-deficient arene. The reaction times for the 6-substituted alkenes were slightly shorter than for cyclization of the 2- and 3-substituted examples. This behavior points to a possible Thorpe-Ingold effect, whereby the C-6 substituent increases the population of the reactive rotamer resulting in an increased reaction rate. It is likely that this tactic can also be applied to pyrroles additionally substituted at the 2- and 3-positions.

Table 3.5 Scope of Indole Annulation



entry	pyrrole	R ²	R ³	R ⁶	product	time (h)	yield (%)
1	2a	-H	-H	-H	3a	12	91
2	2b	0.2	-H	-H	3b	12	67
3	2c	0.2	-H	-H	3c	12	62
4	2d	0.2	-H	-H	3d	12	87
5	2e	-H	-CH ₃	-H	3e	12	94
6	2f	-H	-CH ₂ CH ₃	-H	3f	12	92
7	2g	-H	-Br	-H	3g	12	75
8	4a	-H	-H	-CH ₃	5a	8	88
9	4b	-H	-H	-CH ₂ CH ₃	5b	8	95
10	4c	-H	-H	-CH ₂ Ph	5c	8	96
11	4d	-H	-H	-CH ₂ CH=CH ₂	5d	8	93
12	4e	-H	-H	-CH ₂ C≡CH	5e	8	92
13	4f	-H	-H	-CH ₂ CO ₂ Et	5f	8	72

3.7 One-Pot, Tandem Wittig/Annulation Sequence

In addition, a functionally one-pot reaction was run to indole 3a, shown in Fig. 3.6, in which pyrrole-3-carboxaldehyde and fumaronitrile were reacted in dry THF with PMe₃ as before (Table 1). Taking advantage of the relatively low boiling point of PMe₃, the solvent and any unreacted phosphine were removed by rotary evaporation and the residue taken up in 1,2-DCE. Treatment of this mixture as above with BF₃·OEt₂ gave the desired indole in 77% yield, approximately the theoretical limit from the *E*-isomer, after crystallization of the product from the crude mixture containing unreacted *Z*-isomer.

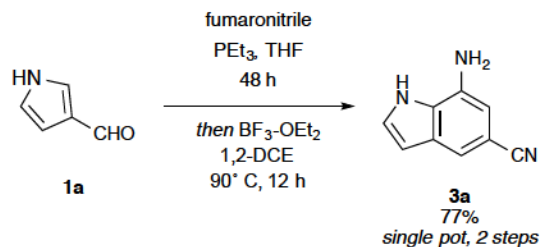


Figure 3.6 One-pot synthesis of indole **3a**

3.8 Application to Synthesis of Benzofurans and Benzothiophenes

Encouraged by the success of this approach, we next tested whether the corresponding furan- and thiophene-3-carboxaldehydes could undergo a similar two-step sequence to the corresponding 7-amino-5-cyanobenzofurans and benzothiophenes, respectively (Fig. 3.7). We hypothesized that, with decreased C-2 nucleophilicity and increased heteroatomic interaction with the $\text{BF}_3 \cdot \text{OEt}_2$, the annulation of these heterocycles would be less facile. First, Wittig reaction using the optimized conditions afforded the olefins **12a-b** in excellent yield and better diastereoselectivity than for the analogous reaction with pyrrole-3-carboxaldehyde. Treatment with $\text{BF}_3 \cdot \text{OEt}_2$ effected annulation to benzofuran **13a** and benzothiophene **13b** in low to moderate yield. As expected, the reaction rates were much slower with conversion stalling around 24 h. Neither additional equivalents of Lewis acid nor longer reaction times improved the yields. It is possible that use of a less oxophilic Lewis acid could improve the yields for these classes of heterocycles.

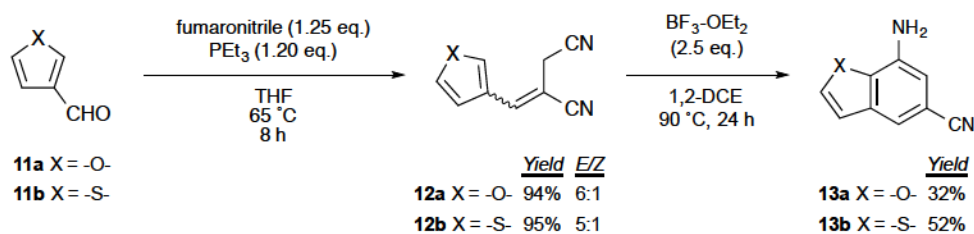


Figure 3.7 Application to the synthesis of benzofuran and benzothiophene derivatives

3.9 Functional Group Transformations

Finally, to illustrate practical applications of this method we chose to demonstrate functional group conversions from the 7-amino-5-cyanoindole intermediates to readily identifiable precursors of the medicinal chemistry targets noted above (Fig. 3.5). First, we utilized Sandmeyer chemistry to substitute the amino group of indole **3a** with chloro or bromo as shown in Fig. 3.8. These aryl halides allow access to a variety of C-7 substituted indoles, such as the nAChR allosteric modulators represented by **7**, through metal-catalyzed coupling reactions. Second, we demonstrated sulfonamide coupling of the aniline with octanesulfonyl chloride, followed by alkaline nitrile hydrolysis to give the GPAT inhibitor analog **9a**. A similar sulfonamide coupling and hydrolysis sequence can be envisioned to access the diversifiable precursor of the BACE1 inhibitors represented by **6**.

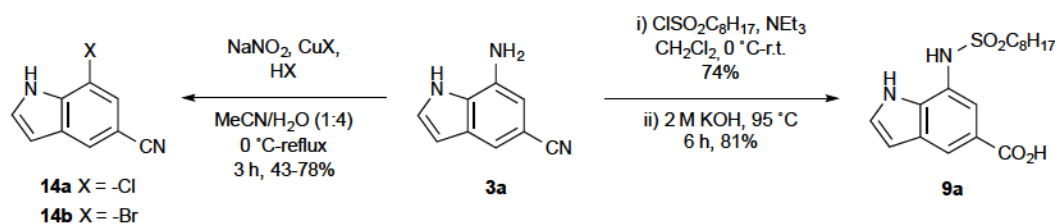


Figure 3.8 Functional group conversion of **3a** to precursors of medicinal chemistry targets

3.10 Conclusions

In conclusion, we have developed a flexible and step-efficient method to obtain highly functionalized 7-aminoindoles from pyrrole-3-carboxaldehydes. This method utilizes a three-component Wittig reaction of pyrrole-3-carboxaldehydes with fumaronitrile and PEt_3 to generate predominantly *cis*-allylic nitriles, which can be optionally elaborated further by a chemoselective alkylation at C-6. These *cis*-allylic nitriles undergo cyclization through an intramolecular Houben-Hoesch reaction to afford highly substituted indoles. A one-pot

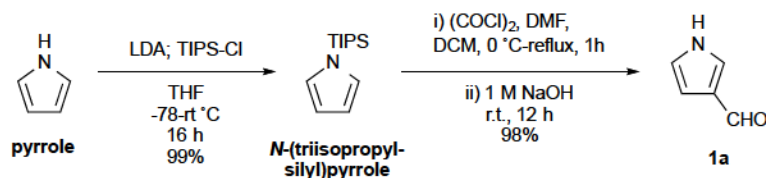
procedure combining the Wittig and Houben-Hoesch reactions was also demonstrated. While the method is substantially linear, the steps are typically high yielding with chromatographic purification minimized or eliminated, and intermediates and products isolated by crystallization. The reactions are scalable and require no special precautions or protecting groups—in sum, attributes favorable for large-scale applications. Further studies will aim to expand the scope of this method and to demonstrate its potential for the synthesis of bioactive targets of interest.

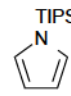
3.11 Experimental

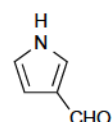
General Information

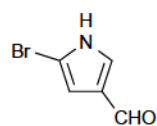
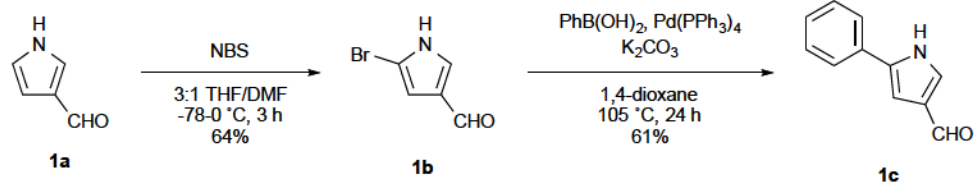
Reactions requiring anhydrous conditions were conducted under an inert atmosphere of argon using anhydrous solvents. CH_2Cl_2 , toluene, and MeOH were distilled over CaH_2 . Et_2O and THF were distilled over Na and benzophenone. All reactions were monitored by analytical thin-layer chromatography (TLC) using indicated solvent systems on Analtech Uniplat Silica Gel TLC plates (250 microns). Melting points were determined on a Thomas-Hoover capillary melting point apparatus and are uncorrected. NMR spectra were recorded on either Bruker Avance 400 MHz or 300 MHz spectrometers as indicated. Chemical shifts (δ) are quoted in parts per million (ppm) and referenced to the following residual solvent signals: ^1H δ = 7.26 (CDCl_3), 2.50 (DMSO-d_6), 3.31 (MeOD), 2.05 (acetone- d_6); ^{13}C δ = 77.0 (CDCl_3), 39.43 (DMSO-d_6), 49.05 (MeOD), 29.84 (acetone- d_6). Coupling constants (J) are given in Hz. Pyrrole and ethyl 4-formylpyrrole-2-carboxylate (2c) were obtained from Sigma-Aldrich.

Preparation of Aldehydes 1a-g

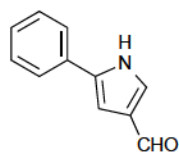


 ***N*-(Triisopropylsilyl)pyrrole.** To a 1.0 M solution of freshly prepared LDA (72.43 mmol) in THF at -78 °C was added pyrrole (5.0 mL, 72.07 mmol). The reaction mixture was allowed to warm to room temperature and stirred for 30 min before cooling to -78 °C, followed by the slow addition of chlorotriisopropylsilane (16.96 mL, 79.27 mmol). The reaction solution was allowed to warm to room temperature and stirred overnight, then quenched with NaHCO₃ (200 mL) and extracted with DCM (3 x 150 mL). The combined organic layers were dried over Na₂SO₄ and concentrated *in vacuo*. Purification by silica gel chromatography (2% EtOAc in hexanes) afforded the TIPS-protected pyrrole as a clear oil (15.9 g, 71.48 mmol, 99%). All spectral data matched literature values.¹⁹

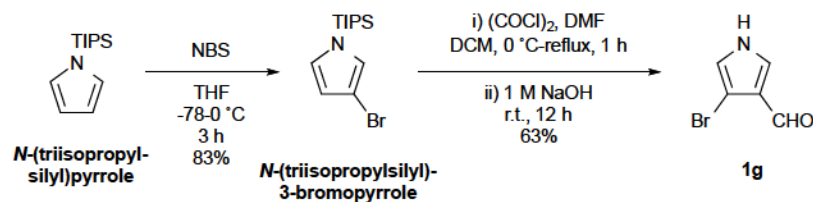
 **Pyrrole-3-carboxaldehyde (1a).** To a 0.18 M solution of oxalyl chloride (5.99 mL, 69.82 mmol) in DCM at 0 °C was added dropwise a 2 M solution of DMF (5.41 mL, 69.82 mmol) in DCM. The reaction mixture was stirred at 0 °C for 30 min before rapid addition of a 1.15 M solution of *N*-triisopropylsilylpyrrole (12.00 g, 53.71 mmol) in DCM. The reaction mixture was heated to reflux and stirred for 30 min. The solvent was removed *in vacuo* and the crude reaction mixture was resuspended in 1 M NaOH (300 mL) and stirred at room temperature for 12 h. The aqueous mixture was extracted with DCM (3 x 150 mL) and the combined organic extracts were dried over Na₂SO₄. Purification by silica gel chromatography (40% EtOAc in hexanes) afforded pyrrole-3-carboxaldehyde as a light brown solid (5.00 g, 98%). All spectral data matched literature values.¹⁹

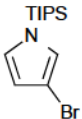


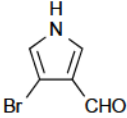
5-Bromo-1H-pyrrole-3-carboxaldehyde (1b). To a stirring solution of pyrrole-3-carboxaldehyde (250 mg, 2.63 mmol) in THF (3.9 mL) at -78°C was added slowly *N*-bromosuccinimide (473 mg, 2.66 mmol) as a solution in DMF (2.0 mL). The reaction mixture was stirred at -78°C for 1 h, then warmed to -10°C over 2 h. The reaction was quenched with ice water, and the product was extracted with EtOAc (3×50 mL). The combined organic extracts were washed with NaHCO_3 and brine, then dried over Na_2SO_4 and concentrated *in vacuo*. The reaction mixture was purified by silica gel chromatography (30% EtOAc/hexanes) to afford 5-bromopyrrole-3-carboxaldehyde (293 mg, 1.68 mmol, 64%). All spectral data matched literature values.²⁰



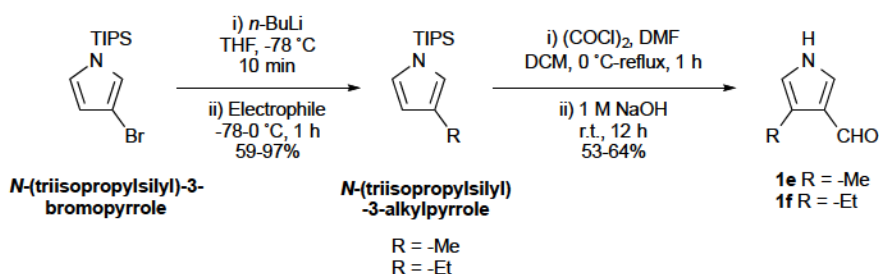
5-Phenyl-1H pyrrole-3-carboxaldehyde (1c). 5-Bromopyrrole-3-carboxaldehyde (50 mg, 0.29 mmol), phenyl boronic acid (42 mg, 0.34 mmol), and potassium carbonate (95 mg, 0.69 mmol) were suspended in dioxane (2.6 mL), and the mixture was degassed with argon. Tetrakis(triphenylphosphine)palladium (0) (17 mg, 5 mol %) was added, then the suspension was degassed again with argon and heated to 105°C for 24 h. The crude product mixture was concentrated, partitioned between EtOAc and water, and extracted with EtOAc (3×15 mL). The combined organic extracts were washed with brine, dried over Na_2SO_4 , and concentrated *in vacuo*. Purification by silica gel chromatography (30% EtOAc/Hexanes) afforded 5-Phenyl-1H pyrrole-3-carboxaldehyde (30 mg, 0.18 mmol, 61%). Spectral data matched literature values.²⁰




***N*-(Triisopropylsilyl)-3-bromopyrrole.** To a stirred solution of *N*-(triisopropylsilyl)pyrrole (214 mg, 0.96 mmol) in anhydrous THF (2.1 mL) at -78 °C was added *N*-bromosuccinimide (170 mg, 0.96 mmol). The reaction mixture was kept at -78 °C for 2 h and then warmed to room temperature. The reaction was quenched with NaHCO₃, extracted with Et₂O (3 × 20 mL), and the combined organic extracts were washed with brine, dried over Na₂SO₄, and concentrated *in vacuo*. The crude product was filtered through a short plug of silica gel, which was eluted with 2% EtOAc in hexanes. Concentration afforded the desired product as a clear oil (238 mg, 78.7 mmol, 82%). Spectral data matched literature values.¹⁹


4-Bromo-1H-pyrrole-3-carboxaldehyde (1g). To a 0.18 M solution of oxalyl chloride (333 μL, 4.3 mmol) in DCM (24 mL) at 0 °C was added dropwise a 2 M solution of DMF (333 μL, 4.3 mmol) in DCM (2.2 mL). The reaction mixture was stirred at 0 °C for 30 min before rapid addition of a 1.15 M solution of 3-bromo-*N*-(triisopropylsilyl)pyrrole (1000 mg, 3.3 mmol) in DCM (2.88 mL). The reaction mixture was heated to reflux and stirred for 30 min. The solvent was removed under reduced pressure, and the crude mixture was resuspended in 1 M NaOH (20 mL) and stirred at room temperature overnight. The reaction was quenched with saturated NH₄Cl, and the product was extracted with EtOAc (3 × 25 mL). The combined organic extracts were washed with brine, dried over Na₂SO₄, and concentrated *in vacuo*. Purification by recrystallization from hot EtOAc and hexanes afforded the aldehyde as a

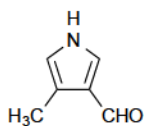
white solid (359 mg, 2.06 mmol, 62%). $^1\text{H-NMR}$ (400 MHz; acetone- d_6): δ 11.12 (s, 1H), 9.80 (s, 1H), 7.59 (d, $J = 2.1$ Hz, 1H), 7.04 (d, $J = 2.1$ Hz, 1H); $^{13}\text{C-NMR}$ (101 MHz, acetone- d_6): δ 184.87, 127.62, 123.83, 121.89, 96.66; HRMS (FAB) calcd for $\text{C}_5\text{H}_4\text{BrNO}$ $[\text{M}]^+$, 172.9476; found, 172.9473.



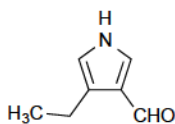
N-(Triisopropylsilyl)-3-methylpyrrole. To a solution of 3-bromo-N-(triisopropylsilyl)pyrrole (400 mg, 1.32 mmol) in THF (6.6 mL) was added *n*-butyllithium (1.85 M, 1.46 mmol) at -78°C . The mixture was stirred at -78°C for 10 min then MeI (107 μL , 1.72 mmol) was added, and the mixture was warmed to 0°C over 1 h. The reaction mixture was quenched by addition of saturated NH_4Cl and extracted with EtOAc (3×25 mL). The combined organic extracts were washed with brine, dried over Na_2SO_4 , and concentrated to dryness to afford the desired alkyl pyrrole as a yellow oil (306 mg, 97%), which was used without purification. Spectral data matched literature values.¹⁵

N-(Triisopropylsilyl)-3-ethylpyrrole. To a solution of 3-bromo-N-(triisopropylsilyl)pyrrole (400 mg, 1.32 mmol) in THF (6.6 mL) was added *n*-butyllithium (1.85 M, 1.46 mmol) at -78°C . The mixture was stirred at -78°C for 10 min then iodoethane (118 μL , 1.72 mmol) was added and the mixture was warmed to 0°C over 1 h. The reaction mixture was quenched using saturated NH_4Cl and extracted with EtOAc (3×25 mL). The combined organic extracts were washed with brine, dried over Na_2SO_4 , and concentrated to

dryness. The residue was purified by silica gel chromatography (1% EtOAc in hexanes) to afford the desired alkyl pyrrole as a clear oil (180 mg, 54%). Spectral data matched literature values.²¹



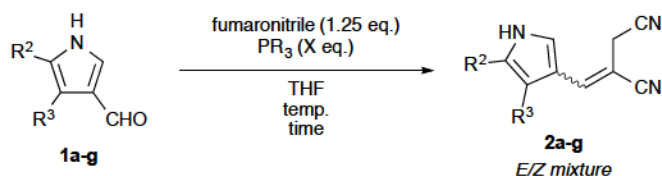
4-Methyl-1H-pyrrole-3-carboxaldehyde (1e). To a 0.18 M solution of oxalyl chloride (136 μ L, 1.58 mmol) in DCM (8.8 mL) at 0 °C was added dropwise a 2 M solution of DMF (122 μ L, 1.58 mmol) in DCM (800 μ L). The reaction mixture was stirred at 0 °C for 30 min before rapid addition of a 1.15 M solution of 3-methyl-*N*-(triisopropylsilyl)pyrrole (300 mg, 1.26 mmol) in DCM (1.1 mL). The reaction mixture was heated to reflux and stirred for 30 min. The solvent was removed *in vacuo*. The crude product mixture was resuspended in 1 M NaOH (15 mL) and stirred at room temperature overnight, then quenched with NH₄Cl and extracted with EtOAc (3 \times 15 mL). The combined organic extracts were washed with brine, dried over Na₂SO₄, and concentrated *in vacuo*. Purification by silica gel chromatography (20% acetone in petroleum ether) afforded the aldehyde as an off-white solid (88 mg, 0.81 mmol, 64%). Spectral data matched literature values.²²



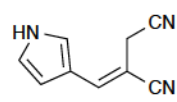
4-Ethyl-1H-pyrrole-3-carboxaldehyde (1f). To a 0.18 M solution of oxalyl chloride (77 μ L, 0.89 mmol) in DCM (5 mL) at 0 °C was added dropwise a 2 M solution of DMF (69 μ L, 0.89 mmol) in DCM (450 μ L). The reaction mixture was stirred at 0 °C for 30 min before rapid addition of a 1.15 M solution of 3-ethyl-*N*-(triisopropylsilyl)pyrrole (180 mg, 0.72 mmol) in DCM (650 μ L). The reaction mixture was heated to reflux and stirred for 30 min. The solvent was removed *in vacuo*. The crude mixture was resuspended in 1 M NaOH (5 mL) and stirred at room temperature overnight, then quenched with NH₄Cl and extracted with EtOAc (3 \times 15 mL). The combined organic extracts were washed with brine, dried over Na₂SO₄, and concentrated *in vacuo*. Purification by silica gel chromatography (20%

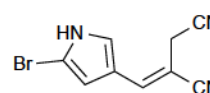
acetone in petroleum ether) afforded the aldehyde as an off-white solid (47 mg, 0.38 mmol, 53%). Spectral data matched literature values.²¹

One-Pot, Three-Component Wittig Reaction

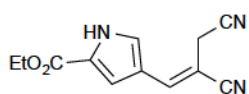


General Procedure. To a stirring solution of the pyrrole-3-carboxaldehyde (1.0 equiv.) in THF (0.25 M) at room temperature was added fumaronitrile (1.25 equiv.) followed by phosphine (X equiv.) dropwise. The reaction mixture was stirred at the denoted temperature until the starting material was no longer visible by TLC, then quenched with aqueous NaHCO_3 and extracted with EtOAc ($\times 3$). The combined organic extracts were washed with brine, dried over Na_2SO_4 , and concentrated *in vacuo*. Generally, purification by silica gel chromatography afforded a mixture of the *E* and *Z* olefin Wittig products due to the similar R_f values of the two isomers. Alternatively, crystallization from EtOAc and hexanes afforded the pure *E* isomer. Spectral data shown below are for the pure *E* isomers.

 **2-((1H-Pyrrol-3-yl)methylene)succinonitrile (2a).** yield: 97%, 3:1 *E/Z*; mp 119-120 °C; $^1\text{H-NMR}$ (400 MHz; CDCl_3): δ 8.73 (s, 1H), 7.34 (s, 1H), 7.11 (q, $J = 2.1$ Hz, 1H), 6.92 (q, $J = 2.1$ Hz, 1H), 6.41 (q, $J = 2.1$ Hz, 1H), 3.52 (s, 2H); $^{13}\text{C-NMR}$ (101 MHz, acetone- d_6): δ 1423.11, 125.20, 121.69, 120.75, 118.89, 117.10, 109.58, 95.26, 19.42; HRMS (FAB) calcd for $\text{C}_9\text{H}_7\text{N}_3$ $[\text{M}]^+$, 157.0640; found, 157.0637.

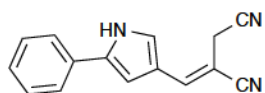
 **2-((5-Bromo-1H-pyrrol-3-yl)methylene)succinonitrile (2b).** yield: 97%,

3:1 *E/Z*; mp 108-109 °C; ¹H-NMR (400 MHz; acetone-*d*₆): δ 11.26 (s, 1H), 7.37 (s, 1H), 7.34 (s, 1H), 6.54 (s, 1H), 3.82 (s, 2H); ¹³C-NMR (101 MHz, acetone-*d*₆): δ 141.65, 126.21, 120.31, 120.25, 116.85, 111.16, 102.25, 96.86, 19.32; HRMS (FAB) calcd for C₉H₆(⁷⁹Br)N₃ [M]⁺, 234.9745; found, 234.9743.



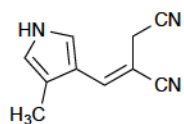
Ethyl 4-(2,3-dicyanoprop-1-en-1-yl)-1H-pyrrole-2-carboxylate (2c).

yield: 96%, 5:1 *E/Z*; mp 134-135 °C; ¹H-NMR (400 MHz; acetone-*d*₆): δ 11.62 (s, 1H), 7.56 (s, 1H), 7.46 (s, 1H), 7.15 (s, 1H), 4.30 (q, *J* = 7.1 Hz, 2H), 3.90 (s, 2H), 1.32 (t, *J* = 7.1 Hz, 3H); ¹³C-NMR (101 MHz, acetone-*d*₆): δ 160.80, 141.91, 128.59, 126.05, 120.13, 119.90, 116.84, 115.70, 98.57, 61.11, 19.57, 14.66; HRMS (EI): Exact mass calcd for C₁₂H₁₁N₃O₂ [M]⁺, 229.0851. Found 229.0854.



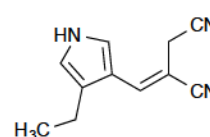
2-((5-Phenyl-1H-pyrrol-3-yl)methylene)succinonitrile (2d). yield:

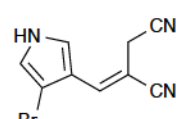
88%, 3:1 *E/Z*; mp 197-198 °C; ¹H-NMR (400 MHz; acetone-*d*₆): δ 11.26 (s, 1H), 7.72 (dd, *J* = 8.5, 1.2 Hz, 2H), 7.43-7.41 (m, 4H), 7.27 (tt, *J* = 1.2 Hz, 1H), 6.95 (t, *J* = 2.1 Hz, 1H), 3.92 (d, *J* = 1.2 Hz, 2H); ¹³C-NMR (101 MHz, acetone-*d*₆): δ 142.59, 135.55, 132.70, 129.76, 127.81, 126.55, 125.07, 120.66, 120.44, 117.13, 106.63, 96.18, 19.54; HRMS (FAB): Exact mass calcd for C₁₅H₁₁N₃ [M]⁺, 233.0953. Found 233.0954.



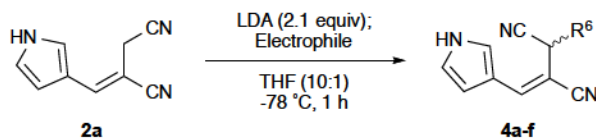
2-((4-Methyl-1H-pyrrol-3-yl)methylene)succinonitrile (2e). yield: 85%,

4:1 *E/Z*; mp 109-111 °C; ¹H-NMR (400 MHz; acetone-*d*₆): δ 10.59 (s, 1H), 7.38 (d, *J* = 1.3 Hz, 1H), 7.26 (t, *J* = 1.2 Hz, 1H), 6.75 (s, 1H), 3.75 (d, *J* = 1.3 Hz, 2H), 2.14 (s, 3H); ¹³C-NMR (101 MHz, acetone-*d*₆): δ 141.32, 122.30, 120.68, 120.56, 118.51, 117.64, 116.98, 95.82, 19.89, 9.90; HRMS (FAB) calcd for C₁₀H₉N₃ [M]⁺, 171.0797; found, 171.0793.

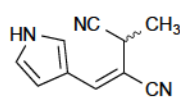

2-((4-Ethyl-1H-pyrrol-3-yl)methylene)succinonitrile (2f). yield: 85%, 4:1 *E/Z*; mp 108-109 °C; ¹H-NMR (400 MHz; acetone-*d*₆): δ 10.63 (s, 1H), 7.40 (s, 1H), 7.26 (s, 1H), 6.77 (s, 1H), 3.76 (s, 2H), 2.59 (q, *J* = 7.5 Hz, 2H), 1.18 (t, *J* = 7.5 Hz, 3H); ¹³C-NMR (101 MHz, acetone-*d*₆): δ 141.23, 127.62, 122.33, 120.67, 117.34, 117.00, 116.71, 95.92, 19.93, 18.57, 14.90; HRMS (FAB) calcd for C₁₁H₁₁N₃ [M]⁺, 185.0953; found, 185.0950.

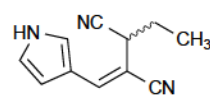

2-((4-Bromo-1H-pyrrol-3-yl)methylene)succinonitrile (2g). yield: 93%, 5:3 *E/Z*; mp 124-125 °C ¹H-NMR (400 MHz; acetone-*d*₆): δ 11.17 (s, 1H), 7.42 (s, 1H), 7.28 (s, 1H), 7.13 (s, 1H), 3.82 (s, 2H); ¹³C-NMR (101 MHz, acetone-*d*₆): δ 140.01, 122.67, 120.84, 119.94, 117.01, 116.62, 100.06, 99.00, 19.93; HRMS (FAB) calcd for C₉H₆(⁷⁹Br)N₃ [M]⁺, 234.9745; found, 234.9739.

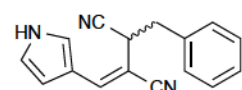
Dianionic Alkylation of 2a

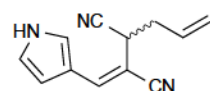


General Procedure. To a stirring 0.3 M solution of alkene **2a** in THF at -78 °C was added 2.2 eq. of LDA dropwise. The reaction mixture was stirred for 20 min and the electrophile (1.05 equiv.) was quickly added. The reaction mixture was allowed to warm to 0 °C over 1 h, then quenched with NH₄Cl and extracted with EtOAc (×3), and the combined organic extracts were washed with brine, dried over Na₂SO₄, and concentrated *in vacuo*. Purification by silica gel chromatography afforded the alkylated products **4a-f**.

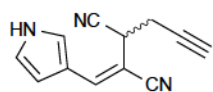

(E)-2-((1H-Pyrrol-3-yl)methylene)-3-methylsuccinonitrile (4a). yield: 77%; ¹H-NMR (400 MHz; acetone-d₆): δ 10.81 (s, 1H), 7.37 (s, 1H), 7.36 (dd, *J* = 2.8, 2.2 Hz, 1H), 7.00 (q, *J* = 2.2 Hz, 1H), 6.50 (dd, *J* = 2.8, 2.2 Hz, 1H), 4.33 (q, *J* = 7.0 Hz, 1H), 1.61 (d, *J* = 7.0 Hz, 3H); ¹³C-NMR (101 MHz, acetone-d₆): δ 142.08, 125.50, 121.87, 120.47, 119.34, 118.63, 109.49, 102.61, 25.97, 18.04; HRMS (FAB): Exact mass calcd for C₁₀H₉N₃ [M]⁺, 171.0797. Found 171.0799.


(E)-2-((1H-Pyrrol-3-yl)methylene)-3-ethylsuccinonitrile (4b). yield: 80%; ¹H-NMR (400 MHz; acetone-d₆): δ 10.79 (s, 1H), 7.41 (s, 1H), 7.36 (m, 1H), 7.00 (m, 1H), 6.50 (m, 1H), 4.15 (t, *J* = 7.5 Hz, 1H), 1.97 (m, 2H), 1.14 (t, *J* = 7.5 Hz, 3H); ¹³C-NMR (101 MHz, acetone-d₆): δ 142.86, 125.62, 121.87, 119.58, 119.54, 118.62, 109.41, 101.29, 32.98, 26.32, 11.57; HRMS (FAB): Exact mass calcd for C₁₁H₁₁N₃ [M]⁺, 185.0953. Found 185.0954.


(E)-2-((1H-Pyrrol-3-yl)methylene)-3-benzylsuccinonitrile (4c). yield: 75%; ¹H-NMR (400 MHz; acetone-d₆): δ 10.77 (s, 1H), 7.43-7.24 (m, 7H), 6.98 (q, *J* = 2.5 Hz, 1H), 6.48 (q, *J* = 2.2 Hz, 1H), 4.51 (t, *J* = 7.9 Hz, 1H), 3.34 (dd, *J* = 13.7, 7.9 Hz, 1H), 3.22 (dd, *J* = 13.7, 7.9 Hz, 1H); ¹³C-NMR (101 MHz, acetone-d₆): δ 143.17, 136.90, 129.96, 129.38, 128.14, 125.60, 121.89, 119.55, 119.26, 118.47, 109.25, 100.80, 38.13, 33.43; HRMS (FAB): Exact mass calcd for C₁₆H₁₃N₃ [M]⁺, 247.1110. Found 247.1107.

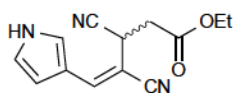

(E)-2-((1H-Pyrrol-3-yl)methylene)-3-allylsuccinonitrile (4d). yield: 67%; ¹H-NMR (400 MHz; acetone-d₆): δ 10.82 (s, 1H), 7.41 (s, 1H), 7.36 (dt, *J* = 3.1, 1.6 Hz, 1H), 7.00 (q, *J* = 2.3 Hz, 1H), 6.51-6.49 (m, 1H), 5.90 (ddt, *J* = 17.1, 10.2, 6.9 Hz, 1H), 5.31 (dq, *J* = 17.1, 1.4 Hz, 1H), 5.20 (dq, *J* = 10.2, 1.4 Hz, 1H), 4.31 (t, *J* = 7.6 Hz, 1H), 2.80-2.63 (m, 2H); ¹³C-NMR (101 MHz, acetone-d₆): δ 142.93, 133.43, 125.68, 121.94,

119.75, 119.50, 119.21, 118.59, 109.39, 100.91, 36.67, 31.45; HRMS (FAB): Exact mass calcd for $C_{12}H_{11}N_3$ $[M]^+$, 197.0953. Found 197.0958.



(*E*)-2-((1H-Pyrrol-3-yl)methylene)-3-(prop-2-yn-1-yl)succinonitrile (**4e**). yield: 72%; 1H -NMR (400 MHz; acetone- d_6): δ 10.83 (s, 1H), 7.47

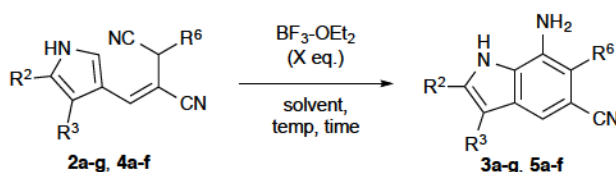
(s, 1H), 7.38 (q, J = 2.3 Hz, 1H), 7.01 (q, J = 2.3 Hz, 1H), 6.51 (q, J = 2.3 Hz, 1H), 4.48 (t, J = 7.4 Hz, 1H), 3.00-2.85 (m, 2H), 2.67 (t, J = 2.7 Hz, 1H); ^{13}C -NMR (101 MHz, acetone- d_6): δ 143.62, 125.92, 122.07, 119.15, 118.53, 118.49, 109.37, 99.99, 79.11, 73.81, 31.48, 22.52; HRMS (FAB): Exact mass calcd for $C_{12}H_9N_3$ $[M]^+$, 195.0797. Found 195.0793.



Ethyl (*E*)-3,4-dicyano-5-(1H-pyrrol-3-yl)pent-4-enoate (**4f**). yield: 80%; 1H -NMR (400 MHz; acetone- d_6): δ 10.85 (s, 1H), 7.44 (s, 1H), 7.39

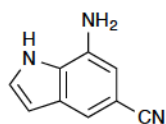
(t, J = 1.4 Hz, 1H), 7.03 (d, J = 2.4 Hz, 1H), 6.52 (q, J = 2.2 Hz, 1H), 4.60 (t, J = 7.4 Hz, 1H), 4.17 (q, J = 7.1 Hz, 2H), 3.15-2.98 (m, 2H), 1.23 (t, J = 7.1 Hz, 4H); ^{13}C -NMR (101 MHz, acetone- d_6): δ 169.54, 143.25, 125.90, 122.06, 119.19, 118.84, 118.61, 109.45, 99.85, 61.88, 36.63, 28.06, 14.34; HRMS (FAB): Exact mass calcd for $C_{13}H_{13}N_3O_2$ $[M]^+$, 243.1008. Found 243.1004.

Intramolecular Houben-Hoesch Annulation to Indoles

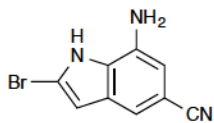


General Procedure. To a stirring 0.1 M solution of alkene **2a-g** or **4a-4f** (1.0 equiv.) in the 1,2-dichloroethane at room temperature was added $BF_3 \cdot OEt_2$ (2.5 equiv.). The reaction mixture was heated to 90 °C and stirred until completion (8-12 h), then cooled to room temperature and

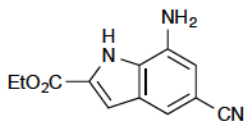
quenched with NaHCO₃. The reaction mixture was extracted with EtOAc (×3), and the combined organic extracts were washed with brine, dried over Na₂SO₄, and concentrated *in vacuo*. Crystallization from hot EtOAc and hexanes afforded the desired indoles.



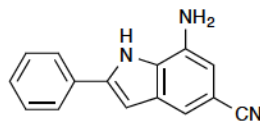
7-Amino-5-cyano-1H-indole (3a). yield: 91%; mp 158-159 °C; ¹H-NMR (400 MHz; acetone-d₆): δ 10.48 (s, 1H), 7.42 (d, *J* = 3.1 Hz, 1H), 7.37 (d, *J* = 1.3 Hz, 1H), 6.70 (d, *J* = 1.3 Hz, 1H), 6.53 (d, *J* = 3.1 Hz, 1H), 5.12 (s, 2H); ¹³C-NMR (101 MHz, acetone-d₆): δ 134.59, 128.53, 127.84, 125.96, 120.91, 115.53, 106.71, 103.08, 103.00; HRMS (FAB) calcd for C₉H₇N₃ [M]⁺, 157.0640; found, 157.0637.



7-Amino-2-bromo-5-cyano-1H-indole (3b). yield: 67%; mp 179-180 °C; ¹H-NMR (400 MHz; acetone-d₆): δ 7.30 (s, 1H), 6.72 (s, 1H), 6.61 (s, 1H), 5.15 (s, 1H); ¹³C-NMR (101 MHz, acetone-d₆): δ 137.84, 130.19, 120.79, 120.54, 114.97, 113.95, 106.15, 106.10, 104.53; HRMS (FAB) calcd for C₉H₆(⁷⁹Br)N₃ [M]⁺, 234.9745; found, 234.9743.

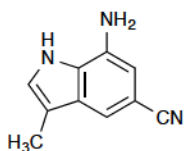


Ethyl 7-amino-5-cyano-1H-indole-2-carboxylate (3c). yield: 62%; mp 202-203 °C; ¹H-NMR (400 MHz; acetone-d₆): δ 11.02 (s, 1H), 7.46 (d, *J* = 1.4 Hz, 1H), 7.21 (d, *J* = 1.6 Hz, 1H), 6.78 (d, *J* = 1.4 Hz, 1H), 5.48 (s, 2H), 4.38 (q, *J* = 7.1 Hz, 2H), 1.37 (t, *J* = 7.1 Hz, 3H); ¹³C-NMR (101 MHz, acetone-d₆): δ 161.84, 136.40, 130.05, 129.75, 128.70, 121.09, 117.44, 109.69, 108.83, 105.67, 61.61, 14.63; HRMS (FAB): Exact mass calcd for C₁₂H₁₁N₃O₂ [M]⁺, 229.0851. Found 229.0855.



7-Amino-5-cyano-2-phenyl-1H-indole (3d). yield: 87%; mp 209-210 °C; ¹H-NMR (400 MHz; acetone-d₆): δ 10.72 (s, 1H), 7.86 (dd, *J* = 8.3, 1.2 Hz, 2H), 7.47 (dd, *J* = 8.3, 7.1 Hz, 2H), 7.37-7.35 (m, 2H), 6.94 (d, *J* = 1.4 Hz, 1H), 6.71 (d, *J* = 1.4 Hz, 1H), 5.23 (s, 2H); ¹³C-NMR (101 MHz, acetone-d₆): δ 140.13, 135.44, 132.85,

130.50, 129.43, 128.82, 126.13, 121.64, 116.02, 108.06, 104.57, 101.09; HRMS (FAB): Exact mass calcd for $C_{15}H_{11}N_3$ $[M]^+$, 233.0953. Found 233.0953.



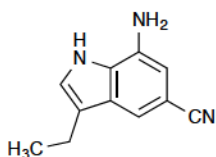
7-Amino-5-cyano-3-methyl-1H-indole (3e). yield: 94%; mp 181-182 °C; 1H -

NMR (400 MHz; acetone- d_6): δ 10.15 (s, 1H), 7.31 (s, 1H), 7.18 (s, 1H),

6.69 (s, 1H), 5.04 (s, 2H), 2.28 (s, 3H); ^{13}C -NMR (101 MHz, acetone- d_6): δ

135.32, 129.66, 128.99, 124.31, 121.90, 114.72, 112.78, 107.66, 103.28, 9.65; HRMS (FAB)

calcd for $C_{10}H_9N_3$ $[M]^+$, 171.0797; found, 171.0795.



7-Amino-5-cyano-3-ethyl-1H-indole (3f). yield: 92%; mp 139-140 °C;

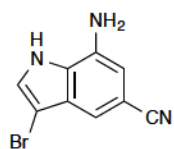
1H -NMR (400 MHz; acetone- d_6): δ 10.16 (s, 1H), 7.35 (s, 1H), 7.20 (s,

1H), 6.69 (s, 1H), 5.05 (s, 2H), 2.74 (q, J = 7.5 Hz, 2H), 1.29 (t, J = 7.5 Hz,

3H); ^{13}C -NMR (101 MHz, acetone- d_6): δ 135.39, 129.12, 128.78, 123.17, 121.91, 114.81,

113.23, 107.65, 103.26, 18.82, 14.96; HRMS (FAB) calcd for $C_{11}H_{11}N_3$ $[M]^+$, 185.0953; found,

185.0960.



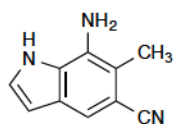
7-Amino-3-bromo-5-cyano-1H-indole (3g). yield: 75%; mp 187-189 °C; 1H -

NMR (400 MHz; acetone- d_6): δ 10.76 (s, 1H), 7.57 (d, J = 1.3 Hz, 1H), 7.22

(d, J = 1.3 Hz, 1H), 6.78 (d, J = 1.3 Hz, 1H), 5.27 (s, 2H).; ^{13}C -NMR (101

MHz, acetone- d_6): δ 135.98, 128.22, 128.10, 126.58, 121.11, 113.83, 108.50, 105.26, 91.80;

HRMS (FAB) calcd for $C_9H_6(^{79}Br)N_3$ $[M]^+$, 236.9745; found, 236.9747.



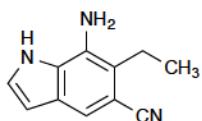
7-Amino-5-cyano-6-methyl-1H-indole (5a). yield: 88%; mp 161-162 °C; 1H -

NMR (400 MHz; acetone- d_6): δ 10.32 (s, 1H), 7.39 (s, 1H), 7.37 (d, J = 3.2

Hz, 1H), 6.47 (d, J = 3.2 Hz, 1H), 4.90 (s, 2H), 2.42 (s, 3H); ^{13}C -NMR (101 MHz, acetone- d_6):

δ 132.77, 129.17, 127.61, 126.49, 121.20, 116.62, 114.06, 105.67, 103.58, 14.92; HRMS (FAB):

Exact mass calcd for $C_{10}H_9N_3$ $[M]$, 171.0797. Found 171.0793.



7-Amino-5-cyano-6-ethyl-1H-indole (5b). yield: 95%; mp 165-166 °C; ¹H-

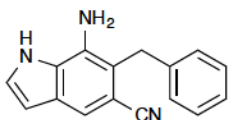
NMR (400 MHz; acetone-d₆): δ 10.34 (s, 1H), 7.40 (s, 1H), 7.37 (dd, *J* =

3.0, 1.8 Hz, 1H), 6.47 (t, *J* = 1.8 Hz, 1H), 4.93 (s, 2H), 2.91 (q, *J* = 7.5 Hz, 2H), 1.22 (t, *J* = 7.5

Hz, 3H); ¹³C-NMR (101 MHz, acetone-d₆): δ 132.05, 129.45, 127.53, 126.54, 121.06, 120.62,

117.08, 105.01, 103.55, 23.02, 14.31; HRMS (FAB): Exact mass calcd for C₁₁H₁₁N₃ [M]⁺,

185.0953. Found 185.0955.



7-Amino-6-benzyl-5-cyano-1H-indole (5c). yield: 96%; mp 170-171 °C;

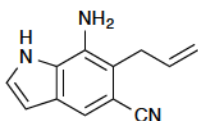
¹H-NMR (400 MHz; acetone-d₆): δ 10.45 (s, 1H), 7.50 (s, 1H), 7.40 (d, *J*

= 3.2 Hz, 1H), 7.27-7.24 (m, 4H), 7.18-7.15 (m, 1H), 6.53 (d, *J* = 3.2 Hz, 1H), 4.87 (s, 2H),

4.30 (s, 2H); ¹³C-NMR (101 MHz, acetone-d₆): δ 140.55, 133.04, 129.43, 129.17, 128.98,

127.99, 126.89, 126.85, 121.34, 117.33, 117.02, 106.16, 103.71, 35.30; HRMS (FAB): Exact

mass calcd for C₁₆H₁₃N₃ [M]⁺, 247.1110. Found 247.1109.



6-Allyl-7-amino-5-cyano-1H-indole (5d). yield: 93%; mp 113-115 °C; ¹H-

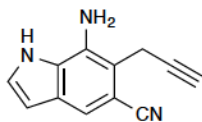
NMR (400 MHz; acetone-d₆): δ 10.43 (s, 1H), 7.43 (s, 1H), 7.39 (d, *J* = 3.1

Hz, 1H), 6.50 (d, *J* = 3.1 Hz, 1H), 5.98 (ddt, *J* = 17.1, 10.1, 6.0 Hz, 1H), 5.09-5.00 (m, 2H), 4.88

(s, 2H), 3.65 (dt, *J* = 6.0, 1.7 Hz, 2H); ¹³C-NMR (101 MHz, acetone-d₆): δ 136.08, 132.84,

129.75, 129.03, 127.87, 126.72, 121.00, 117.24, 115.64, 105.66, 103.65, 33.99; HRMS (FAB):

Exact mass calcd for C₁₂H₁₁N₃ [M]⁺, 197.0953. Found 197.0960.



7-Amino-5-cyano-6-(prop-2-yn-1-yl)-1H-indole (5e). yield: 92%; mp

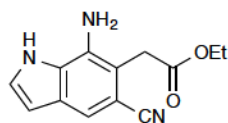
182-183; ¹H-NMR (400 MHz; acetone-d₆): δ 10.52 (s, 1H), 7.45 (s, 1H),

7.43 (m, 1H), 6.52 (m, 1H), 5.08 (s, 2H), 3.80 (d, *J* = 2.8 Hz, 2H), 2.52 (t, *J* = 2.8 Hz, 1H); ¹³C-

NMR (101 MHz, acetone-d₆): δ 133.06, 129.30, 128.18, 127.09, 120.61, 117.30, 112.97, 105.01,

103.77, 81.35, 70.97, 19.32; HRMS (FAB): Exact mass calcd for $C_{12}H_9N_3$ $[M]^+$, 195.0797.

Found 195.0796.



Ethyl 2-(7-amino-5-cyano-1H-indol-6-yl)acetate (5f). yield: 72%; mp

177-178 °C; 1H -NMR (400 MHz; acetone- d_6): δ 10.51 (s, 1H), 7.46 (s,

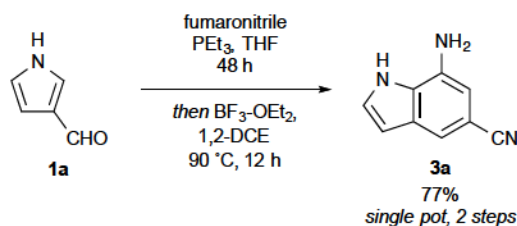
1H), 7.42 (t, J = 2.3 Hz, 1H), 6.52 (t, J = 2.0 Hz, 1H), 5.07 (s, 2H), 4.12 (q, J = 7.0 Hz, 2H), 3.91

(s, 2H), 1.21 (t, J = 7.0 Hz, 3H). ^{13}C -NMR (101 MHz, acetone- d_6): δ 171.32, 133.88, 129.43,

128.24, 127.05, 120.73, 117.41, 111.71, 106.22, 103.81, 61.39, 35.72, 14.49; Exact mass calcd for

$C_{13}H_{13}N_3O_2$ $[M]^+$, 243.1008. Found 243.1007.

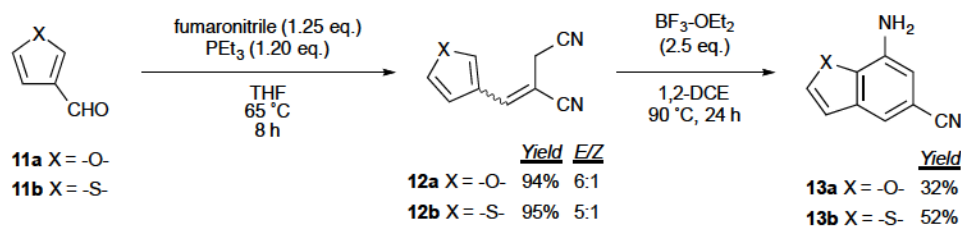
One-Pot Wittig/Houben-Hoesch Indole Synthesis



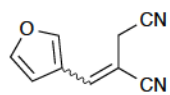
Procedure. To a stirring solution of pyrrole-3-carboxaldehyde (100 mg, 1.05 mmol) in THF (2.1 mL) at room temperature was added fumaronitrile (103 mg, 1.31 mmol) followed by trimethylphosphine (131 μ L, 1.26 mmol) dropwise. The reaction mixture was stirred for 48 h, then concentrated on a rotary evaporator. The residue was then taken up in 1,2-DCE (10.5 mL) and $BF_3 \cdot OEt_2$ (324 μ L, 2.63 mmol) was added dropwise. The reaction mixture was heated to 90 °C and stirred for 12 h, then cooled to room temperature and quenched with $NaHCO_3$. The crude product mixture was extracted with EtOAc (3×20 mL), and the combined organic extracts were washed with brine, dried over sodium sulfate, and concentrated *in vacuo*. The crude product was run through a short plug of silica gel, which was eluted with 30%

acetone/petroleum ether, then recrystallized from hot EtOAc and hexanes to afford indole **3a** (128 mg, 0.81 mmol, 77%).

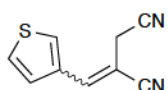
Preparation of Benzofuran **13a** and Benzothiophene **13b**



General Procedure for Wittig Olefination. To a stirring solution of the heteroaryl-3-carboxaldehyde (1.0 equiv.) in THF (0.25 M) at room temperature was added fumaronitrile (1.25 equiv.) followed by triethylphosphine (1.20 equiv.) dropwise. The reaction mixture was stirred at 65 °C until the starting material was no longer visible by TLC (typically 8 h), then quenched with NaHCO₃ and extracted with EtOAc (×3). The combined organic extracts were washed with brine, dried over Na₂SO₄, and concentrated *in vacuo*. Purification by silica gel chromatography afforded a mixture of the *E*- and *Z*-olefin Wittig products due to the similar R_f values of the two isomers. Crystallization was unable to separate the two isomers, which were used as an *E/Z* mixture (6:1 for **12a**, 5:1 for **12b**) for the cyclization reaction. The spectroscopic data is given for the *E*-isomer.

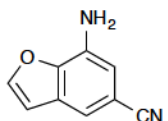


2-(Furan-3-ylmethylene)succinonitrile (12a**).** ¹H-NMR (400 MHz; acetone-d₆): δ 8.10 (s, 1H), 7.77 (d, *J* = 1.4 Hz, 1H), 7.47 (s, 1H), 6.87 (d, *J* = 1.4 Hz, 1H), 3.91 (d, *J* = 1.2 Hz, 2H); ¹³C-NMR (101 MHz, acetone-d₆): δ 147.62, 146.04, 139.13, 120.97, 119.42, 116.56, 110.56, 102.43, 19.60; HRMS (EI): Exact mass calcd for C₉H₆N₂O [M]⁺, 158.0480. Found 158.0483.

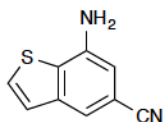


2-(Thiophen-3-ylmethylene)succinonitrile (12b). $^1\text{H-NMR}$ (400 MHz; acetone- d_6): δ 7.93 (d, J = 2.8 Hz, 1H), 7.68 (dd, J = 5.1, 2.8 Hz, 1H), 7.61 (s, 1H), 7.40 (dd, J = 5.1, 1.3 Hz, 1H), 3.96 (d, J = 1.3 Hz, 2H); $^{13}\text{C-NMR}$ (101 MHz, acetone- d_6): δ 142.24, 135.29, 131.58, 128.88, 128.44, 119.50, 116.60, 102.85, 19.75; HRMS (EI): Exact mass calcd for $\text{C}_9\text{H}_6\text{N}_2\text{S}$ $[\text{M}]^+$, 174.0252; Found 174.0257.

General Procedure for Annulation to Benzofuran 13a and Benzothiophene 13b. To a stirring 0.1 M solution of alkene 12a-b (1.0 equiv.) in 1,2-dichloroethane at room temperature was added $\text{BF}_3 \cdot \text{OEt}_2$ (2.5 equiv.). The reaction mixture was heated to 90 °C and stirred for 24 h. The reaction stalled around 24 h and did not progress further even with addition of excess Lewis acid or extended reaction time. The reaction mixture was then cooled to room temperature and quenched with NaHCO_3 . The reaction mixture was extracted with EtOAc (x3), and the combined organic extracts were washed with brine, dried over Na_2SO_4 , and concentrated *in vacuo*. Recrystallization from hot EtOAc and hexanes afforded the desired heterocycles 13a-b.

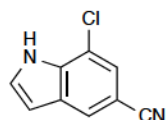
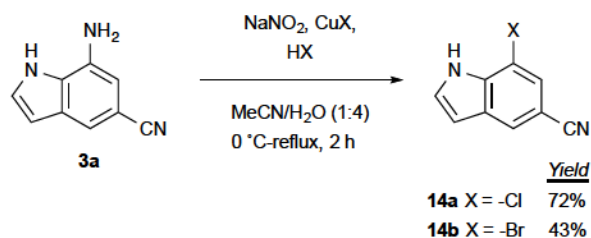


7-Amino-5-cyanobenzofuran (13a). yield: 32%; mp 197-198 °C; $^1\text{H-NMR}$ (400 MHz; MeOD): δ 8.09 (d, J = 2.2 Hz, 1H), 8.03 (d, J = 1.3 Hz, 1H), 7.55 (d, J = 1.3 Hz, 1H), 7.11 (d, J = 2.2 Hz, 1H); $^{13}\text{C-NMR}$ (101 MHz, MeOD): δ 150.02, 149.94, 131.47, 125.69, 122.07, 122.04, 120.74, 119.32, 108.61; HRMS (FAB) calcd for $\text{C}_9\text{H}_6\text{N}_2\text{O}$ $[\text{M}]^+$, 158.0480; found, 158.0479.

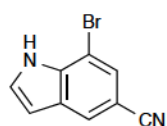


7-Amino-5-cyanobenzothiophene (13b). yield: 52%; mp 123-124 °C; $^1\text{H-NMR}$ (300 MHz; acetone- d_6): δ 7.77 (d, J = 5.4 Hz, 1H), 7.63 (d, J = 1.4 Hz, 1H), 7.48 (d, J = 5.4 Hz, 1H), 6.92 (d, J = 1.4 Hz, 1H), 5.50 (s, 2H); $^{13}\text{C-NMR}$ (101 MHz, acetone- d_6): δ 144.62, 141.81, 130.72, 128.82, 125.73, 120.43, 117.85, 109.78, 109.60; HRMS (FAB) calcd for $\text{C}_9\text{H}_6\text{N}_2\text{S}$ $[\text{M}]^+$, 174.0252; found, 174.0258.

Elaboration of 3a: Sandmeyer Reaction



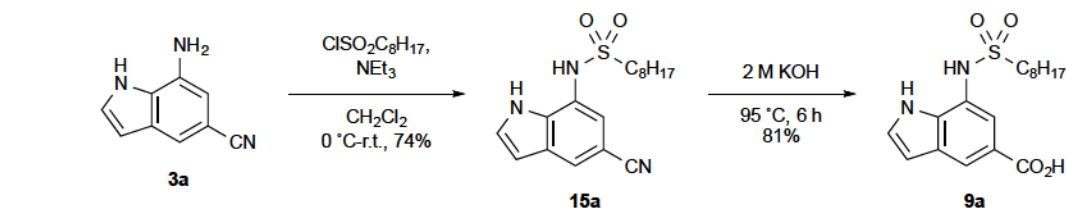
7-Chloro-5-cyano-1H-indole (14a). To a stirring solution of 7-amino-5-cyano[1H]indole•HCl (100 mg, 0.52 mmol) in 4.3 mL MeCN and 4.3 mL water at 0 °C was added 0.3 mL concentrated HCl. Sodium nitrite (71 mg, 1.03 mmol) was then added as a solution in 4.3 mL water. The reaction mixture was allowed to warm to room temperature over 30 min before addition of CuCl (256 mg, 2.58 mmol) as a solution in 8.6 mL water. The reaction mixture was heated to reflux for 3 h, then the MeCN was evaporated. The reaction mixture was diluted with water (100 mL) and extracted with EtOAc (3 × 30). The combined organic extracts were washed with brine, dried over Na₂SO₄, and concentrated *in vacuo*. Crystallization from hot EtOAc and hexanes afforded the chlorinated indole (71 mg, 0.40 mmol, 72%). ¹H-NMR (400 MHz; acetone-d₆): δ 11.15 (s, 1H), 8.06 (s, 1H), 7.64 (t, *J* = 3.0 Hz, 1H), 7.53 (d, *J* = 1.6 Hz, 1H), 6.76 (dd, *J* = 3.0, 1.6 Hz, 1H); ¹³C-NMR (101 MHz, acetone-d₆): δ 135.10, 129.50, 128.53, 124.94, 122.90, 118.96, 117.25, 103.99, 103.32; HRMS (FAB) calcd for C₉H₅ClN₂ [M]⁺, 176.0141; found, 176.0153.



7-Bromo-5-cyano-1H-indole (14b). To a stirring solution of the 7-amino-5-cyano[1H]indole•HCl (100 mg, 0.52 mmol) in 4.3 mL MeCN and 4.3 mL water at 0 °C was added the HBr (48% solution in water, 0.3 mL). Sodium nitrite (72 mg, 1.03 mmol) was then added as a solution in 4.3 mL water. The reaction mixture was allowed to warm to room temperature over 30 min before addition of CuBr (370 mg, 2.58 mmol) as a solution in

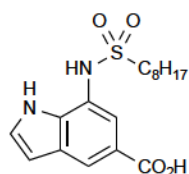
8.6 mL water. The reaction mixture was heated to reflux for 3 h, then the MeCN was evaporated. The reaction mixture was diluted with water (100 mL) and extracted with EtOAc (3 × 30 mL). The combined organic extracts were dried over Na₂SO₄ and concentrated *in vacuo*. Purification by recrystallization from EtOAc and hexanes afforded the pure bromoindole (49 mg, 0.22 mmol, 43%). ¹H-NMR (400 MHz; acetone-d₆): δ 11.01 (s, 1H), 8.09 (s, 1H), 7.66 (s, 1H), 7.63 (s, 1H), 6.79 (s, 1H); ¹³C-NMR (101 MHz, acetone-d₆): δ 136.62, 129.01, 128.51, 125.89, 125.37, 118.85, 104.73, 104.11, 103.66; HRMS (FAB) calcd for C₉H₅⁷⁹BrN₂ [M]⁺, 219.9636; found, 219.9637; C₉H₅⁸¹BrN₂ [M]⁺, 221.9616; found, 221.9615.

Elaboration of 3a: Preparation of GPAT Inhibitor Analog 9a.



N-(5-cyano-1H-indol-7-yl)octane-1-sulfonamide (15a). To a stirring solution of indole **3a** (68 mg, 0.43 mmol) in CH₂Cl₂ (1 mL) at 0 °C was added octanesulfonyl chloride (101 μL, 0.52 mmol) followed by NEt₃ (121 μL, 0.87 mmol) dropwise. The reaction mixture was allowed to warm to room temperature and stirred for 24 h. The reaction was quenched by addition of 20 mL NaHCO₃ and extracted with CH₂Cl₂ (3 × 15 mL). The combined organic extracts were dried over Na₂SO₄, and concentrated *in vacuo*. Purification by flash chromatography (20% EtOAc/Hexanes) afforded the pure sulfonamide (106 mg, 0.32 mmol, 74%). ¹H-NMR (400 MHz; acetone-d₆): δ 10.71 (s, 1H), 8.73 (s, 1H), 7.95 (d, *J* = 1.1 Hz, 1H), 7.60 (t, *J* = 2.8 Hz, 1H), 7.46 (d, *J* = 1.2 Hz, 1H), 6.70 (dd,

$J = 3.2, 1.9 \text{ Hz}$, 1H), 3.24–3.20 (m, 2H), 1.84–1.76 (m, 2H), 1.39 (quintet, $J = 7.1 \text{ Hz}$, 2H), 1.24 (m, $J = 11.5 \text{ Hz}$, 8H), 0.85 (t, $J = 6.9 \text{ Hz}$, 3H); ^{13}C NMR (100 MHz; acetone- d_6): δ 132.4, 130.0, 128.0, 123.6, 123.2, 119.7, 117.5, 103.3, 102.7, 51.0, 31.5, 28.76, 28.74, 27.8, 23.3, 22.3, 13.4; HRMS (EI) calcd for $\text{C}_{17}\text{H}_{23}\text{N}_3\text{O}_2\text{S} [\text{M}]^+$, 333.1511; found, 333.1510.



7-(octylsulfonamido)-1H-indole-5-carboxylic acid (9a). To a stirring solution the cyanoindole **15a** (33 mg, 0.10 mmol) at room temperature was added 2 M KOH (1 mL). The reaction mixture was stirred at 95 °C for 6 h, then quenched with 1 M HCl (3 mL). The white precipitate was filtered, washed with cold water, and dried. Purification by flash chromatography (20% acetone/77% petroleum ether/3% AcOH) afforded the pure carboxylic acid **9a** (28 mg, 0.080 mmol, 81%). ^1H -NMR (400 MHz; acetone- d_6): δ 10.60 (s, 1H), 8.28 (s, 1H), 7.90 (s, 1H), 7.50 (s, 1H), 6.67 (s, 1H), 3.15 (m, 2H), 1.81 (m, 2H), 1.37 (m, 2H), 1.22 (m, 8H), 0.84 (t, $J = 6.8 \text{ Hz}$, 3H); ^{13}C -NMR (101 MHz, acetone- d_6): δ 168.62, 134.35, 130.56, 127.86, 127.70, 122.73, 122.23, 118.15, 104.44, 51.52, 32.41, 30.09, 29.89, 28.75, 24.23, 23.22, 14.31; HRMS (EI) calcd for $\text{C}_{17}\text{H}_{24}\text{N}_2\text{O}_4\text{S} [\text{M}]^+$, 352.1457; found, 352.1456.

3.12 References

1. Wydysh, E.A.; Medghalchi, S.M.; Vadlamudi, A.; Townsend, C.A. *J. Med. Chem.* **2009**, *52*, 3317–3327.
2. B Kuhajda, F. P.; Aja, S.; Tu, Y.; Han, W. F.; Medghalchi, S. M.; Meskini, El, R.; Landree, L. E.; Peterson, J. M.; Daniels, K.; Wong, K.; Wydysh, E. A.; Townsend, C. A.; Ronnett, G. V. *Am. J. Physiol. Regul. Integr. Comp. Physiol.* **2011**, *301*, R116–R130.

3. Outlaw, V. K.; Wydysh, E. A.; Vadlamudi, A.; Medghalchi, S. M.; Townsend, C. A. *Med. Chem. Comm.* **2014**, *5*, 826–830.
4. Sharma, V.; Kumar, P.; Pathak, D. *J. Het. Chem.* **2010**, *41*.
5. Fischer, E.; Hess, O. *Ber. Chem. Ges.* **1884**, *17*, 559.
6. Bischler, A. *Chem. Ber.* **1892**, *25*, 2860.
7. Sugasawa, T.; Adachi, M.; Sasakura, K.; Kitagawa, A. *J. Org. Chem.* **1979**, *44*, 578–586.
8. Larock, R. C.; Yum, E. K. *J. Am. Chem. Soc.* **1991**, *113*, 6689.
9. Hegedus, L. S.; Toro, J. L.; Miles, W. H.; Harrington, P. J. *J. Org. Chem.* **1987**, *52*, 3319–3322.
10. Mori, M.; Chiba, K.; Ban, Y. *Tetrahedron Letters* **1977**, *18*, 1037–1040.
11. Reissert, A. *Ber. Chem Ges.* **1897**, *30*, 1030.
12. Bartoli, G.; Palmieri, G.; Bosco, M.; Dalpozzo, R. *Tet. Lett.* **1989**, *30*, 2129.
13. For recent reviews, see: a) Taber, D. F.; Tirunahari, P. K. *Tetrahedron* **2011**, *67*, 7195–7210.
b) Cacchi, S.; Fabrizi, G. *Chem. Rev.* **2005**, *105*, 2873–2920.
14. For pyrrole-based indole synthesis, see: a) Moskal, J.; van Leusen, A. M. *J. Org. Chem.* **1986**, *51*, 4131.; b) Ishibashi, H.; Tabata, T.; Hanaoka, K.; Iriyama, H.; Akamatsu, S.; Ikeda, M. *Tet. Lett.* **1993**, *34*, 489.; c) Della Rossa, C.; Kneeteman, M.; Mancini, P. *Tet. Lett.* **2007**, *48*, 1435.; d) Kim, M.; Vedejs, E. *J. Org. Chem.* **2004**, *69*, 6945.; e) Iwasaki, M.; Kobayashi, Y.; Li, J.-P.; Matsuzaka, H.; Ishii, Y.; Hidai, M. *J. Org. Chem.* **1991**, *56*, 1922.; f) Katritzky, A. R.; Le-doux, S.; Nair, S. K. *J. Org. Chem.* **2003**, *68*, 5728.; g) Asao, N.; Ai-kawa, H. *J. Org. Chem.* **2006**, *71*, 5249.; h) Zhao, J.; Hughes, C. O.; Toste, F. D. *J. Am. Chem. Soc.* **2006**, *128*, 7436.
15. Muchowski, J. M.; Naef, R. *Helv. Chim. Act.* **1984**, *67*, 1168–1172.

16. Charrier, N.; Clarke, B.; Cutler, L.; Demont, E.; Dingwall, C.; Dunsdon, R.; East, P.; Hawkins, J.; Howes, C.; Hussain, I.; Jeffrey, P.; Maile, G.; Matico, R.; Mosley, J.; Naylor, A.; O'Brien, A.; Red-shaw, S.; Rowland, P.; Soleil, V.; Smith, K. J.; Sweitzer, S.; Theobald, P.; Vesey, D.; Walter, D. S.; Wayne, G. *J. Med. Chem.* **2008**, *51*, 3313–3317.
17. Sams, A. G.; Eskildsen, J.; Bastlund, J. F. Intl. Patent WO 2012/131031 A1, October 4, 2012.
18. a) Hedaya, E.; Theodoropoulos, S. *Tetrahedron* **1968**, *24*, 2241–2254.; b) Eyjólfsson, R. *Acta. Chem. Scand.* **1970**, *24*, 3075–3078.; c) Balasubramanian, V.; Tongare, D. B.; Gosavi, S. S.; Babar, S. M. *Proc. Indian Acad. Sci., Chem. Sci.* **1993**, *105*, 265–271.; d) McCombie, S. W.; Luchaco, C. A. *Tet. Lett.* **1997**, *38*, 5775–5776.; e) Marcq, V.; Mirand, C.; Decarme, M.; Emonard, H.; Horne-beck, W. *Bioorg. Med. Chem. Lett.* **2003**, *13*, 2843–2846.
19. Bray, B. L.; Mathies, P. H.; Naef, R.; Solas, D. R.; Tidwell, T. T.; Artis, D. R.; Muchowski, J. *M. J. Org. Chem.* **1990**, *55*, 6317–6328.
20. Arikawa, Y.; Nishida, H.; Kurasawa, O.; Hasuoka, A.; Hirase, K.; Inatomi, N.; Hori, Y.; Matsukawa, J.; Imanishi, A.; Kondo, M.; Tarui, N.; Hamada, T.; Takagi, T.; Takeuchi, T.; Kajino, M. *J. Med. Chem.* **2012**, *55*, 4446–4456.
21. Stefan, K.-P.; Schuhmann, W.; Parlar, H.; Korte, F. *Chem. Ber.* **1989**, *122*, 169–174.
22. Dawadi, P. B. S.; Lugtenburg, J. *Eur. J. Org. Chem.* **2008**, 2288–2292.

Chapter 4

One-Pot Synthesis of Highly Substituted *N*-Fused Heteroaromatic Bicycles from Azole Aldehydes

4.1 Introduction

In Chapter 3, new methodology was described for the synthesis of substituted indole-containing compounds. This route was devised for the rapid access and diversification of indole-based inhibitors of glycerol-3-phosphate acyltransferase (GPAT). In addition to the indole bicycle, compounds containing *N*-fused heteroaromatic bicycles, as shown in Fig. 4.1, were also of interest. Although isosteric to the indole structure, each *N*-fused heteroaromatic bicyclic core presents a distinct array of H-bond donors and acceptors and a unique electronic structure. The heteroaromatic bicycles targeted included the indolizine, imidazo[1,2-*a*]pyridine, and imidazo[1,5-*a*]pyridine nuclei. Because no sufficient method existed for the synthesis of these 5,7-disubstituted structures, a route was devised for their ready preparation.

N-fused aromatic heterocycles, such as the indolizine and imidazopyridine classes, are attractive synthetic targets owing to their pharmacological potential and unique electronic properties. The wide array of biological effects elicited by members of these heteroaromatic classes has been well documented, including antimicrobial,¹ antiviral,² antiinflammatory,³ antitubercular,⁴ anticancer,⁵ antinociceptive,⁶ antiprotozoal,⁷ and hypnoselective⁸ activities. In addition, these scaffolds, notably the imidazopyridines, have found utility as *N*-heterocyclic carbene (NHC) ligands in complexes with promising catalytic reactivity⁹ or as inks and dyes. As a consequence of their diverse uses, several synthetic methods have been developed for their

preparation. Traditional syntheses employ substituted pyridines to annulate the 5-membered portion of the bicyclic system.¹⁰⁻¹¹ For example, the most common indolizine syntheses involve the euphonious Tschitschibabin reaction or its conceptual variants, and proceed by reaction of 2-alkylpyridines with α -halo ketones.^{10a} More recently, strategies have been developed to access these bicycles from their 5-membered heterocyclic precursors.¹² Lee and Kim, for example, demonstrated the aldol-type cyclization of *N*-substituted 2-acetylpyrroles under alkaline conditions to furnish 6,8-disubstituted indolizines.^{12c}

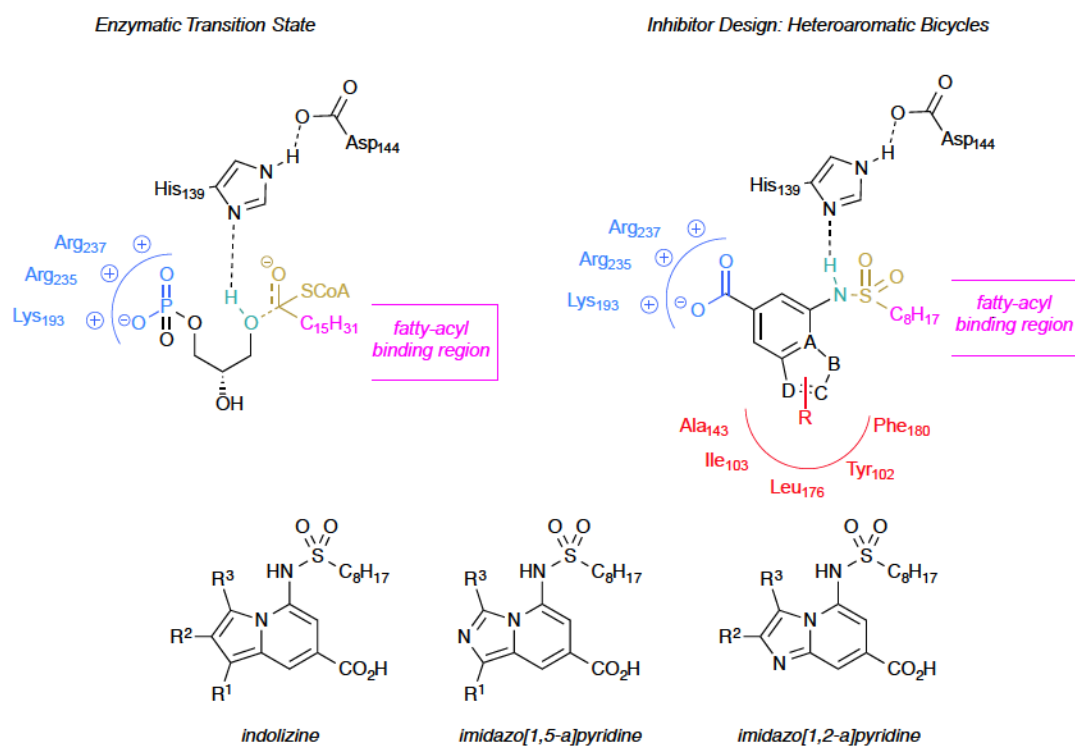


Figure 4.1 Design of GPAT inhibitors containing *N*-fused heteroaromatic bicycles

4.2 Design of Synthetic Route

Despite recent developments to *N*-fused heteroaromatic bicycles, to our knowledge no routes exist that allow the direct synthesis of 5-amino-substituted indolizines. We recently

reported a flexible, efficient route to highly substituted 7-aminoindoles from pyrrole-3-carboxaldehydes.¹³ This route utilized a one-pot, three component Wittig olefination of the aldehydes with a trialkylphosphine and fumaronitrile to afford predominantly *E*-alkenes, followed by Lewis acid-mediated intramolecular Houben-Hoesch reaction to the corresponding indoles. We envisioned a mechanistically related route to obtain the 5-aminoindolizine, 5-aminoimidazo[1,2-*a*]pyridine, and 5-aminoimidazo[1,5-*a*]pyridine classes, as shown in Fig. 4.2. In this case, rather than nucleophilic attack of the pyrrolic α -carbon on a Lewis acid-activated nitrile, we reasoned that the relative acidity of the azolic N-H proton would allow for facile deprotonation to a nucleophilic azolide anion followed by cycloaromatization. Alternatively, a second deprotonation could furnish an allylic dianion that could react selectively with electrophiles prior to cyclization to allow for substituent control at the 6-position.

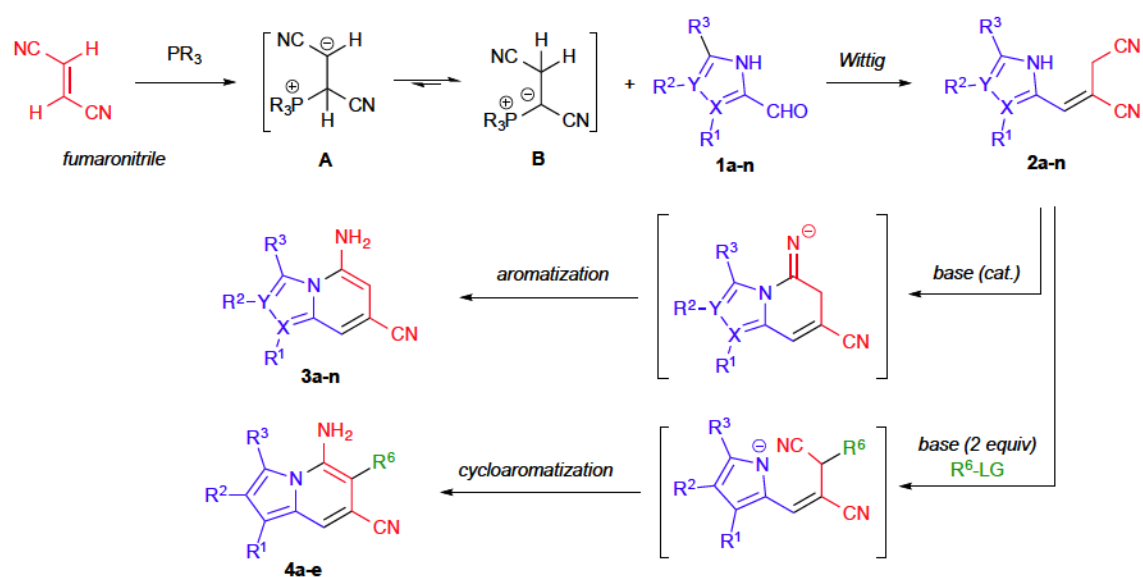
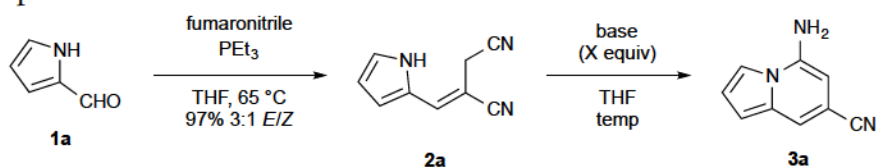


Figure 4.2 Proposed route to *N*-fused heterocycles

4.3 Optimization of Method

Extending the conditions established in our laboratory,¹⁴ Wittig olefination of commercially-available pyrrole-2-carboxaldehyde afforded alkene **2a** in excellent yield and good diastereoselectivity as shown in Table 4.1. To establish an optimal annulation procedure, the *E*-isomer, purified by recrystallization from the diastereomeric mixture, was then subjected to a variety of conditions. Under the Lewis acidic conditions employed previously for the Houben-Hoesch annulation to 7-aminoindoles ($\text{BF}_3 \cdot \text{OEt}_2$), no desired cyclization was observed. Similarly, treatment with LDA at -78°C resulted in the isolation of only starting material. At 0°C , however, treatment with stoichiometric amounts of the strong bases LDA or LiHMDS effected rapid and complete conversion to the indolizine **3a**. The weaker bases KOH and K_2CO_3 also exhibited the desired cyclization although higher temperatures were required. For KOH, complete conversion to the indolizine was observed at room temperature after 15 minutes. K_2CO_3 was far less efficient and required reflux temperature, longer reaction time, and afforded lower yields. We hypothesized that the initial cyclized product, an anilide anion, could also act as a base itself thereby necessitating only a catalytic amount of base to initiate the cycle. Indeed, treatment with catalytic amounts of LDA at 0°C or KOH at room temperature effected complete conversion to the cyclized product. Due to the milder conditions, short reaction time, low cost, and ease of workup, we proceeded with catalytic KOH as the optimal method for annulation.

Table 4.1 Optimization of Reaction Conditions



entry	reagent	X	temp ($^\circ\text{C}$)	time (h)	yield of 3a (%)
1	$\text{BF}_3 \cdot \text{OEt}_2^a$	2.5	90	12	0
2	LDA	1.0	-78	1	0
3	LDA	1.0	0	0.5	98
4	LDA	0.4	0	0.5	97
5	LiHMDS	1.0	0	0.5	97
6	KOH	4.0	23	0.25	97
7	KOH	0.4	23	0.25	96
8	K_2CO_3	4.0	70	1	86

^aReaction run in 1,2-dichloroethane rather than THF.

4.4 Scope of Method

The mild and efficient cyclization conditions encouraged us to combine the Wittig olefination and cyclization steps into a tandem, one-pot synthesis of highly substituted *N*-fused heteroaromatic bicycles from azole aldehydes as shown in Fig. 4.3. The unadorned pyrrole-2-carboxaldehyde **1a** was reacted as before with PEt_3 and fumaronitrile at $65\text{ }^\circ\text{C}$, but for the one-pot procedure, the *E/Z* mixture was cooled to room temperature and catalytic KOH was added. The *E*-isomer was completely converted to 5-amino-7-cyanoindolizine within 30 minutes while the *Z*-isomer was left unreacted. The 74% yield for this reaction approaches the stoichiometric conversion of the 3:1 *E/Z* mixture. To demonstrate the scope of the olefination/cyclization sequence, a variety of substituted pyrrole and imidazole aldehydes was employed. Under the conditions used before, aldehydes **1b-n** underwent alkene formation and cyclization to indolizines, imidazo[1,2-*a*]pyridines, and imidazo[1,5-*a*]pyridines in moderate to good yields.

Like the unsubstituted pyrrole-2-aldehyde, yields approached the stoichiometric limit for the *E*-isomer present in the diastereomeric mixture of the crude Wittig reaction. The imidazole aldehydes exhibited much faster reaction rates for the Wittig reaction but much slower rates of annulation. The additional nitrogen on the imidazole likely activates the aldehyde for attack by the phosphonium ylide but the increased acidity of the imidazole stabilizes the azolide anion, thereby decreasing its nucleophilicity and slowing cyclization.

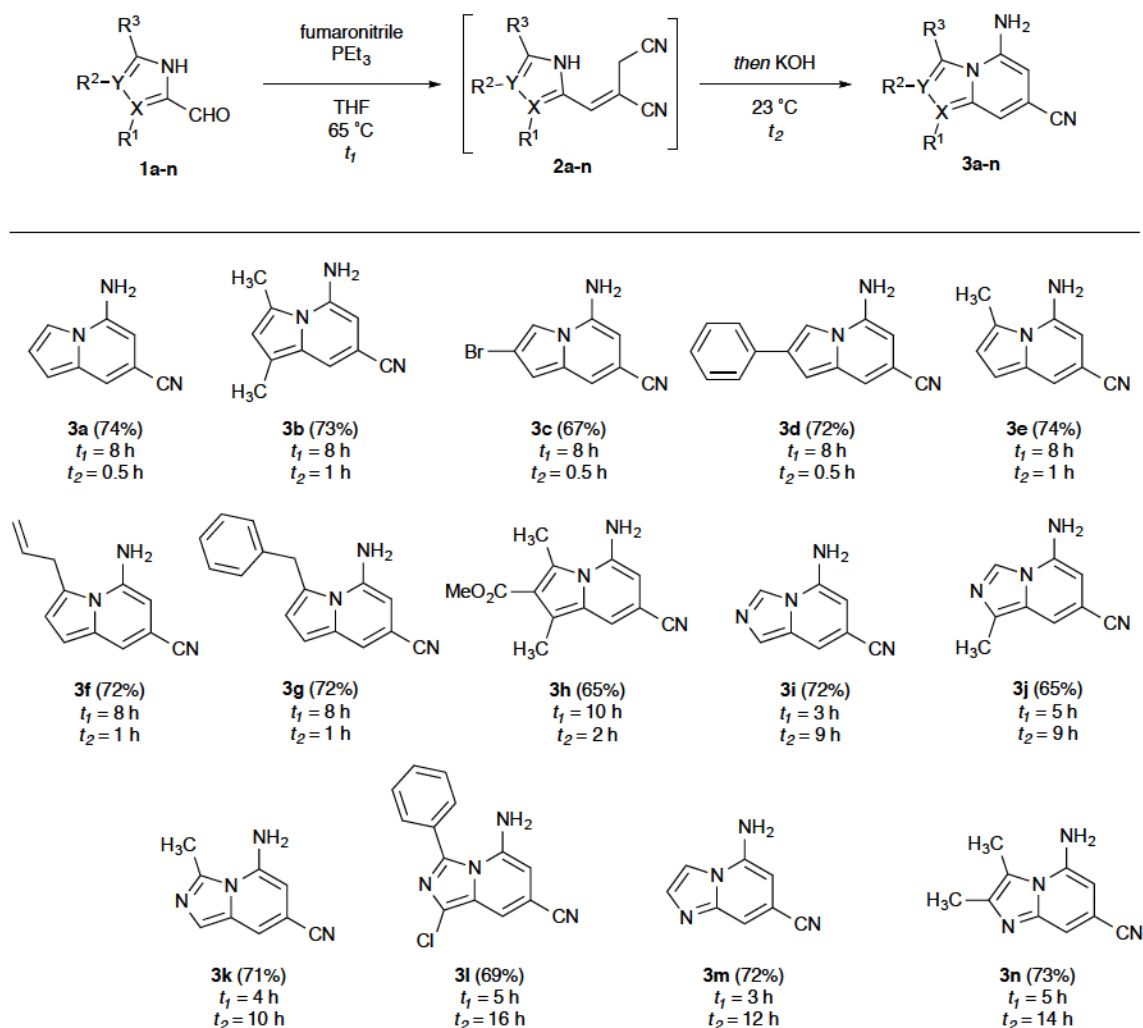


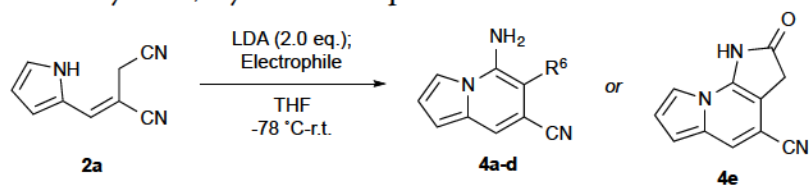
Figure 4.3 Scope of one-pot annulation of azole aldehydes

The conditions were tolerant of a range of substituents including halide, ester, and aryl functionalities, as well as alkyl substituents at each of the possible positions on the azole aldehydes. Deactivated azole aldehydes, for example those containing halogen and ester functionalities, showed a modest decline in yield. Aldehydes with substituents at the α -position (e.g. **1b,h,l**) showed a moderate decrease in cyclization rate, potentially due to the A^{1,3} strain present between the C-3 and C-5 substituents in the cyclized products.

4.5 Dianionic Approach to C-6 Substituted Indolizines

With no cyclization occurring at -78 °C, we hypothesized that the dianion of alkene **2a** formed at low temperatures could be reacted with electrophiles regioselectively at the allylic position. The resulting alkylated monoanions would then cyclize *in situ* upon warming. This method would allow for selective installation of C-6 substituents in the indolizine products. A set of electrophiles was chosen and the results are summarized in Table 4.2. Selective addition of alkyl-, allyl-, propargyl-, benzyl-, and α -keto halides was achieved at -78 °C. After 1 h of alkylation, the acetone/CO₂ bath was removed effecting rapid cyclization to the 5,6,7-trisubstituted indolizines **4a-e** as the reaction mixture warmed to room temperature. These tandem alkylation/cyclization reactions exhibited excellent yields. The activated electrophiles afforded slightly higher yields than the non-activated MeI. Notably, the reaction with ethyl bromoacetate effected selective alkylation of the dianion, annulation to the indolizine, and further condensation to the γ -lactam **4e** in a single pot, highlighting the efficiency and synthetic potential of this method.

Table 4.2 Tandem Alkylation/Cyclization Sequence



entry	electrophile	product	R ⁶	yield (%)
1	MeI	4a	-CH ₃	87
2	BnBr	4b	-CH ₂ CH=CH	98
3	allyl-Br	4c	-CH ₂ C≡CH	94
4	propargyl-Br	4d	-CH-CH ₂ Ph	98
5	BrCH ₂ CO ₂ Et	4e		90

4.6 Conclusions

In conclusion, we have developed a one-pot, olefination/cyclization sequence for the synthesis of highly-substituted indolizines, imidazo[1,2-*a*]pyridines, and imidazo[1,5-*a*]pyridines from pyrrole-2-, imidazole-2-, and imidazole-4-carboxaldehydes, respectively. Wittig olefination of the aldehydes with an ylide formed *in situ* from fumaronitrile and triethylphosphine affords *E*-enriched alkenes, which undergo cycloaromatization when treated with catalytic and mild bases, allowing for control of the C-1, C-2, and C-3 substituents. Alternatively, dianions formed from the isolable *E*-isomers undergo selective alkylation at -78 °C followed by spontaneous cyclization upon warming to room temperature, allowing for C-6 substituent control. The efficiency and tailorability of this method simplifies the generation of large arrays of functionalized heteroaromatic compounds. Isosteres and nitrogen-rich homologs of indole present geometrically definable hydrogen bond donors and acceptors that greatly expand the usefulness of this privileged nucleus in medicinal chemistry. The substituents and

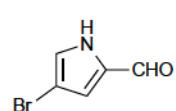
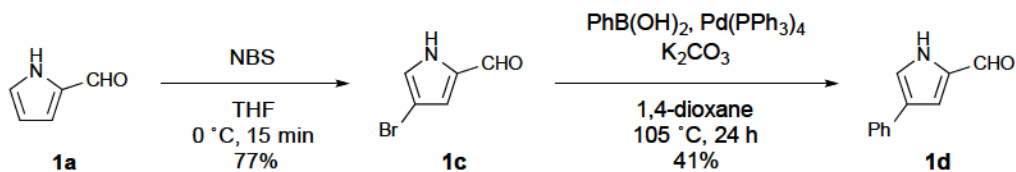
substitution patterns readily achievable by this approach enrich and complement those available by current methods.¹⁴

4.7 Experimental

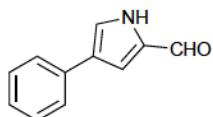
General Information

Reactions requiring anhydrous conditions were conducted under an inert atmosphere of argon using anhydrous solvents. DCM and toluene were distilled over CaH₂. Et₂O and THF were distilled over Na and benzophenone. All reactions were monitored by analytical thin-layer chromatography (TLC) using indicated solvent systems on Analtech Uniplat Silica Gel TLC plates (250 microns). All NMR spectra were recorded on either Bruker Avance 400 MHz or 300 MHz spectrometers as indicated. Chemical shifts (δ) are quoted in parts per million (ppm) and referenced to the following residual solvent signals: ¹H δ = 7.26 (CDCl₃), 2.50 (DMSO-d₆), 3.31 (MeOD), 2.05 (acetone-d₆); ¹³C δ = 77.0 (CDCl₃), 39.43 (DMSO-d₆), 49.05 (MeOD), 29.84 (acetone-d₆). Coupling constants (*J*) are given in Hz. All IR data were obtained on Triethylphosphine, fumaronitrile, pyrrole-2-carboxaldehyde (**1a**), 3,5-dimethylpyrrole-2-carboxaldehyde (**1b**), 5-formyl-2,4-dimethyl-1*H*-pyrrole-3-carboxylic acid, 4-imidazolecarboxaldehyde (**1i**), 4-methyl-5-imidazolecarboxaldehyde (**1j**), 2-methyl-1*H*-imidazole-4-carboxaldehyde (**1k**), 5-chloro-2-phenyl-1*H*-imidazole-4-carboxaldehyde (**1l**), imidazole-2-carboxaldehyde (**1m**), and 4,5-dimethyl-1*H*-imidazole-5-carbaldehyde (**1n**) were obtained from Sigma-Aldrich.

Preparation of Aldehydes



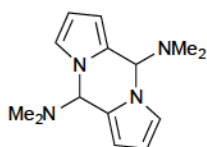
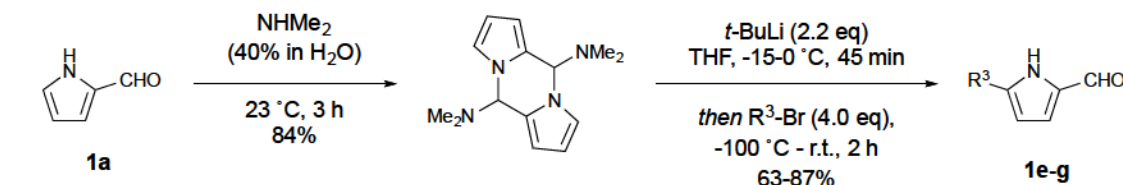
4-Bromo-1H-pyrrole-2-carbaldehyde (1c). To a stirred solution of pyrrole-2-carboxaldehyde (100 mg, 1.05 mmol) in THF (1.1 mL) at 0 °C was added *N*-bromosuccinimide (187 mg, 1.05 mmol) as a single portion. The reaction mixture was stirred for 15 min at 0 °C before the solvent was removed *in vacuo*. The crude mixture was suspended in water, the suspension was filtered, and the filtrand was washed with water. Crystallization of the filtrand from hot ethanol and water afforded the desired 4-bromopyrrole-2-carbaldehyde as a tan solid (183 mg, 0.80 mmol, 77%). Spectral data matched literature values.¹⁵ ¹H-NMR (400 MHz; acetone-*d*₆): δ 11.57–11.28 (s, 1H), 9.52 (s, 1H), 7.30 (d, *J* = 2.5 Hz, 1H), 7.05 (d, *J* = 2.5 Hz, 1H).



4-Phenyl-1H-pyrrole-2-carbaldehyde (1d). The 4-bromopyrrole-2-carbaldehyde (250 mg, 1.44 mmol), phenyl boronic acid (210 mg, 1.72 mmol), and potassium carbonate (477 mg, 3.45 mmol) were suspended in dioxane (13 mmol), and the suspension was degassed with argon. Tetrakis(triphenylphosphine)palladium (83 mg, 5 mol%) was added, and the suspension was degassed again with argon and heated to 105 °C for 24 h. The reaction mixture was concentrated to dryness, and the residue was taken up in 20 mL EtOAc and 20 mL water. The mixture was extracted with EtOAc (3 × 20 mL), and the combined organic extracts were washed with brine, dried over sodium sulfate, and concentrated *in vacuo*. Purification by flash chromatography (12→20% acetone/petroleum ether) afforded the desired 4-phenylpyrrole-2-carboxaldehyde as a white solid (101 mg, 0.59 mmol, 41%) as well as

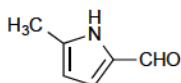
re-isolated starting material (98 mg, 0.56 mmol, 39%). Spectral data matched literature values.¹⁶

¹H-NMR (400 MHz; acetone-d₆): δ 9.59 (s, 1H), 7.68–7.64 (m, 3H), 7.38–7.34 (m, 3H), 7.23–7.19 (m, 1H).



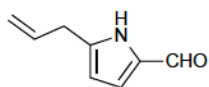
Pyrrole-2-carbaldehyde dimethylamine dimer. A solution of pyrrole-2-carboxaldehyde 3.0 g, 31.55 mmol) in dimethylamine (6.3 mL, 40% in H₂O) was stirred at room temperature for 3 h. The precipitated solid was

collected by filtration and dried in *vacuo*. The crude solid was recrystallized from hot EtOAc and hexanes to afford the dimer as a light pink solid (3.26 g, 13.3 mmol, 84%). Spectral data matched literature values.¹⁷

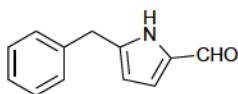


5-Methyl-1H-pyrrole-2-carbaldehyde (1e). A 1.7 M solution of *t*-BuLi in pentane (1.06 mL, 1.80 mmol) was added dropwise to a stirred solution of the pyrrole-2-carbaldehyde dimethylamine dimer (200 mg, 0.82 mmol) in anhydrous THF at –15 °C. The reaction mixture was stirred for 15 min at this temperature and then for 30 min at 0 °C by which time it had become deep violet in color. The reaction mixture was cooled to –100 °C and MeI (204 μL, 3.27 mmol) was added in one portion. The reaction mixture was allowed to warm to –30 °C over 1.5 h and then 23 °C for 1 h. Water (20 mL) and saturated aqueous sodium bicarbonate (20 mL) were added and the mixture was heated to 80 °C for 15 h. The mixture was poured into a concentrated sodium bicarbonate solution and extracted with DCM (3 × 20 mL). The combined organic extracts were dried over Na₂SO₄ and concentrated. Purification by flash chromatography (20% acetone in petroleum ether) afforded 5-methylpyrrole-2-carbaldehyde

as an off-white solid (156 mg, 1.43 mmol, 87%). Spectral data matched literature values.¹⁷ ¹H-NMR (400 MHz; acetone-d₆): δ 10.86 (s, 1H), 9.37 (s, 1H), 6.87 (s, 1H), 6.03 (s, 1H), 2.33 (s, 3H).

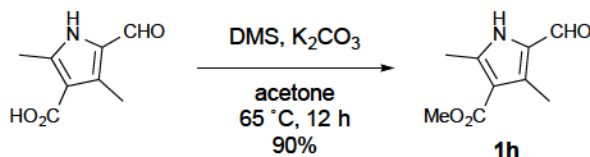


5-Allyl-1H-pyrrole-2-carbaldehyde (1f). A 1.7 M solution of *t*-BuLi in pentane (1.06 mL, 1.80 mmol) was added dropwise to a stirred solution of the pyrrole-2-carbaldehyde dimethylamine dimer (200 mg, 0.82 mmol) in anhydrous THF at –15 °C. The reaction mixture was stirred for 15 min at this temperature and then for 30 min at 0 °C by which time it had become deep violet in color. The reaction mixture was cooled to –100 °C and allyl bromide (283 µL, 3.27 mmol) was added in one portion. The reaction mixture was allowed to warm to –30 °C over 1.5 h and then 23 °C for 1 h. Water (20 mL) and saturated aqueous sodium bicarbonate (20 mL) were added and the mixture was heated to 80 °C for 15 h. The mixture was poured into a concentrated sodium bicarbonate solution and extracted with DCM (3 × 20 mL). The combined organic extracts were dried over Na₂SO₄ and concentrated. Crystallization from EtOAc and hexanes afforded 5-allylpyrrole-2-carbaldehyde as an off-white solid (140 mg, 1.04 mmol, 63%). Spectral data matched literature values.¹⁷ ¹H-NMR (400 MHz; acetone-d₆): δ 10.92 (s, 1H), 9.41 (s, 1H), 6.91 (s, 1H), 6.09 (s, 1H), 5.99 (ddt, *J* = 17.0, 10.1, 6.7 Hz, 1H), 5.14 (d, *J* = 17.0 Hz, 1H), 5.07 (d, *J* = 10.1 Hz, 1H), 3.48 (d, *J* = 6.7 Hz, 2H).



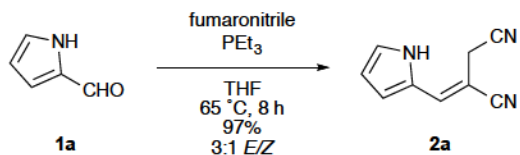
5-Benzyl-1H-pyrrole-2-carbaldehyde (1g). A 1.7 M solution of *t*-BuLi in pentane (1.06 mL, 1.80 mmol) was added dropwise to a stirred solution of the pyrrole-2-carbaldehyde dimethylamine dimer (200 mg, 0.82 mmol) in anhydrous THF at –15 °C. The reaction mixture was stirred for 15 min at this temperature and then for 30 min at 0 °C by which time it had become deep violet in color. The reaction mixture was cooled to –100 °C and BnBr (390 µL, 3.27 mmol) was added in one portion. The reaction

mixture was allowed to warm to -30 °C over 1.5 h and then 23 °C for 1 h. Water (20 mL) and saturated aqueous sodium bicarbonate (20 mL) were added and the mixture was heated to 80 °C for 15 h. The mixture was poured into a concentrated sodium bicarbonate solution and extracted with DCM (3 × 20 mL). The combined organic extracts were dried over Na₂SO₄ and concentrated. Crystallization from EtOAc and hexanes afforded 5-benzylpyrrole-2-carbaldehyde as an off-white solid (208 mg, 1.12 mmol, 69%). ¹H-NMR (400 MHz; acetone-d₆): δ 10.99 (s, 1H), 9.41 (s, 1H), 7.31–7.21 (m, 5H), 6.90 (d, *J* = 1.7 Hz, 1H), 6.07 (d, *J* = 1.7 Hz, 1H); ¹³C-NMR (101 MHz, acetone-d₆): δ 178.61, 141.72, 140.04, 133.75, 129.50, 129.32, 127.22, 122.03, 110.46, 34.42; HRMS (FAB) calcd for C₁₂H₁₁NO [M]⁺, 185.0841; found, 185.0840; [M+H]⁺, 186.0919; found, 186.0914.



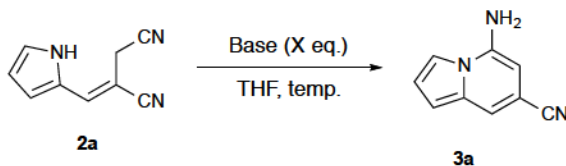
Methyl 5-formyl-2,4-dimethyl-1H-pyrrole-3-carboxylate (1h). To a stirring solution of 5-formyl-2,4-dimethylpyrrole-3-carboxylic acid (100 mg, 0.60 mmol) in acetone (6.0 mL) was added potassium carbonate (91 mg, 0.66 mmol) followed by dimethyl sulfate (60 μL, 0.63 mmol). The reaction mixture was stirred at 23 °C for 12 h, then filtered over Celite. The filter pad was washed with EtOAc and the filtrate was concentrated. Crystallization from hot EtOAc and hexanes afforded the desired product as a white solid (98 mg, 0.54 mmol, 90%). ¹H-NMR (400 MHz; acetone-d₆): δ 11.06 (s, 1H), 9.68 (s, 1H), 3.78 (s, 3H), 2.54 (s, 3H), 2.52 (s, 3H); ¹³C-NMR (101 MHz, acetone-d₆): δ 177.97, 165.80, 143.32, 134.47, 129.54, 114.13, 50.85, 13.89, 10.61; HRMS (FAB) calcd for C₉H₁₁NO₃ [M]⁺, 181.0739; found, 181.0739; [M+H]⁺, 182.0817; found, 182.0818.

Preparation of Alkene 2a



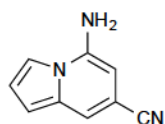
(E)-2-((1H-pyrrol-2-yl)methylene)succinonitrile (2a). To a stirring solution of pyrrole-2-carboxaldehyde (100 mg, 1.05 mmol) in THF (4.2 mL) at room temperature was added fumaronitrile (103 mg, 1.31 mmol) followed by triethylphosphine (186 μL , 1.26 mmol) dropwise. The reaction mixture was stirred at 65 $^\circ\text{C}$ for 8 h, then quenched with saturated NaHCO_3 (15 mL) and extracted with EtOAc (3×10 mL). The combined organic extracts were washed with brine, dried over Na_2SO_4 , and concentrated *in vacuo*. Purification by flash chromatography (20% acetone in petroleum ether) afforded a 3:1 mixture of *E* and *Z* isomers as a white solid (161 mg, 1.02 mmol, 97%). Recrystallization from hot EtOAc and hexanes gave 116 mg (70%) of pure *E*-isomer. mp 148-149 $^\circ\text{C}$; $^1\text{H-NMR}$ (400 MHz; acetone- d_6): δ 10.76 (s, 1H), 7.39 (s, 1H), 7.20 (m, 1H), 6.75 (m, 1H), 6.39 (m, 1H), 3.83 (s, 2H); $^{13}\text{C-NMR}$ (101 MHz, acetone- d_6): δ 137.17 (CH), 126.95 (C), 124.65 (CH), 120.47 (C), 116.73 (C), 115.97 (CH), 112.60 (CH), 94.97 (C), 19.80 (CH_2); HRMS (FAB) calcd for $\text{C}_9\text{H}_7\text{N}_3$ $[M]^+$, 157.0640; found, 157.0640.

Optimizing Conditions for Annulation of 2a to Indolizine 3a



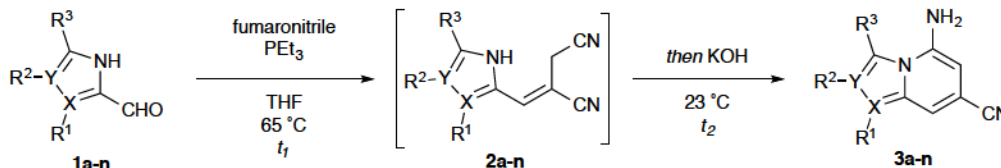
General Procedure. To a stirring solution of alkene **2a** (50 mg, 0.32 mmol) in THF (3.2 mL) was added the base as a single portion. The mixture was stirred at the temperature indicated

until conversion was complete as determined by TLC. The reaction was quenched with saturated NH_4Cl (10 mL) and extracted with EtOAc (3×10 mL). The combined organic extracts were washed with brine, dried over Na_2SO_4 , and concentrated *in vacuo*. Purification by crystallization from hot EtOAc and hexanes afforded the indolizine **3a**. See Table 1 in the manuscript for specific information regarding temperature, base identity, number of base equivalents, reactions times, and yields.



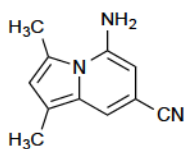
5-Aminoindolizine-7-carbonitrile (3a). mp 219-200 °C; ^1H -NMR (400 MHz; acetone- d_6): δ 7.63 (d, $J = 1.7$ Hz, 1H), 7.44 (s, 1H), 6.96 (t, $J = 3.2$ Hz, 1H), 6.69 (d, $J = 3.2$ Hz, 1H), 6.06 (s, 2H), 5.95 (d, $J = 1.7$ Hz, 1H); ^{13}C -NMR (101 MHz, acetone- d_6): δ 142.05 (C), 133.18 (C), 120.43 (C), 116.24 (CH), 115.07 (CH), 111.15 (CH), 104.18 (CH), 102.18 (C), 87.93 (CH); IR (cm^{-1}) 3427, 3335, 3029, 2217, 1651, 1629, 1538; HRMS (EI) calcd for $\text{C}_9\text{H}_7\text{N}_3$ $[M]^+$, 157.0640; found, 157.0641.

One-Pot Wittig/Annulation Sequence

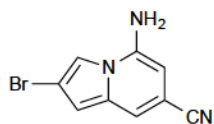


General Procedure. THF at room temperature was added fumaronitrile (1.25 equiv.) followed by triethylphosphine (1.20 equiv.) dropwise. The reaction mixture was heated to 65 °C. The reaction was monitored by TLC for disappearance of starting material as described in Figure 4.2 (3-10 h), then allowed to cool to room temperature. KOH (0.40 equiv.) was added as a single portion, and the reaction mixture was stirred for the time described in Figure 4.2 (0.5-16 h) at room temperature. The reaction was quenched with saturated NH_4Cl and extracted with EtOAc ($\times 3$). The combined organic extracts were washed with brine, dried over Na_2SO_4 , and

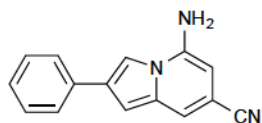
concentrated *in vacuo*. Purification by either flash chromatography (eluted with ~20% acetone in petroleum ether for the indolizines, ~40% acetone in petroleum ether for the imidazopyridines) or crystallization afforded the desired cyclized products.



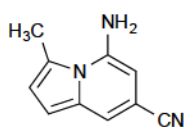
5-amino-1,3-dimethylindolizine-7-carbonitrile (3b). 73% yield; mp 156-158 °C; $^1\text{H-NMR}$ (300 MHz; acetone- d_6): δ 7.25 (d, J = 1.6 Hz, 1H), 6.42 (s, 1H), 5.68 (d, J = 1.6 Hz, 1H), 5.42 (s, 2H), 2.96 (s, 3H), 2.26 (s, 3H); $^{13}\text{C-NMR}$ (101 MHz, acetone- d_6): δ 144.65 (C), 131.99 (C), 123.79 (C), 120.61 (C), 119.44 (CH), 115.98 (CH), 112.77 (C), 98.97 (C), 89.53 (CH), 16.01 (CH_3), 10.52 (CH_3); IR (cm^{-1}) 3429, 3347, 3083, 2917, 2203, 1636, 1607, 1558; HRMS (FAB) calcd for $\text{C}_{11}\text{H}_{11}\text{N}_3$ $[\text{M}]^+$, 185.0953; found, 185.0955.



5-Amino-2-bromoindolizine-7-carbonitrile (3c). 67% yield; mp 202-203 °C; $^1\text{H-NMR}$ (400 MHz; acetone- d_6): δ 7.74 (s, 1H), 7.41 (s, 1H), 6.77 (s, 1H), 6.19 (s, 2H), 6.04 (s, 1H); $^{13}\text{C-NMR}$ (101 MHz, acetone- d_6): δ 141.61 (C), 133.65 (C), 119.84 (C), 113.51 (CH), 110.96 (CH), 105.85 (C), 105.81 (CH), 104.07 (C), 88.97 (CH); IR (cm^{-1}) 3438, 3342, 3145, 2221, 1632, 1541, 1322; HRMS (FAB) calcd for $\text{C}_9\text{H}_6(^{79}\text{Br})\text{N}_3$ $[\text{M}]^+$, 234.9745; found, 234.9741; $\text{C}_9\text{H}_6(^{81}\text{Br})\text{N}_3$ $[\text{M}]^+$, 236.9725; found, 236.9737.

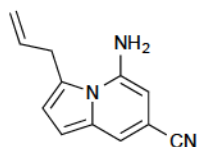


5-Amino-2-phenylindolizine-7-carbonitrile (3d). 72% yield; mp 230-232 °C; $^1\text{H-NMR}$ (400 MHz; acetone- d_6): δ 8.07 (s, 1H), 7.77 (d, J = 7.4 Hz, 2H), 7.44–7.40 (m, 3H), 7.28 (t, J = 7.4 Hz, 1H), 7.06 (s, 1H), 6.13 (s, 2H), 5.99 (s, 1H); $^{13}\text{C-NMR}$ (101 MHz, acetone- d_6): δ 142.01 (C), 135.58 (C), 134.14 (C), 131.92 (C), 129.73 (CH), 127.86 (CH), 126.87 (CH), 120.31 (C), 114.73 (CH), 108.16 (CH), 102.95 (C), 101.36 (CH), 88.48 (CH); IR (cm^{-1}) 3429, 3336, 3139, 2217, 1603, 1495; HRMS (FAB) calcd for $\text{C}_{15}\text{H}_{11}\text{N}_3$ $[\text{M}]^+$, 233.0953; found, 233.0955.



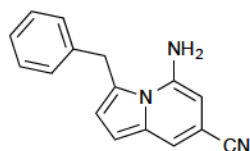
5-Amino-3-methylindolizine-7-carbonitrile (3e). 74% yield; mp 134-135

°C; $^1\text{H-NMR}$ (400 MHz; acetone- d_6): δ 7.31 (s, 1H), 6.57 (d, $J = 3.9$ Hz, 1H), 6.50 (d, $J = 3.9$ Hz, 1H), 5.77 (s, 1H), 5.53 (s, 2H), 3.00 (s, 3H); $^{13}\text{C-NMR}$ (101 MHz, acetone- d_6): δ 144.91 (C), 134.75 (C), 124.74 (C), 120.29 (C), 117.97 (CH), 117.48 (CH), 103.76 (CH), 100.68 (C), 90.08 (CH), 16.23 (CH_3); IR (cm^{-1}) 3414, 3343, 2208, 1634, 1542, 1472; HRMS (FAB) calcd for $\text{C}_{10}\text{H}_9\text{N}_3$ $[\text{M}]^+$, 171.0797; found, 171.0794.



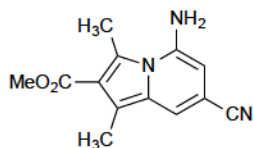
3-Allyl-5-aminoindolizine-7-carbonitrile (3f). 72% yield; $R_f = 0.30$ (25%

acetone/petroleum ether); $^1\text{H-NMR}$ (400 MHz; acetone- d_6): δ 7.39 (s, 1H), 6.69 (d, $J = 4.0$ Hz, 1H), 6.60 (d, $J = 4.0$ Hz, 1H), 6.23 (ddt, $J = 17.0, 10.5, 5.7$ Hz, 1H), 5.86 (s, 1H), 5.45 (s, 2H), 5.20 (dd, $J = 10.5, 1.1$ Hz, 1H), 4.98 (dd, $J = 17.0, 1.1$ Hz, 1H), 4.17 (d, $J = 5.7$ Hz, 2H); $^{13}\text{C-NMR}$ (101 MHz, acetone- d_6): δ 144.48 (C), 139.11 (CH_2), 135.20 (C), 126.57 (C), 120.15 (C), 118.19 (CH), 117.51 (CH), 117.28 (CH), 104.10 (CH), 101.06 (C), 90.84 (CH), 34.25 (CH_2); IR (cm^{-1}) 3399, 3331, 2208, 1633, 1540, 1440; HRMS (FAB) calcd for $\text{C}_{12}\text{H}_{11}\text{N}_3$ $[\text{M}]^+$, 197.0953; found, 197.0960.



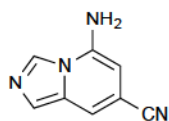
5-Amino-3-benzylindolizine-7-carbonitrile (3g). 72% yield; mp 121-

122 °C; $^1\text{H-NMR}$ (400 MHz; acetone- d_6): δ 7.39 (s, 1H), 7.32 (t, $J = 7.5$ Hz, 2H), 7.23 (t, $J = 7.3$ Hz, 1H), 7.14 (d, $J = 7.6$ Hz, 2H), 6.61 (s, 2H), 5.79 (s, 1H), 5.27 (br. s, 2H), 4.77 (s, 2H); $^{13}\text{C-NMR}$ (101 MHz, acetone- d_6): δ 144.47 (C), 141.47 (C), 135.42 (C), 129.70 (CH), 129.15 (CH), 127.42 (CH), 127.25 (C), 120.08 (C), 119.42 (CH), 117.58 (CH), 104.11 (CH), 101.22 (C), 90.95 (CH), 35.87 (CH_2); IR (cm^{-1}) 3413, 3343, 2210, 1635, 1540, 1472; HRMS (FAB) calcd for $\text{C}_{16}\text{H}_{13}\text{N}_3$ $[\text{M}]^+$, 247.1110; found, 247.1108.



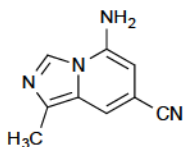
Methyl 5-amino-7-cyano-1,3-dimethylindolizine-2-carboxylate (3h).

65% yield; $R_f = 0.30$ (25% acetone/petroleum ether); $^1\text{H-NMR}$ (400 MHz; acetone- d_6): δ 7.42 (s, 1H), 5.80 (s, 1H), 5.62 (br. s, 2H), 3.88 (s, 3H), 3.26 (s, 3H), 2.44 (s, 3H); $^{13}\text{C-NMR}$ (101 MHz, acetone- d_6): δ 166.74 (C), 145.41 (C), 131.46 (C), 128.62 (C), 119.93 (C), 119.57 (C), 116.97 (CH), 114.72 (C), 101.27 (C), 91.39 (CH), 51.41 (CH_3), 14.20 (CH_3), 10.83 (CH_3); IR (cm^{-1}) 3428, 3335, 3139, 2983, 2217, 1738, 1628, 1537, 1220; HRMS (FAB) calcd for $\text{C}_{13}\text{H}_{13}\text{N}_3\text{O}_2$ $[\text{M}]^+$, 243.1008; found, 243.1007.



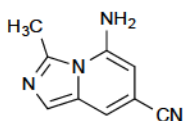
5-aminoimidazo[1,5-a]pyridine-7-carbonitrile (3i). 72% yield; mp 226-227

$^{\circ}\text{C}$; $^1\text{H-NMR}$ (300 MHz; acetone- d_6): δ 8.47 (s, 1H), 7.61 (s, 1H), 7.58 (d, $J = 1.3$ Hz, 1H), 6.40 (s, 2H), 5.93 (d, $J = 1.3$ Hz, 1H); $^{13}\text{C-NMR}$ (101 MHz, acetone- d_6): δ 140.79 (C), 130.80 (C), 126.83 (C), 124.46 (CH), 119.60 (C), 114.00 (CH), 105.13 (CH), 88.64 (CH); IR (cm^{-1}) 3401, 3136, 2222, 1659, 1544, 1118; HRMS (FAB) calcd for $\text{C}_8\text{H}_6\text{N}_4$ $[\text{M}]^+$, 159.0671; found, 159.0669.



5-amino-1-methylimidazo[1,5-a]pyridine-7-carbonitrile (3j). 65% yield;

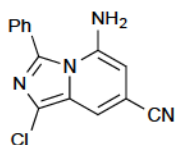
mp 233-234 $^{\circ}\text{C}$; $^1\text{H-NMR}$ (400 MHz; MeOD): δ 8.30 (s, 1H), 7.38 (s, 1H), 5.75 (s, 1H), 2.47 (s, 3H); $^{13}\text{C-NMR}$ (100 MHz, MeOD): δ 141.22 (C), 132.51 (C), 127.72 (C), 125.40 (CH), 120.12 (C), 113.82 (CH), 104.49 (C), 88.51 (CH), 12.37 (CH_3); IR (cm^{-1}) 3398, 3331, 2209, 1633, 1541, 1441; HRMS (FAB) calcd for $\text{C}_9\text{H}_8\text{N}_4$ $[\text{M}]^+$, 172.0749; found, 172.0744.



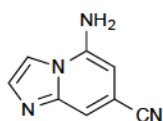
5-amino-3-methylimidazo[1,5-a]pyridine-7-carbonitrile (3k). 71% yield;

mp 214-215 $^{\circ}\text{C}$; $^1\text{H-NMR}$ (400 MHz; MeOD): δ 8.30 (s, 1H), 7.38 (s, 1H), 5.75 (s, 1H), 2.47 (s, 3H); $^{13}\text{C-NMR}$ (100 MHz, MeOD): δ 141.22 (C), 132.51 (C), 127.72 (C), 125.40 (CH), 120.12 (C), 113.82 (CH), 104.49 (C), 88.51 (C), 12.37 (CH_3); IR (cm^{-1})

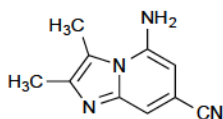
3437, 3340, 2221, 1645, 1539, 1431; HRMS (FAB) calcd for $C_9H_9N_4$ $[M+H]^+$, 173.0828; found, 173.0828.



5-amino-1-chloro-3-phenylimidazo[1,5-a]pyridine-7-carbonitrile (3l). 69% yield; mp 201-202 °C; 1H -NMR (400 MHz; acetone- d_6): δ 8.04 (d, J = 6.8 Hz, 2H), 7.53-7.48 (m, 4H), 7.24 (s, 1H), 4.63-4.45 (m, 2H); ^{13}C -NMR (101 MHz, DMSO- d_6): δ 146.75 (C), 133.45 (C), 131.82 (C), 129.71 (CH), 128.90 (CH), 128.56 (CH), 125.50 (CH), 122.06 (C), 119.21 (C), 117.11 (C), 99.07 (C), 18.44 (CH_2); IR (cm^{-1}) 3190, 2207, 1621, 1479; HRMS (FAB) calcd for $C_{14}H_9^{35}ClN_4$ $[M]^+$, 269.0594; found, 269.0587; $C_{14}H_9^{37}ClN_4$ $[M]^+$, 271.0565; found, 271.0566.

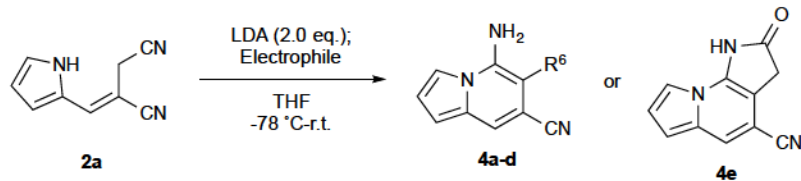


5-aminoimidazo[1,2-a]pyridine-7-carbonitrile (3m). 72% yield; R_f = 0.35 (40% acetone/petroleum ether); 1H -NMR (400 MHz; acetone- d_6): δ 7.98 (s, 1H), 7.75 (d, J = 1.4 Hz, 1H), 7.43 (s, 1H), 6.52 (s, 1H), 6.24 (d, J = 1.4 Hz, 1H); ^{13}C -NMR (101 MHz, MeOD): δ 144.74 (C), 143.53 (C), 133.74 (CH), 117.93 (C), 110.24 (C), 109.22 (CH), 107.97 (CH), 90.10 (CH); IR (cm^{-1}) 3382, 3152, 2233, 1664, 1544, 1494; HRMS (EI) calcd for $C_8H_6N_4$ $[M+H]^+$, 159.0671; found, 159.0667.

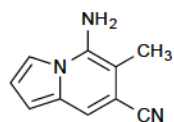


5-amino-2,3-dimethylimidazo[1,2-a]pyridine-7-carbonitrile (3n). 73% yield; mp 220-221 °C; 1H -NMR (400 MHz; MeOD): δ 7.09 (s, 1H), 6.01 (s, 1H), 2.80 (s, 3H), 2.31 (s, 3H); ^{13}C -NMR (101 MHz, MeOD): δ 146.83 (C), 145.52 (C), 142.59 (C), 119.31 (C), 110.87 (CH), 110.82 (C), 109.74 (C), 93.60 (CH), 12.91 (CH_3), 11.54 (CH_3); IR (cm^{-1}) 3443, 2226, 1656, 1532, 1381; HRMS (FAB) calcd for $C_{10}H_{10}N_4$ $[M+H]^+$, 187.0984; found, 187.0985.

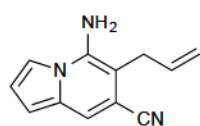
One-Pot Alkylation/Cyclization Sequence of 2a to Indolizines 4a-e



General Procedure. To a stirring solution of alkene **2a** (100 mg, 0.63 mmol) in THF (6.3 mL) at -78 °C was added freshly prepared 1.0 M LDA (1.27 mL, 1.27 mmol) dropwise. The mixture was allowed to stir at -78 °C for 45 min before slow addition of the electrophile (1.0 equiv). The reaction mixture was stirred at -78 °C for 1.5 h, then allowed to warm to room temperature over 10 minutes. The reaction was quenched with saturated NH_4Cl (15 mL) and the crude mixture was extracted with EtOAc (3 \times 15 mL). The combined organic extracts were washed with brine, dried over Na_2SO_4 , and concentrated *in vacuo*. Purification by flash chromatography (eluted with ~20% acetone in petroleum ether) or crystallization from hot EtOAc and hexanes afforded the desired indolizines.

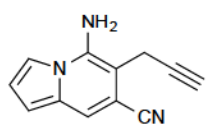


5-amino-6-methylindolizine-7-carbonitrile (4a). 87% yield; R_f = 0.30 (20% acetone/petroleum ether); $^1\text{H-NMR}$ (400 MHz; acetone- d_6): δ 7.62-7.62 (m, 1H), 7.47 (s, 1H), 6.92 (dd, J = 4.0, 2.8 Hz, 1H), 6.63 (dd, J = 4.0, 1.1 Hz, 1H), 5.78 (s, 2H), 2.34 (s, 3H); $^{13}\text{C-NMR}$ (101 MHz, acetone- d_6): δ 132.75 (C), 129.17 (C), 127.60 (C), 126.49 (CH), 121.21 (CH), 116.63 (CH), 114.07 (C), 105.65 (CH), 103.57 (C), 14.91 (CH_3); IR (cm^{-1}) 3368, 3326, 2213, 1651, 1529, 1319; HRMS (FAB) calcd for $\text{C}_{10}\text{H}_9\text{N}_3$ $[\text{M}]^+$, 171.0797; found, 171.0794.

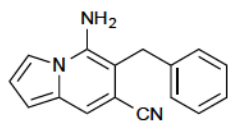


6-allyl-5-aminoindolizine-7-carbonitrile (4b). 98% yield; R_f = 0.30 (20% acetone/petroleum ether); $^1\text{H-NMR}$ (400 MHz; acetone- d_6): δ 7.66-7.65 (m, 1H), 7.52 (s, 1H), 6.94 (t, J = 3.7 Hz, 1H), 6.66 (d, J = 3.7 Hz, 1H), 6.02-5.92 (m, 1H), 5.80

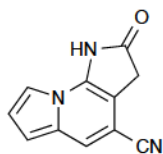
(s, 2H), 5.09 (d, $J = 17.2$ Hz, 1H), 5.04 (d, $J = 10.0$ Hz, 1H), 3.55 (d, $J = 5.9$ Hz, 2H); ^{13}C -NMR (100 MHz, acetone- d_6): δ 138.90 (C), 135.75 (CH), 132.33 (C), 119.63 (C), 116.25 (CH), 115.93 (CH), 115.74 (CH), 111.10 (CH), 104.61 (C), 103.85 (CH), 96.08 (C), 32.62 (CH_2); IR (cm^{-1}) 3399, 3331, 2208, 1634, 1540, 1440; HRMS (FAB) calcd for $\text{C}_{12}\text{H}_{11}\text{N}_3$ $[\text{M}]^+$, 197.0953; found, 197.0958.



5-amino-6-(prop-2-yn-1-yl)indolizine-7-carbonitrile (4c). 94% yield; $R_f = 0.30$ (20% acetone/petroleum ether); ^1H -NMR (400 MHz; acetone- d_6): δ 7.70 (m, 1H), 7.53 (s, 1H), 6.96 (t, $J = 3.7$ Hz, 1H), 6.68 (d, $J = 3.7$ Hz, 1H), 6.01 (s, 2H), 3.72 (d, $J = 2.6$ Hz, 2H), 2.52 (t, $J = 2.6$ Hz, 1H); ^{13}C -NMR (101 MHz, acetone- d_6): δ 139.08 (C), 132.31 (C), 119.27 (C), 116.52 (CH), 116.00 (CH), 111.48 (CH), 104.29 (CH), 103.87 (C), 93.88 (C), 81.32 (C), 71.01 (CH), 18.26 (CH_2); IR (cm^{-1}) 3428, 3336, 3309, 2216, 1629, 1536, 1323; HRMS (FAB) calcd for $\text{C}_{12}\text{H}_9\text{N}_3$ $[\text{M}]^+$, 195.0796; found, 197.0795.



5-amino-6-benzylindolizine-7-carbonitrile (4d). 98% yield; $R_f = 0.25$ (20% acetone/petroleum ether); ^1H -NMR (400 MHz; acetone- d_6): δ 7.68 (m, 1H), 7.56 (s, 1H), 7.27 (d, $J = 4.3$ Hz, 4H), 7.18 (q, $J = 4.3$ Hz, 1H), 6.96 (t, $J = 3.7$ Hz, 1H), 6.69 (d, $J = 3.7$ Hz, 1H), 5.86 (s, 2H), 4.20 (s, 2H); ^{13}C -NMR (101 MHz, acetone- d_6): δ 140.43, 139.32, 132.38, 129.22, 128.90, 127.01, 119.87, 116.37, 116.13, 111.35, 105.00, 104.04, 97.52, 34.01; IR (cm^{-1}) 3340, 2216, 1698, 1639, 1538; HRMS (FAB) calcd for $\text{C}_{16}\text{H}_{13}\text{N}_3$ $[\text{M}]^+$, 247.1110; found, 247.1099.



2-oxo-2,3-dihydro-1H-pyrrolo[2,3-e]indolizine-4-carbonitrile (4e). 90% yield; $R_f = 0.30$ (25% acetone/petroleum ether); ^1H -NMR (300 MHz; acetone- d_6): δ 10.62 (s, 1H), 7.73 (s, 1H), 7.65 (dd, $J = 1.7, 0.7$ Hz, 1H), 7.04 (dd, $J = 4.1, 2.7$ Hz, 1H), 6.83 (dd, $J = 4.1, 0.7$ Hz, 1H); ^{13}C -NMR (101 MHz, acetone- d_6): δ 175.53

(C), 137.22 (C), 133.31 (C), 118.43 (CH), 118.19 (C), 117.61 (CH), 111.62 (CH), 105.33 (CH), 98.82 (C), 98.51 (C), 36.07 (CH₂); IR (cm⁻¹) 3336, 3231, 2217, 1640, 1539, 1380; HRMS (FAB) calcd for C₁₁H₇N₃O [M]⁺, 197.0589; found, 197.0595.

4.8 References

1. a) Hazra, A.; Mondal, S.; Maity, A.; Naskar, S.; Saha, P.; Paira, R.; Sahu, K. B.; Paira, P.; Ghosh, S.; Sinha, C.; Samanta, A.; Banerjee, S.; Mondal, N. B. *Eur. J. Med. Chem.* **2011**, *46*, 2132–2140; b) Darwish, E. S. *Molecules* **2008**, *13*, 1066–1078.
2. a) Reddy, M. V.; Rao, M. R.; Rhodes, D.; Hansen, M. S.; Rubins, K.; Bushman, F. D.; Venkateswarlu, Y.; Faulkner, D. J. *J. Med. Chem.* **1999**, *42*, 1901; b) Facompré, M.; Tardy, C.; Bal-Mahieu, C.; Colson, P.; Perez, C.; Manzanares, I.; Cuevas, C.; Bailly, C. *Cancer Research* **2003**, *63*, 7392–7399.
3. a) Hagishita, S.; Yamada, M.; Shirahase, K.; Okada, T.; Mura-kami, Y.; Ito, Y.; Matsuura, T.; Wada, M.; Kato, T.; Ueno, M.; Chikazawa, Y.; Yamada, K.; Ono, T.; Teshirogi, I.; Ohtani, M. *J. Med. Chem.* **1996**, *39*, 3636–3658; b) Yokota, Y.; Hanasaki, K.; Ono, T.; Nakazato, H.; Kobayashi, T.; Arita, H. *Biochim. Biophys. Acta.* **1999**, *1438*, 213–222.
4. a) Dannhardt, G.; Meindl, W.; Gussmann, S.; Ajili, S.; Kappe, T. *Eur. J. Med. Chem.* **1987**, *22*, 505–510; b) Gundersen, L. L.; Negussie, A. H.; Rise, F.; Ostby, O. B. *Arch. Pharm. Pharm. Med. Chem.* **2003**, *336*, 191–195.
5. a) Cheng, Y.; An, L. K.; Wu, N.; Wang, X. D.; Bu, X. Z.; Huang, Z. S.; Gu, L. Q. *Bioorg. Med. Chem.* **2008**, *16*, 4617–4625; b) James, D.A.; Koya, K.; Li, H.; Liang, G.; Xia, Z.; Ying, W.; Wu, Y.; Sun, L. *Bioorg. Med. Chem. Lett.* **2008**, *18*, 1784–1787; c) Shen, Y. M.; Lv, P. C.; Chen, W.; Liu, P. G.; Zhang, M. Z.; Zhu, H. L. *Eur. J. Med. Chem.* **2010**, *45*, 3184–3190; d)

- Bloch, W. M.; Derwent-Smith, S. M.; Issa, F.; Morris, J. C.; Rendina, L. M.; Sumby, C. J. *Tetrahedron* **2011**, *67*, 9368–9375.
6. Vaught, J. L.; Carson, J. R.; Carmosin, R. J.; Blum, P. S.; Persico, F. J.; Hageman, W. E.; Shank, R. P.; Raffa, R. B. *J. Pharmacol. Exp. Ther.* **1990**, *255*, 1–10.
 7. Ismail, M. A.; Arafa, R. K.; Wenzler, T.; Brun, R.; Tanious, F. A.; Wilson, W. D.; Boykin, D. W. *Bioorg. Med. Chem.* **2008**, *16*, 683–691.
 8. Depoortere, H.; Zivkovic, B.; Lloyd, K. G.; Sanger, D. J.; Perrault, G.; Langer, S. Z.; Bartholini, G. *J. Pharmacol. Exp. Ther.* **1986**, *237*, 649–658.
 9. a) Alcarazo, M.; Roseblade, S. J.; Cowley, A. R.; Fernández, R.; Brown, J. M.; Lassaletta, J. *M. J. Am. Chem. Soc.* **2005**, *127*, 3290–3291. Klingele, J.; Kaase, D.; Hilgert, J.; Steinfeld, G.; Klingele, M. H.; Lach, J. *Dalton Trans.* **2010**, *39*, 4495.
 10. For pyridine-based indolizine syntheses see: a) Tschitschibabin, A. E. *Ber. Dtsch. Chem. Ges.* **1927**, *60*, 1607. b) Behnisch, R. *Houben-Weyl, Methoden der Organischen Chemie*; Thieme: Stuttgart, 1994; *E6b1*, 323-450. c) Uchida, T.; Matsumoto, K. *Synthesis* **1976**, *209*. d) Katritzky, A. R.; Qui, G.; Yang, B.; He, H.-Y. *J. Org. Chem.* **1999**, *64*, 7618. e) Kostik, E. I.; Abiko, A.; Oku, A. *J. Org. Chem.* **2001**, *66*, 2618–2623. f) Smith, C. R.; Bunnelle, E. M.; Rhodes, A. J.; Sarpong, R. *Org. Lett.* **2007**, *9*, 1169–1171; g) Basavaiah, D.; Devendar, B.; Lenin, D.; Satyanarayana, T. *Synlett.* **2009**, 411–416.
 11. For pyridine-based imidazopyridine syntheses see: a) Barun, O.; Ila, H.; Junjappa, H.; Singh, O. M. *J. Org. Chem.* **2000**, *65*, 1583–1587; b) Loones, K. T. J.; Maes, B. U. W.; Meyers, C.; Deruytter, J. *J. Org. Chem.* **2006**, *71*, 260–264; c) Chernyak, N.; Gevorgyan, V. *Angew. Chem., Int. Ed.* **2010**, *49*, 2743–2746; d) Seregin, I. V.; Schammel, A. W.; Gevorgyan, V. *Org. Lett.* **2007**, *9*, 3433–3436; e) Katritzky, A. R.; Xu, Y.-J.; Tu, H. *J. Org. Chem.* **2003**, *68*, 4935–

- 4937; f) Masquelin, T.; Bui, H.; Brickley, B.; Stephenson, G.; Schwerkoske, J.; Hulme, C. *Tetrahedron Lett.* **2006**, 47, 2989–2991.
12. For syntheses originating from 5-membered ring see: a) Kim, M.; Vedejs, E. *J. Org. Chem.* **2004**, 69, 6945–6948. b) Zhu, H.; Stöckigt, J.; Yu, Y.; Zou, H. *Org. Lett.* **2011**, 13, 2792–2794. c) Lee, J. H.; Kim, I. *J. Org. Chem.* **2013**, 78, 1283–1288. d) Kucukdisli, M.; Opatz, T. *J. Org. Chem.* **2013**, 78, 6670–6676; e) Galons, H.; Bergerat, I.; Combet Farnoux, C.; Miocque, M. *Synthesis* **1982**, 1103; f) Knölker, H. J.; Hitzemann, R.; Boese, R. *Chem. Ber.* **1990**, 123, 327–339; g) Virieux, D.; Guillouzac, A.-F.; Cristau, H.-J. *Tetrahedron* **2006**, 62, 3710–3720.
13. Outlaw, V. K.; Townsend, C. A. *Org. Lett.* **2014**, 16, 6334–6337.
14. Singh, G. S.; Mmatli, E. E. *Eur. J. Med. Chem.* **2011**, 46, 5237–5257.
15. Kraye, M.; Balasubramanian, T.; Ruzié, C.; Ptaszek, M.; Cramer, D. L.; Taniguchi, M.; Lindsey, J. S. *J. Porphyr. Phthalocyanines* **2009**, 13, 1098–1110.
16. Bergauer, M.; Gmeiner, P. *Synthesis* **2002**, 2, 0274–0278.
17. Muchowski, J. M.; Hess, P. *Tetrahedron Lett.* **1988**, 29, 777–780.

Chapter 5

Summary and Conclusions

5.1 Obesity Epidemic

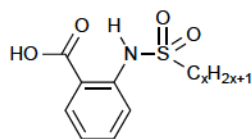
The prevalence of obesity in the human population has rapidly increased over the last few decades. As a result, obesity-related diseases, such as heart disease^{1,2}, stroke³, and type 2 diabetes⁴, are on the rise, causing a staggering medical and financial burden.⁵ Despite the increased incidence of obesity, few pharmacological options exist to combat the disease. The primary mode of action for recent drugs involves targeting receptors within the CNS to elicit the feeling of satiety and reduce food intake. Unfortunately, several of these drugs have been removed from the market for their severe side effects, such as anxiety, depression, and suicidal intentions. Outside of the CNS, only one clinically-used drug, orlistat, acts in the peripheral tissues to treat obesity. Orlistat inhibits pancreatic lipases to prevent the breakdown and absorption of dietary triglycerides. While this promotes modest weight loss, excretion of the unabsorbed fat leads to undesirable side effects, such as fecal incontinence and fat-soluble vitamin deficiency, that limit the therapeutic benefit of the drug. Due to the side effects of the current therapies, new targets are needed to treat a growing obese population.

5.2 GPAT as a Therapeutic Target for Obesity

Potential methods for treating obesity include the inhibition of the biosynthesis of TAG, the major component of animal body fat, and the stimulation of fatty acid metabolism. GPAT catalyzes the first committed and rate-limiting step in TAG biosynthesis, the acylation of G3P with long chain fatty acyl-CoAs.⁶ The activity of GPAT is linked to the activity of CPT1, the

enzyme responsible for the rate-limiting step in the β -oxidation of fatty acids. GPAT and CPT1 are both located on the outer mitochondrial membrane where they compete for fatty acyl-CoA substrates.⁷ Studies have shown that GPAT plays a major role in the partitioning of fatty acyl-CoA substrates between the TAG biosynthesis and fatty acid metabolic pathways.^{8,9} Inhibition of GPAT, therefore, has the potential to limit TAG biosynthesis while stimulating β -oxidation through CPT1, making it an attractive target for obesity therapy.

Our lab recently described the design, synthesis, and evaluation of sulfonamidobenzoic and sulfonamidophosphonic acids as the first-reported small molecule inhibitors of GPAT.¹⁰ These compounds were designed to mimic key interactions of the proposed enzymatic transition state. The *o*-substituted (nonanesulfonamido)benzoic acid **1b**, shown in Fig. 5.1, demonstrated modest inhibitory activity of $24.7 \pm 2.1 \mu\text{M}$ against GPAT *in vitro* and was selected as the best candidate for studies in DIO mice. The *in vivo* results were quite promising, with treated mice showing sustained weight loss of 15.6–17.6% even after cessation of treatment.¹¹ These results verified that GPAT inhibition, in general, and the sulfonamidobenzoic acid scaffold, in particular, has potential as an obesity therapeutic.



1a ($x = 16$) $\text{IC}_{50} = 18.3 \pm 1.9 \mu\text{M}$

1b ($x = 9$) $\text{IC}_{50} = 24.7 \pm 2.1 \mu\text{M}$

1c ($x = 8$) $\text{IC}_{50} = 25.7 \pm 2.4 \mu\text{M}$

Figure 5.1 Structures and *in vitro* inhibitory data for *o*-(alkanesulfonamido)benzoic acids **1a–c**

5.3 Second-Generation GPAT Inhibitors: Probing for an Active Site Hydrophobic Pocket

Given the encouraging results of **1a–c** *in vivo*, the sulfonamidobenzoic acid scaffold was used for the design and synthesis of more potent analogs. In order to design these second generation

inhibitors, modeling studies were performed with the octyl analog **1c** in the active site of the GPAT squash homolog.¹² The energy-minimized docked inhibitor, shown in Fig. 5.2, was found to bind in the active site of GPAT with its carboxylate anion positioned in the putative phosphate binding domain comprised of three conserved cationic residues (Lys193, Arg235, and Arg237). The lipophilic C₈-tail of the sulfonamide was bound within a long hydrophobic tunnel hypothesized as the fatty acyl-CoA substrate binding site. In addition, a complex network of hydrophobic cavities and tunnels were observed that wound throughout the enzyme. One of these cavities was positioned extending from the C-4 and C-5 positions of the benzoic acid ring and lined with the hydrophobic and aromatic residues Phe98, Gly99, Tyr102, Ile103, Ala143, Leu176, Pro179, and Phe180. We directed the design of our second-generation of inhibitors to bind within this cavity.

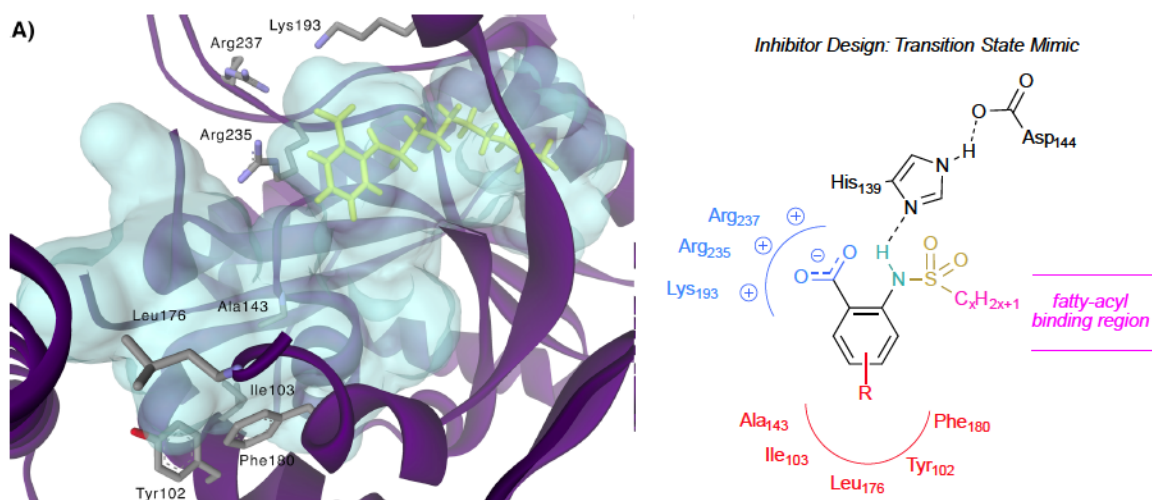


Figure 5.2 (Octanesulfonamido)benzoic acid docked in GPAT and proposed inhibitor analogs

A series of analogs of docked inhibitor **1b** was designed and synthesized with aromatic substituents appended to the 4- and 5-positions using a series of linker regions. The aryl moieties were chosen to encourage π -stacking with aromatic residues in the hydrophobic pocket while

the linkers were chosen to sample different orientations and geometries for extension of the substituent into the pocket. This set of compounds was evaluated *in vitro* for GPAT inhibition.

In general, hydrophobic and chloro substituents led to an increase in inhibitory activity, as shown in Fig. 5.3. Conversely, more polar and hydrogen-bonding substituents, such as fluoro and hydroxyl moieties, showed a decrease in inhibitory activity. While the observed effects of substituting at the 4- and 5-positions of the benzoic acid were modest, the data were consistent with the presence of a hydrophobic pocket as identified by *in silico* studies. One inhibitor, *p*-biphenylketone-substituted **5**, exhibited a 3-fold increase in inhibitory activity and, at 8.5 μ M, represents the most potent GPAT inhibitor reported to date. The benzophenone moiety in this compound could allow for photocrosslinking experiments to ascertain the binding site of the inhibitor on GPAT or any off-target proteins.

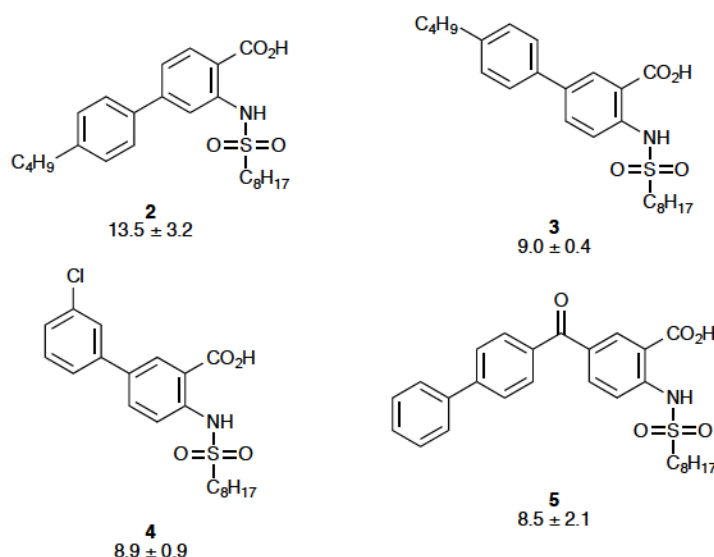


Figure 5.3 Hydrophobic- and chloro-substituted inhibitors with most potent activity

5.4 Development of Methodology to Access Substituted Indoles

While several analogs of the sulfonamidobenzoic acid scaffold demonstrated promising inhibitory activity against GPAT *in vitro*, their polyaromatic structure resulted in poor solubility

that precluded *in vivo* testing. To improve solubility, a related series of compounds was designed, replacing the simple benzoic acid with carboxylic acid-substituted heteroaromatic structures. The first heteroaromatic scaffold focused on a 7-aminoindole-5-carboxylic acid structure, shown in Fig. 5.4. With no existing method to rapidly synthesize this library of compounds, we devised a new, practical route for their preparation.¹³

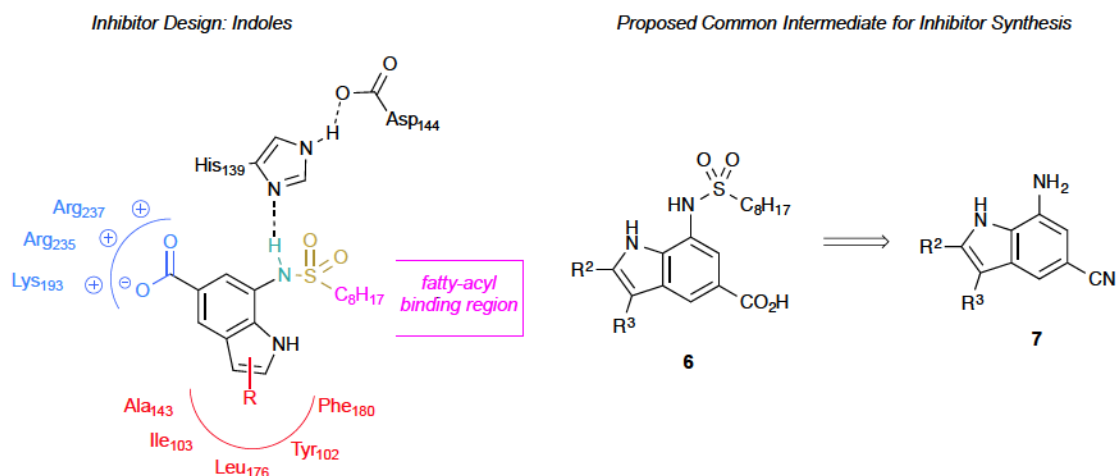


Figure 5.4 Design of indole-based GPAT inhibitors and proposed synthetic intermediate

The new route, shown in Fig. 5.5, commences with a one-pot, three-component Wittig reaction of substituted pyrrole-3-carboxaldehydes, such as **8**, with fumaronitrile and a trialkylphosphine. This reaction was optimized to afford predominantly the *E*-alkenes **9**, which are required for the subsequent reaction. The allylic nitriles undergo a Lewis-acid mediated cycloaromatization to afford 2- and 3-substituted 7-amino-5-cyanoindoles such as **10** in high yield. Alternatively, the *E*-alkenes can also be further functionalized at the allylic position prior to cyclization. Dianion formation, achieved by addition of 2 equivalents of LDA, reacts with a host of electrophiles selectively at the allylic position, which upon annulation, furnish indoles additionally substituted at C-6 such as **12**. The substituted 7-amino-5-cyanoindoles can then be

readily converted to GPAT inhibitors or a number of other medicinal chemistry targets in the literature.

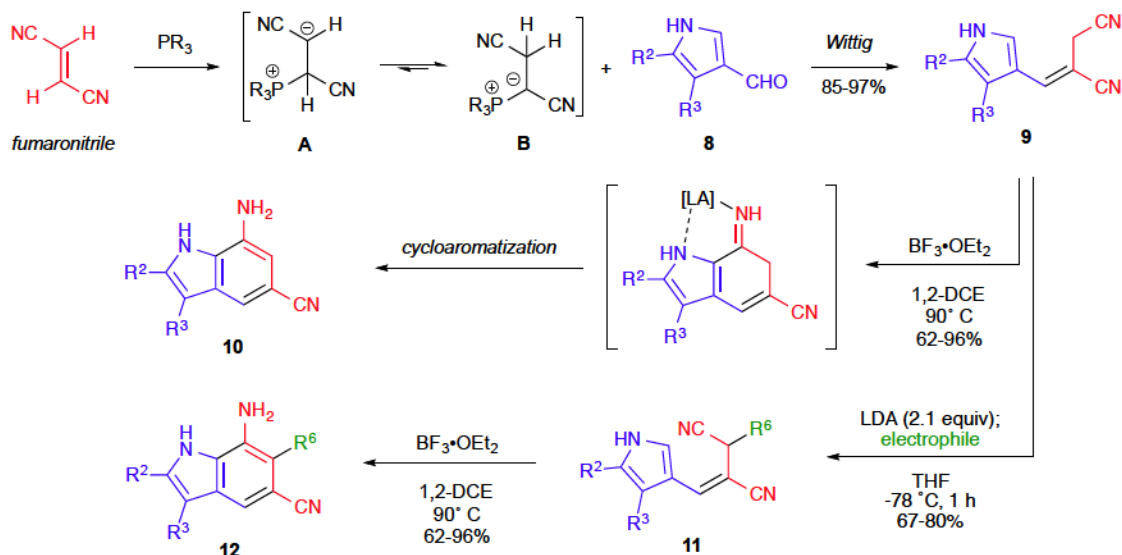


Figure 5.5 Synthesis of 2-, 3-, and 6-substituted 7-amino-5-cyanoindoles

5.5 Development of Methodology to Access Substituted *N*-Fused Heteroaromatic Bicycles

In addition to indole-based compounds, *N*-fused heteroaromatic analogs were also desired. These structures, including indolizine (13), imidazo[1,2-*a*]pyridine (14), and imidazo[1,5-*a*]pyridine (15) heterocycles, are isosteric with indole, but each provides a unique electronic structure that can subtly alter inhibitor binding within the GPAT active site. Like with the indoles, no sufficient method existed for the direct synthesis of the desired 5-amino-7-cyano-substituted bicyclic structures, thereby necessitating the development of a new route.¹⁴

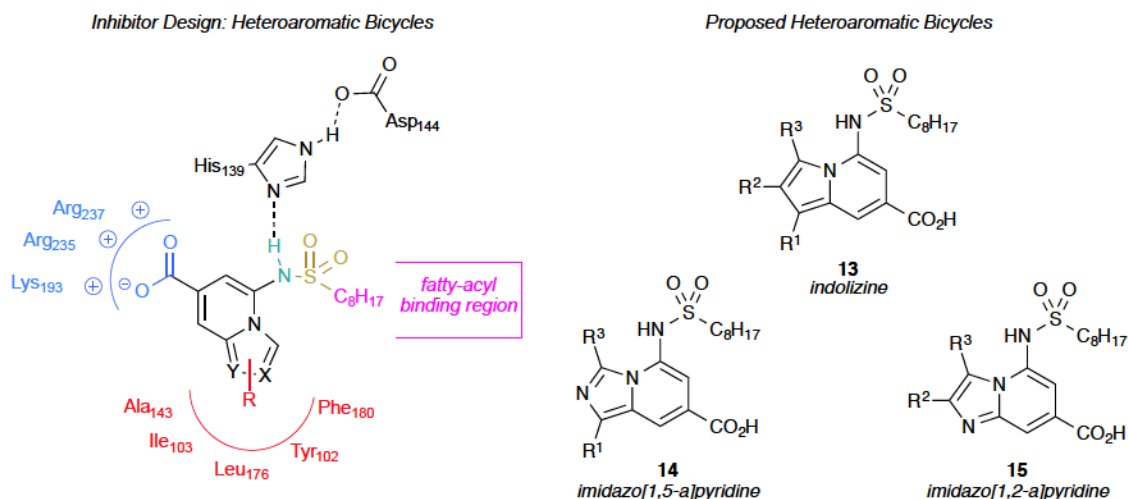


Figure 5.6 Design of *N*-fused heteroaromatic bicyclic inhibitors of GPAT

Mechanistically related to the indole method mentioned *vide supra*, our route to the *N*-fused heteroaromatic bicycles involves a three-component Wittig reaction. Rather than the 3-formylpyrroles used previously, substituted azole-2-carboxaldehydes, such as **16**, undergo olefination in the presence of fumaronitrile and triethylphosphine to afford predominantly *E*-alkenes. Deprotonation of this intermediate to the azolide anion, promoted by *in situ* addition of catalytic KOH, followed by cycloaromatization, furnished the target heteroaromatic structures in a single pot in good yield.

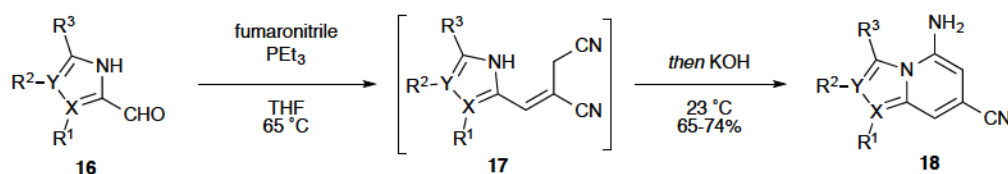


Figure 5.7 One-pot synthesis of *N*-fused heteroaromatic bicycles

Alternatively, addition of 2 equivalents of strong base (e.g., LDA, LiHMDS) to the isolable Wittig product promotes a second deprotonation allylic to the nitrile. This formed dianion reacts with electrophiles selectively at the allylic position at $-78\text{ }^{\circ}\text{C}$. The resulting monoanion

then undergoes the desired annulation when warmed to room temperature to afford 6-substituted heterocycles.

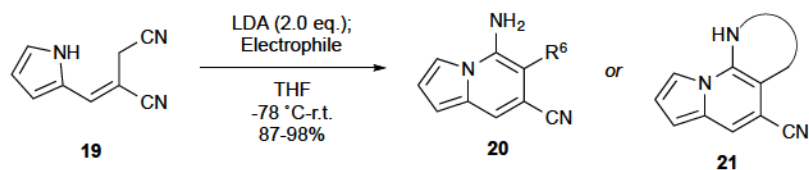


Figure 5.8 Tandem alkylation/cycloaromatization route to 6-substituted indolizines

5.6 Conclusions

The inhibition of GPAT remains a valid strategy for combating obesity. Even modest inhibition of the enzyme by sulfonamidobenzoic acids has demonstrated significant and sustained weight loss. This thesis has been devoted to the design and synthesis of more potent GPAT inhibitors. Docking studies of compound **1c** in the GPAT active site have suggested the presence of a hydrophobic pocket extending from the 4- and 5-positions. Synthesis and evaluation of several analogs substituted at these positions have indicated that hydrophobic and chloro substituents result in more effective GPAT inhibitors than incorporation of more polar groups, potentially validating our inhibitor binding model.

The design and syntheses of related heterocyclic analogs, including indoles, indolizines, and imidazopyridines, were also undertaken. This required new methodology to be developed in order to efficiently synthesize appropriately substituted heterocycles. While related, the routes to the indole and *N*-fused heteroaromatic classes were mechanistically distinct. Both relied heavily on a one-pot, three-component Wittig reaction of azole aldehydes. For the indoles, Lewis acid-mediated activation of the nitrile resulted in the intramolecular Houben-Hoesch-type reaction followed by aromatization. In contrast, base-catalyzed deprotonation of the azole was required to promote cycloaromatization. Both routes, however, represent practical,

inexpensive, and efficient methods for the preparation of these important classes of heterocycles. The rapid generation of heterocyclic analogs will aid in our ongoing research to discover more potent GPAT inhibitors and further pursue our approach to develop a new pharmacological treatment for obesity.

5.7 References

1. Poirier, P., Giles, T.D., Bray, G.A. *Arterioscler. Thromb. Vasc. Biol.* **2006**, 26, 968–976.
2. Yusuf, S., Hawken, S., Ounpuu, S. *Lancet* **2004**, 364, 937–952.
3. Hall, J.E. *Hypertension* **2003**, 41, 625–633.
4. Haslam, D.W., James, W.P. *Lancet*, **2005**, 366, 1197–1209.
5. Flegal, K.M., Carroll, M.D., Ogden, C.L., Curtin, L.R. *J. Am. Chem. Assoc.* **2010**, 303, 235-241.
6. Coleman, R. A.; Lewin, T. M.; Muoio, D. M. *Annu. Rev. Nutr.* **1998**, 18, 331-351.
7. Van der Leij, F. R.; Kram, A. M.; Bartelds, B.; Roelofsen, H.; Smid, G. B.; Takens, J.; Zammit, V. A.; Kuipers, J. R. G. *Biochem. J.* **1999**, 341, 777-784.
8. Lindén, D.; William-Olsson, L.; Ahnmark, A.; Ekroos, K.; Hallberg, C.; Sjögren, H. P.; Becker, B.; Svensson, L.; Clapham, J. C.; Oscarsson, J.; Schreyer, S. *FASEB J.* **2006**, 20, 434-443.
9. Hammond, L. E.; Neschen, S.; Romanelli, A. J.; Cline, G. W.; Ilkayeva, O. R.; Shulman, G. I.; Muoio, D. M.; Coleman, R. A. *J. Biol. Chem.* **2005**, 280, 25629-25636.
10. Wydysh, E. A.; Medghalchi, S. M.; Vadlamudi, A.; Townsend, C. A. *J. Med. Chem.* **2009**, 52, 3317–3327.

11. Kuhajda, F. P.; Aja, S.; Tu, Y.; Han, W. F.; Medghalchi, S. M.; Meskini, El, R.; Landree, L. E.; Peterson, J. M.; Daniels, K.; Wong, K.; Wydysh, E. A.; Townsend, C. A.; Ronnett, G. V. *Am. J. Physiol. Regul. Integr. Comp. Physiol.* **2011**, *301*, R116–R130.
12. Outlaw, V. K.; Wydysh, E. A.; Vadlamudi, A.; Medghalchi, S. M.; Townsend, C. A. *Med. Chem. Commun.* **2014**, *5*, 826–830.
13. Outlaw, V. K.; Townsend, C. A. *Org. Lett.* **2014**, *16*, 6334–6337.
14. Outlaw, V. K.; d'Andrea, F. B.; Townsend, C. A. *Org. Lett.* **2015**, *17*, 1822–1825.

Victor K. Outlaw

Department of Chemistry • Johns Hopkins University
309 W. Johnson Street, #736 • Madison, WI 53703
757.651.8132 (cell) • 434.516.7915 (lab) • victoroutlaw@jhu.edu

Education

2006-2015 *Johns Hopkins University*, Baltimore, Maryland
• Ph.D. Chemistry, 2015
• M.Sc. Chemistry, 2009

2002-2006 *University of Virginia*, Charlottesville, Virginia
• B.Sc. Chemistry, 2006

Research

2006-2015 **Graduate Research with Craig A. Townsend**
Department of Chemistry, Johns Hopkins University
• *Design, Synthesis, and Evaluation of Glycerol-3-Phosphate Acyltransferase (GPAT) Inhibitors as Anti-Obesity Therapeutics*
• *Development of Heterocyclic Methodology: Efficient and Flexible Synthesis of Highly-Substituted Indoles and N-Fused Aromatic Heterocycles*

2004-2006 **Undergraduate Research with Timothy L. Macdonald**
Department of Chemistry, University of Virginia
• *Synthesis of Analogs of Sphingosine-1-Phosphate (S1P) for the Evaluation of Subtype-Selective Activity against S1P Receptors*

Teaching and Mentorship

2013-2015 Undergraduate Research Mentor: Organic Synthesis and Methodology
2013-2015 Chem 205-206: Introduction to Organic Chemistry, Head Teaching Fellow
2012 Chem 205-206: Introduction to Organic Chemistry, Tutor
2007-2010 Chem 205-206: Introduction to Organic Chemistry
Fall 2006 Chem 101: Introduction to General Chemistry I
2005-2006 Chem 241-2: Introduction to Organic Chemistry, Tutor
2004 Chem 181-2L: Principle Chemical Reactions Lab for Majors

Awards and Honors

2014 Sheppard Memorial Fund Award, Johns Hopkins University
2005 Undergraduate Research Fellowship, University of Virginia

Publications

Outlaw, V. K.; Wydysh, E. A.; Vadlamudi, A.; Medghalchi, S. M.; Townsend, C. A. "Design, Synthesis, and Evaluation of 4- and 5-Substituted *o*-(Octanesulfonamido)benzoic Acids as Inhibitors of Glycerol-3-Phosphate Acyltransferase" *Med. Chem. Commun.* **2014**, *5*, 826–830.

Outlaw, V. K.; Townsend, C. A. "A Practical Route to Substituted 7-Aminoindoles from Pyrrole-3-carboxaldehydes" *Org. Lett.* **2014**, *16*, 6334–6337.

Outlaw, V. K.; D'Andrea, F. B.; Townsend, C. A. "One-Pot Synthesis of Highly-Substituted N-Fused Heteroaromatic Bicycles from Azole Aldehydes" *Org. Lett.* **2015**, *17*, 1822–1825.

Presentations

Outlaw, V. K.; Wydysh, E. A.; Vadlamudi, A.; Medghalchi, S. M.; Townsend, C. A. "Tipping the Balance between Fat Synthesis and Fat Burning: Inhibition of Glycerol-3-Phosphate Acyltransferase" Poster, Bioorganic Gordon Research Conference. Andover, New Hampshire, June 2014.